Annelid chaetae

Ultrastructure, arrangement and phylogenetic significance

Dissertation

zur

Erlangung des Doktorgrades (Dr. rer. nat.)

der

Mathematisch-Naturwissenschaftlichen Fakultät

der

Rheinischen Friedrich-Wilhelms-Universität Bonn

vorgelegt von

Julian Müller

aus

Bonn

Bonn, 03.03.2022

Angefertigt mit Genehmigung der Mathematisch-Naturwissenschaftlichen Fakultät der Rheinischen Friedrich-Wilhelms-Universität Bonn

1. Gutachter: Prof. Dr. Thomas Bartolomaeus
Institut für Evolutionsbiologie und Ökologie, Universität Bonn

2. Gutachter: Prof. Dr. Heike Wägele
Zoologisches Forschungsmuseum Alexander Koenig

Tag der Promotion: 12.07.2022
Erscheinungsjahr: 2022

Danksagung

It's the beauty in the flaw, the grace of imperfection
Now I'm twisted out of form, by unnatural selection
- Haken, „A cell divides" (Vector)

An erster Stelle möchte ich mich bei Prof. Dr. Bartolomaeus für die Aufnahme in seine Arbeitsgruppe, die Vergabe des Dissertationsthemas und vor allem seine ständige Betreuung und die wertvolle Bereitstellung seiner Erfahrung bedanken. Außerdem danke ich Prof. Dr. Heike Wägele für die Übernahme des Zweitgutachtens sowie Prof. Dr. Lukas Schreiber und Prof. Dr. Gerd Bendas für ihre Teilnahme an der Promotionskommission.

Den größten Dank schulde ich Dr. Ekin Tilic, der nicht nur im Zuge meiner Bachelor-Arbeit bereits mein Interesse an Anneliden und Untersuchungen ihrer Borsten geweckt hat, sondern auch als äußerst hilfsbereiter und geduldiger Kollege einen großen Anteil am Abschluss dieser Doktorarbeit hat. Weiterhin bin ich allen Kollegen der AG Bartolomaeus, insbesondere Dr. Patrick Beckers und Dr. Jörn von Döhren, für das Diskutieren und Bereitstellen von Daten und ihre permanente Unterstützung in technischen und fachlichen Fragen dankbar.

Darüber hinaus danke ich allen technischen Angestellten, die durch die Organisation diverser Geburtstags-, Karnevals- oder Abschiedsfeiern die Atmosphäre aufgelockert und dem Alltag die nötigen Unterbrechungen beschert haben. Besonders hervorheben möchte ich Tatjana Bartz, deren umfangreiche Hilfe im Labor und am Mikrotom essentiell für diese Arbeit war. In diesem Zusammenhang möchte ich auch Dr. Gregor Kirfel vom Institut für Zellbiologie der Universität Bonn für seine Zeit und Hilfe bei der Benutzung des dortigen Rasterelektronenmikroskops danken. Außerdem danke ich Kirsten Hennes für ihre unermüdliche Hilfe bei jeder administrativen und bürokratischen Hürde.

Auch wenn nicht mehr einzeln aufgezählt, bin ich jedem aktuellen und ehemaligen Mitglied des Instituts dankbar, mit dem ich während meiner Zeit als Doktorand zusammenarbeiten und meinen Alltag teilen durfte. Besondere Grüße gehen an den Friday-Club, mit dem sich so manche Woche äußerst angenehm ausklingen ließ.

Zu guter Letzt gilt mein allergrößter Dank meinen beiden Mitdoktoranden und Freunden Christina Sagorny und Sabrina Kuhl, mit denen ich nicht nur ein Büro, sondern auch Eis im Sommer, Kekse im Winter, Unterkünfte während Tagungen, den ein oder anderen Frustmoment, aber natürlich in erster Linie eine wunderschöne Doktorandenzeit teilen durfte!

Summary

With approximately 21,000 described species, Annelida represent one of the largest and best studied group of marine invertebrates. Their anatomy is characterized by a metameric organization, which covers potential for an extraordinarily diverse morphology and, therefore, the adaptation to basically every habitat and ecological niche. Each segment of their body bears equivalent structures, which comprise a pair of coelomic cavities, a pair of metanephridia and two pairs of parapodia. These parapodia are equipped with the most representative morphological structure of annelids, the chaetae.

Chaetae are chitinous, extracellular structures, which are formed within a follicle of invaginated epidermal cells. The basalmost cell of this follicle, the chaetoblast, secretes chitin, which accumulates between the cell's microvilli brush border. With ongoing secretion, the chitinous mass is pushed apically through the follicle until it eventually pierces the cuticle, thus forming the chaeta. Hollow canals are left inside the chaetae, where the microvilli of the chaetoblast were during chaetal formation. That way, a typical transverse-sectional honey-comb like pattern is generated, which guarantees mechanical stability and flexibility at the same time. The highly dynamic nature of the chaetoblast's microvilli pattern during the chaetogenesis facilitates the formation of numerous different shapes of chaetae. Chaetae often fulfil essential functions for the lifestyle of the respective species, which eminently influences their exact shape. Several chaetal follicles form a chaetal sac, in most cases one per parapodial ramus. Within a chaetal sac, new chaetae are formed at distinct formative sites. The number and positions of these formative sites determine the eventual arrangement pattern of the chaetae. Formation, diversity and arrangement of chaetae represent relevant characters for identification and description of species as well as phylogenetic and evolutionary analyses.

The vast morphological diversity of annelids always made it difficult to properly resolve their inner systematics. During the last decade, however, phylotranscriptomic studies revealed an updated and stable phylogenetic tree. This "new" annelid phylogeny demands a re-evaluation of morphological characters in order to understand their evolution and test established homology-hypotheses. In the course of three studies presented in this thesis, I investigated chaetal characteristics of several, predominantly basally branching annelid taxa. The first two studies examined the formation and arrangement of chaetae in Magelonidae and Oweniidae, together constituting the sister group to all remaining annelids. The third study focussed on the understudied family of Euphrosinidae, the sister group to Amphinomidae, which are notorious for their calcified, defensive stinging bristles. Additional unpublished

results covered insights into chaetal properties of the two largest annelid groups including data on Sternaspidae (Sedentaria) and Nephtyidae as well as Glyceridae (both Errantia).

All presented results support the hypothesis that chaetae are primarily arranged in one transverse row per parapodial ramus with a single formative site, which is located ventrally in the notopodium and dorsally in the neuropodium. More complex arrangement patterns like staggered rows (Magelonidae), bundles (Oweniidae, Euphrosinidae) or huge patches (Oweniidae) of chaetae are the result of a shift or multiplication of formative sites or constitute a modified, spirally curled up row. Moreover, comparisons of several internal, supportive chaetae in different annelid groups substantiate that this type of chaetae, often referred to as "aciculae", evolved several times independently. Aciculae of Errantia and Amphinomida differ regarding their shape, arrangement and composition and the arcuate chaetae in abdominal segments of Magelonidae actually constitute internal hooded hooks. Furthermore, it could be shown that chaetae of Euphrosinidae feature incorporated calcium compounds just like those of Amphinomidae. Combined with the findings concerning ultrastructure and arrangement, this third study sheds light on the chaetal properties found in the ground pattern of Amphinomida.

Altogether, the here presented results demonstrate the vast variability of chaetae, support the phylogenetic significance of their arrangement and help understanding the evolution of these characteristic structures.

Table of contents

Table of contents

Manuskripte

Die aufgelisteten Manuskripte/Publikationen sind im Zuge der Dissertation entstanden.

Manuskript 1 Müller, J. & Bartolomaeus, T. (in revision). Chaetal arrangement and type diversity in *Magelona mirabilis* (Magelonidae, Annelida) with ultrastructural details of the internal support chaetae. *Journal of Morphology*.

Manuskript 2 Müller, J., Bartolomaeus, T., & Tilic, E. (2022). Formation and degeneration of scaled capillary notochaetae in *Owenia fusiformis* Delle Chiaje, 1844 (Oweniidae, Annelida). *Zoomorphology*, *141*(1), 43–56. https://doi.org/10.1007/s00435-021-00547-z.

Manuskript 3 Müller, J., Schumacher, A., Borda, E., Rouse, G. W., Bartolomaeus, T., & Tilic, E. (2021). “Brittleworms”: Ultrastructure and arrangement of the calcified chaetae of *Euphrosine* (Amphinomida, Annelida). *Invertebrate Biology*, *140*(4), e12353. https://doi.org/10.1111/ivb.12353.

Introduction 1

1.1 Background

Except for a few familiar but rather unusual representatives like earthworms and leeches, annelids may not constitute the best-known - not to mention most popular - animal clade among non-biologists. Nonetheless, they always played a prominent role in natural history, which led to an extensive research catalogue underlining the interest and fascination for these segmented worms among scientists (Read, 2019).

With roughly 21,000 described species, Annelida represent the second largest group of the Lophotrochozoa after Mollusca (Read & Fauchald, 2022). Compared to larger metazoan taxa like Nematoda, Arthropoda or Vertebrata, Annelida constitute a rather medium-sized clade regarding species numbers, but they are extraordinarily rich in individuals (Hutchings, 1998). Annelids have conquered basically every possible habitat and ecological niche (Rouse & Pleijel, 2001; Díaz-Castañeda & Reish, 2009). The majority of annelid species occur in marine benthic environments covering plenty of different substrates like soft sediment (Labrune et al., 2007), hydrothermal vents (Shank et al., 1998), cold seeps (Levin et al., 2006) and even shells or skeletons of other marine animals (Blake, 1969; Glover et al., 2005). Besides the benthos, also pelagic and tidal zones serve as habitats for numerous annelids (Robbins, 1965; Gouveneaux et al., 2018; Zanol et al., 2021) and even fresh water (Glasby & Timm, 2008) as well as terrestrial terrains (Rousset et al., 2008) have been colonized by these originally marine creatures (Martinez-Acosta & Zoran, 2015).

It comes with their extensive distribution and abundance that annelids adopted a broad variety of lifestyles and ecological roles. While many annelids are predatory, like the venomous Glyceridae (Reumont et al., 2014) or representatives of the Eunicida, which are equipped with massive jaws (Paxton, 2000, 2009), some have a parasitic (Øresland & Pleijel, 1991), symbiotic (Jennings & Gelder, 1976) or commensal lifestyle (Zimmermann et al., 2011). The major part of annelids, however, are deposit or suspension feeders, which is also hypothesized to constitute the ancestral state in this group (Weigert et al., 2014). This feeding habit often correlates with a burrowing lifestyle so that the animals are hidden within the sediment and only display their retractable feeding structures like palps or tentacles (Lewis, 1968; Weigert et al., 2014). In the course of this sediment dwelling way of life, some annelids evolved the ability to build tubes supported by cement-like substances secreted to enhance the stability of their burrows (Barnes, 1965; Stewart et al., 2004; Noffke et al., 2009). Some annelids literally dig even deeper and developed an infaunal lifestyle, feeding on sediment (Shelley et al., 2008). Due to this

bioturbation, they fulfil a decisive role in the ecological system by significantly influencing the constitution of the sediment (Krantzberg, 1985; Levin et al., 2003; Volkenborn et al., 2007).

1.2 Annelid morphology

The key to the vast variety of lifestyles and habitats found in annelids lies in their highly flexible morphology. The most significant characteristic of annelids is their metameric body plan, which means that they are subdivided into numerous segments along the anterior-posterior-axis. All of these segments share the same composition and bear equivalent structures (Purschke, 2002; Fig. 1.2.1A). Each segment contains one pair of metanephridia (Bartolomaeus, 1999), one pair of coelomic cavities (Bartolomaeus, 1994; Rieger & Purschke, 2005) and two pairs of laterally protruding appendages called parapodia (Fauchald, 1977; Fig. 1.2.1B). These parapodia are biramous, being subdivided into a dorsal notopodium and a ventral neuropodium (Grzimek, 1971). Both parapodial rami possess a complex system of musculature and are often equipped with branchiae serving as respirational structures (Tzetlin & Filippova, 2005; Struck, 2011). Furthermore, they carry various taxon-specific appendages like cirri, lobes or lamellae so that their appearance can be extraordinarily diverse among different taxa (Fauchald, 1977). Finally, each parapodial ramus bears one bundle of chitinous chaetae, one of the most representative annelid characters (Fauchald, 1977; Hausen, 2005a). Apart from in the parapodia, musculature is present throughout the whole body organized as outer circular and inner longitudinal muscles (Tzetlin & Filippova, 2005). The annelid integument is composed of a monolayered and occasionally multi- or monociliated epidermis that is covered by a thin and flexible collagenous cuticle and contains numerous secretory and sensory cells, (Welsch et al., 1984; Bartolomaeus, 1995a; Hausen, 2005b).

The only constant deviations from the repetitive, segmental body plan can be found in the first (prostomium) segment with the main sensory organs and the brain and the last segment (pygidium) with the anus (Westheide, 1997). The second segment, the peristomium, additionally carries the mouth. New segments are produced during the entire lifespan of the animals at the meristematic zone, which is located immediately anteriorly to the pygidium (Balavoine, 2014). This formation of new segments already starts in the early ontogenetic stage as a trochophore larva (Balavoine, 2014; Fig. 1.2.1C). Thus, the successive growth of new segments could be described as an additional, “doubled” ontogenesis, which continues even after the juveniles performed the change from a pelagic to a benthic lifestyle (Fig. 1.2.1C).

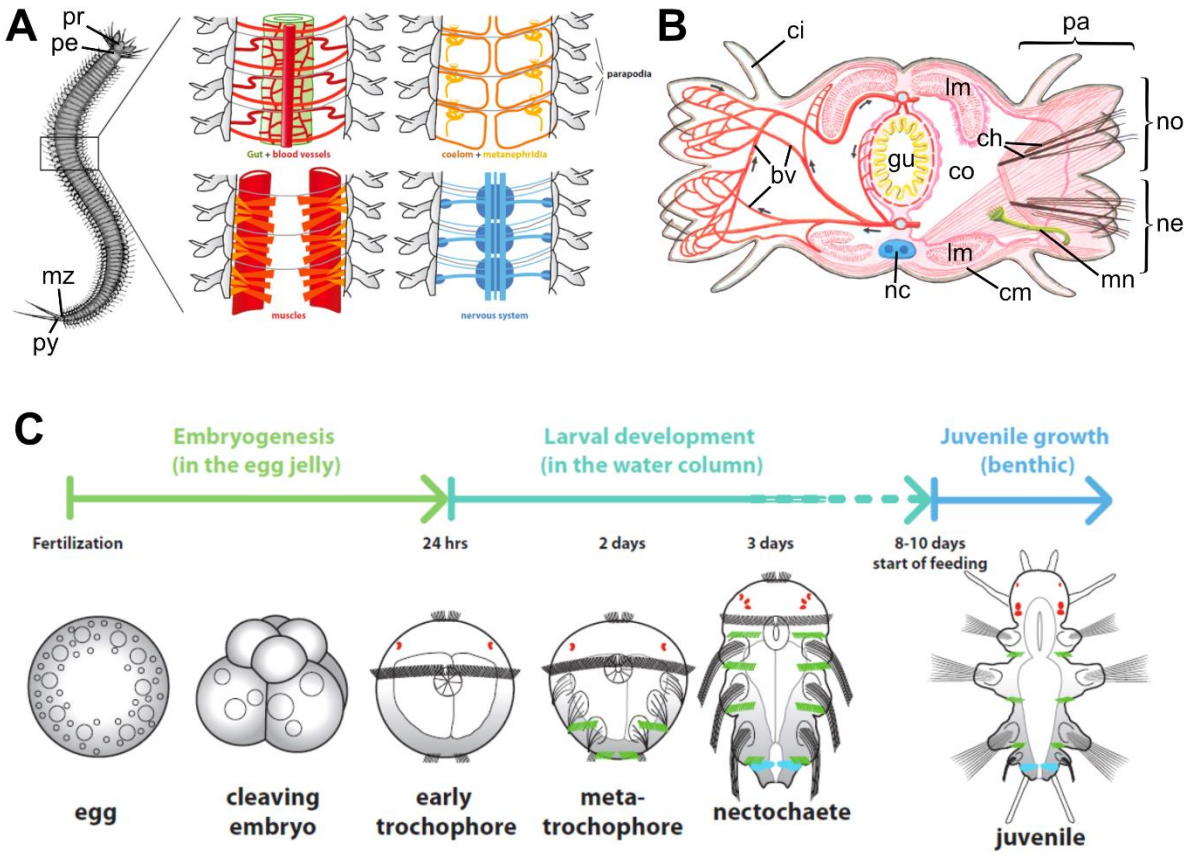

Fig. 1.2.1 Annelid morphology and development. **A** Schematic drawing of a typical segmented annelid from a dorsal view. A section of four segments is shown more detailed four times, illustrating the location of varying internal structures. Modified after Balavoine (2014). **B** Exemplary schematic transverse section through an annelid segment showing typical structures and organs, appearing in all segments. Modified after Grzimek (1971). **C** Schematic depiction of the annelid development including the spiral cleavage, the pelagic trochophore larva and the juvenile benthic, already segmented worm. From Balavoine (2014). *bv* blood vessel, *ch* chaetae, *ci* cirrus, *cm* circular muscles, *co* coelomic cavity, *gu* gut, *lm* longitudinal muscles, *mn* metanephridium, *mz* meristematic zone, *nc* nerve cord, *ne* neuropodium, *no* notopodium, *pa* parapodium, *pe* peristomium, *pr* prostomium, *py* pygidium.

The segmented body plan of annelids, and therefore the possibility of individual variation or fusion of single segments, holds great potential in terms of fast and effective evolutionary adaptation and eventually resulted in an extraordinary morphological diversity (Purschke, 2002). Accordingly, it is hypothesized that the annelid ground pattern comprised a homogeneously segmented marine worm of simple organization, lacking any appendages along the whole body (Fauchald, 1974a, 1977). Deviating from this presumed common ancestor, many annelids developed specialized segments and even functionally and morphologically differentiated tagmata. Analog to arthropods, this can often be observed as a subdivision into

thorax and abdomen, but with varying appearances and numbers of segments (Jones, 1968; Nilsen & Holthe, 1985). The most peculiar form of tagmatization may be found in the Chaetopteridae with three distinct body regions, which again contain anatomically varying segments (Barnes, 1964; Irvine & Martindale, 2000). Some annelid groups like Echiura, Sipuncula, Siboglinidae or Sternaspidae convergently deviate from the ground pattern by the secondary loss of inner segmentation (Vejdovský, 1882; McHugh, 2000; Purschke, 2002; Dordel et al., 2010).

The exceptionally high diversity in relation to their species number always made annelids particularly interesting for morphological studies in order to comprehend the evolution of key structures and to draw phylogenetic implications (e.g. Rouse & Fauchald, 1997; Westheide et al., 1999). In that regard, the here presented thesis focusses on examining various morphological aspects of the annelid chaetae.

1.3 Chaetae

Chaetogenesis

Chaetae are extracellular structures that are formed within a follicle of invaginated epidermal cells (O'Clair & Cloney, 1974). A specialized epidermal cell, the chaetoblast, which is equipped with a distinct microvilli pattern, constitutes the basal end of the follicle (O'Clair & Cloney, 1974). The chaetoblast secretes β-chitin, cross-linked by proteins, that accumulates between the microvilli and polymerizes (Lotmar & Picken, 1950; George & Southward, 1973). In some cases the chaetal material contains additional inorganic substances like calcium carbonate (McIntosh, 1876) or iron (Bartolomaeus, 1992) incorporated within the chitinous mass. By constant secretion the thus forming chaeta is permanently pushed apically through the follicular space, eventually breaking through the cuticle (Fig. 1.3.1A). This way, hollow canals arise at the positions of the microvilli, leaving a typical honeycomb-like pattern in transverse sections of the chaeta (Bouligand, 1967). In most cases, this canal meshwork consists of larger, thin-walled canals in the centre of the chaeta and smaller ones with thick lamellae in its periphery, which guarantees an extraordinary flexibility as well as stability (Kryvi & Sørvig, 1990; Merz & Woodin, 1991; Hausen, 2005a; Fig. 1.3.1B).

The follicle cells participate in chaetogenesis as well by releasing additional chaetal material, producing an outer enamel layer (Hausen & Bartolomaeus, 1998; Hausen, 2005a). This enamel layer surrounds the whole chaeta, providing a strengthened periphery with a smooth surface and is adhered by hemidesmosomes to the follicle cell’s microvilli filled with

intermediate filaments (Bartolomaeus, 1995b). Furthermore, modification of the enamel or the contribution of additional chitin by the follicle cells can lead to the creation of fine external ornamentations (Tilic, Geratz, et al., 2021; Tilic, Neunzig, & Bartolomaeus, 2021). Due to the dynamic nature of the chaetoblast's microvilli brush border during chaetogenesis and distinct modifications by the follicle cells, numerous variations in terms of size and shape can be found among annelid chaetae (Fig. 1.3.1C-N).

Shapes and functions

The simplest form of annelid chaetae are capillary chaetae, representing long and slender hair-like bristles (Fig. 1.3.1C). By flattening or stretching of parts of the chaeta, more definite shapes

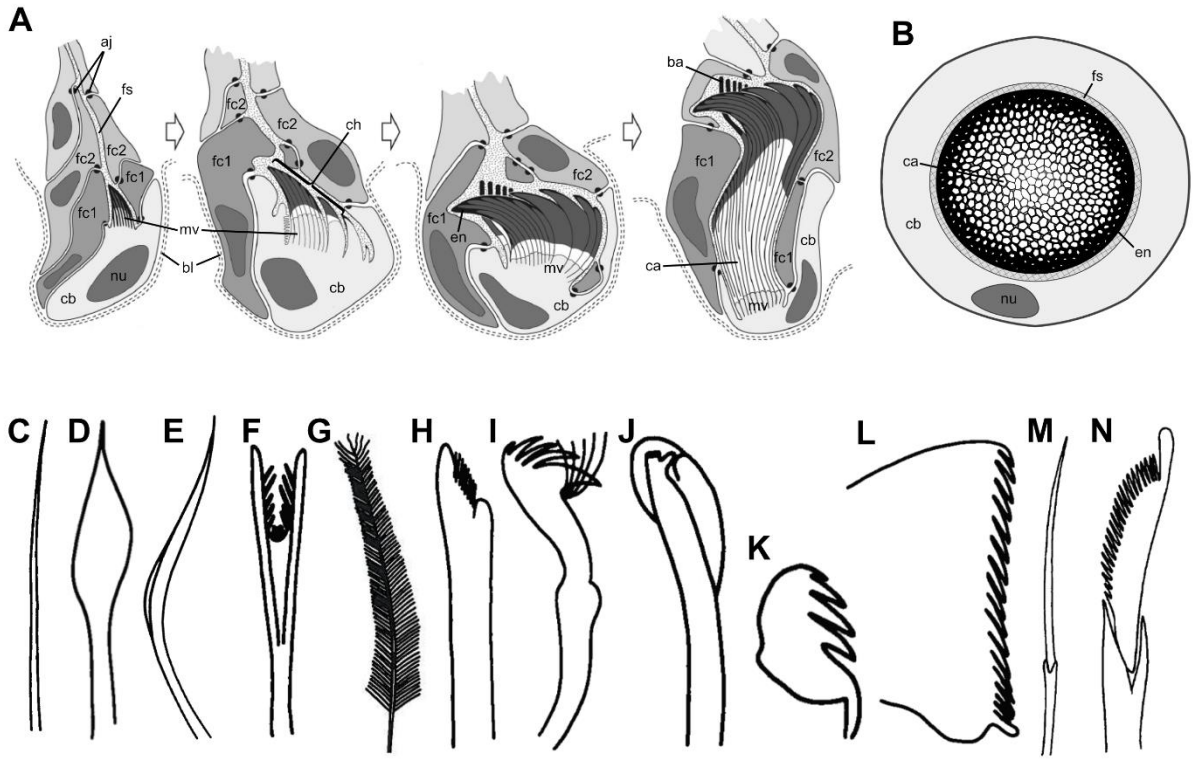

Fig. 1.3.1 Chaetogenesis and chaetal shapes of annelids. **A** Schematic drawing of the chaetogenesis of a bearded hook in four steps. Note the enamel layer and how every barbule is formed by one single microvillus each. Modified after Tilic et al. (2015). **B** Schematic drawing of the typical appearance of a transverse section through a chaeta with the thickness of the chitinous lamellae differing between centre and periphery. Based on personal data. **C-N** Schematic drawings of various types of annelid chaetae, not to scale. Modified after Gardiner (1992). **C** Capillary chaeta. **D** Spatulate chaeta. **E** Limbate chaeta. **F** Forked chaeta. **G** Featherlike chaeta. **H** Stout chaeta with terminal hairs. **I** Bearded hook. **J** Hooded hook. **K** Small uncinus. **L** Large uncinus. **M** Compound chaeta. **N** Compound chaeta with toothed blade. *aj* adhaerens junction, *ba* barbule, *bl* basal lamina, *cb* chaetoblast, *ch* chaeta, *en* enamel, *fc* follicle cell, *fs* follicular space, *mv* microvilli, *nu* nucleus.

like spatulate (Fig. 1.3.1D) or limbate chaetae (Fig. 1.3.1E) may develop. More derived forms would be forked chaetae (Fig. 1.3.1F). Some carry fine substructures, which are formed by single microvilli of the chaetoblast (Fig. 1.3.1A, G-I). Extraordinarily widespread among annelids are hooks or uncini, which are equipped with varying numbers of distinct teeth (Fig. 1.3.1I-L). A very specialized form, emphasizing the great potential of the chaetogenetic process to create complex shapes, can be found in compound chaetae (Fig. 1.3.1M, N). Those consist of two variably designed parts, which are connected via a flexible joint (Gustus & Cloney, 1973). Additionally, several annelid taxa possess enlarged, stout chaetae, which do not stand out by a specialized shape but differ from other chaetae in being embedded within the tissue and not piercing the cuticle. These so-called aciculae act as supportive skeletal elements and serve as muscle attachment points (Hausen, 2005a; Tilic et al., 2016).

The shape of chaetae is directly influenced by ecological factors, which is the cause for their vast diversity and makes them fulfil plenty of different functions (Merz & Woodin, 2006). Jointed chaetae, for example, support the locomotion by increasing the traction with the substrate and enhancing the swimming stroke (Merz & Edwards, 1998). In Amphinomidae, on the other hand, calcareous chaetae serve as defensive tools (Eckert, 1985; Schulze et al., 2017). Numerous studies deal with the variety of hooked chaetae and their connection to a tubiculous lifestyle by functioning as anchors within the worm's tube (e.g. Knight-Jones, 1981; Woodin & Merz, 1987; Merz & Woodin, 2000). Simple capillary chaetae are generally thought to improve the animals' perception of the environment, acting as mechano-receptors (Woodin et al., 2003; Merz & Woodin, 2006). They have also been recognized to support the irrigation of tubes by stabilizing the worm's position within the tube during peristaltic movement (Sendall et al., 1995; Merz & Woodin, 2006).

The diversity of chaetae is not restricted to different species, but various chaetal types can even be formed within single individuals. They potentially differ between noto- and neuropodia of the same segment as well as, if present in the respective species, between different tagmata (Jones, 1968; Meyer & Bartolomaeus, 1996; Britayev & Martin, 2019). In many of such cases, one parapodial ramus bears hooked chaetae, and the other one capillary ones, but different chaetal types can also be found within one ramus (Bartolomaeus, 1995b; Bartolomaeus & Meyer, 1997; Bartolomaeus, 2002; Tilic et al., 2014; Tilic, Döhren, et al., 2015).

Arrangement of chaetae

Independently from the exact chaetal type, the number of chaetae found in each segment is immensely variable among species. Representatives of the Tomopteridae, for example, carry only one large acicula per parapodium in the second segment, while some Oweniidae bear up to over 7,000 uncini per segment (Fauchald, 1977; Capa et al., 2019). Irrespective of the final number, chaetae are not formed all at once, but successively and in a certain order (Pilgrim, 1977). This consecutive formation takes place in chaetal sacs, which constitute an aggregation of chaetal follicles and, thus, consist of epidermal tissue embedded in the mesoderm and underlined by a common basal lamina (Bouligand, 1967; Bartolomaeus, 2002). In the vast majority of annelids each parapodial ramus bears one chaetal sac, containing all chaetae of that ramus, even if there are various types (Hausen, 2005a; Tilic et al., 2014). Within these chaetal sacs, chaetae are formed at distinct formative sites. Constant formation of new chaetae at the same spot leads to a shift of older chaetae in a certain direction, eventually reaching the degeneration site, which often lies at the formative site's opposite end of the chaetal sac (Bartolomaeus, 1998; Fig. 1.3.2A). New chaetae are formed and degenerated during the entire lifespan of the animals (Bartolomaeus, 1998; Kolbasova et al., 2014).

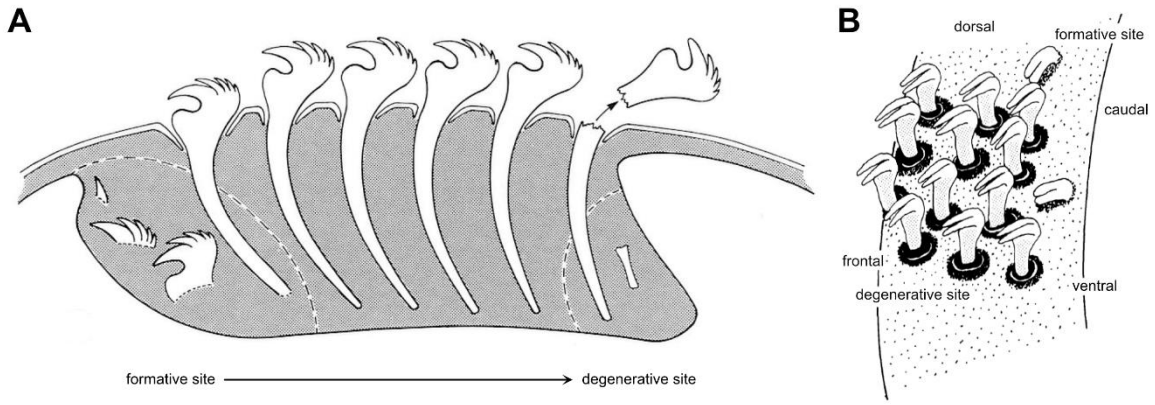

Fig. 1.3.2 Arrangement of annelid chaetae. **A** Schematic longitudinal section through a chaetal sac with one formative site. Due to the constant generation of new chaetae, older ones shift towards the opposite end of the sac, where they degenerate. Modified after Bartolomaeus (1998). **B** Schematic drawing of the formation of a neuropodial patch of oweniid uncini with a dorso-caudal formative site and a ventro-frontal degenerative site. Modified after Meyer & Bartolomaeus (1996).

Combined with the size and dimension of the chaetal sac, the direction of chaetal formation terminates in a definite arrangement of a group of chaetae (Fig. 1.3.2B). Additional

formative sites result in additional groups and, potentially, further types of chaetae in a chaetal sac (Tilic et al., 2014; Tilic et al., 2019). In most taxa that have been investigated in this regard, chaetae are arranged in transverse rows, with a single ventral formative site in the notopodium and a dorsal one in the neuropodium (Hausen & Bartolomaeus, 1998; Schweigkofler et al., 1998; Hausen, 2005a; Kolbasova et al., 2014). Other arrangement patterns include doubled rows, fascicles, bundles or patches of chaetae (Meyer & Bartolomaeus, 1996; Hausen & Bartolomaeus, 1998; Hausen & Bleidorn, 2006; Tilic et al., 2017). The formation processes and involvement of formative sites in such patterns are still not fully understood and further investigations on this characteristic are needed in order to comprehend the evolution of chaetal arrangement in annelids.

Phylogenetic significance

Due to their unique development and immense diversity, chaetae have been playing a major role in annelid research for over a century by now (Vejdovský, 1882; Schepotieff, 1903, 1904; Gustafson, 1930; Bobin, 1944; Lippert & Gentil, 1963; O'Clair & Cloney, 1974). Since their shape and structure are taxon-specific, they have become the best investigated morphological characters in annelids and acquired enormous relevance for species identification as well as phylogenetic and evolutionary analyses (e.g. George & Southward, 1973; Fauchald, 1977; Fitzhugh, 1989; Bartolomaeus, 1995b; Fauchald & Rouse, 1997; Rouse & Fauchald, 1997; Hausen, 2005a). However, due to the enormous flexibility of the chaetogenetic process and the fact that the appearances of chaetae are strongly driven by ecological restraints, several shape-based homology hypotheses are questionable and, in some cases, contradict more recent phylogenomic data (Bartolomaeus, 1995b; Meyer & Bartolomaeus, 1996; Bartolomaeus & Meyer, 1997; Bartolomaeus, 1998; Merz & Woodin, 2000; Hausen, 2005a).

The arrangement of chaetae, including positions and numbers of formative and degenerative sites, though, have been proved to be of high phylogenetic significance (Meyer & Bartolomaeus, 1996; Bartolomaeus et al., 2005; Hausen, 2005a; Hoffmann & Hausen, 2007; Kieselbach & Hausen, 2008; Tilic, Döhren, et al., 2015). This is supported by the fact that extracellular, ectodermal chitinous structures describable as chaetae or something complementary are not solely found in annelids, but only their specific arrangement counts as an annelid apomorphy (Bartolomaeus, 1998). Aside from few ultrastructural differences, chaetae are also present in brachiopods and similar structures a reported from cephalopods (Gustus & Cloney, 1972; Brocco et al., 1974). Additionally, Gordon (1975) discussed some

correlations to bryozoan gizzard teeth. This morphological resemblance of annelid chaetae to other lophotrochozoan group's structures still complicates the phylogenetic placement of Annelida.

1.4 Phylogenetic placement of Annelida

As their most remarkable morphological trait, the metameric organization of annelids was the basis for their primary phylogenetic placement as sister group to the arthropods, both summarized as Articulata (Cuvier, 1817). This long-lasting idea of a clade including all segmented animals was challenged and, consequently, falsified at the end of the last millennium by the re-evaluation of morphological characters and the advent of molecular data (Eernisse et al., 1992; Giribet & Ribera, 1998; Irvine & Martindale, 2000). Since then, it is widely accepted that protostomes comprise Ecdysozoa (including arthropods) and Lophotrochozoa (including annelids) as two large sister groups (Halanych et al., 1995; Aguinaldo et al., 1997; Bourlat et al., 2008).

The inner phylogeny of the Lophotrochozoa has been under constant discussion ever since this fundamental change in protostome systematics (Bleidorn, 2019). Therefore, the position of annelids within lophotrochozoans has changed multiple times. Over the past two decades, they have been placed into a sister group relationship with Nemertea (Kocot et al., 2017), clades consisting of Phoronida plus Bryozoa (Helmkampf et al., 2008a), Brachiozoa plus Mollusca (Paps et al., 2009) respectively Nemertea (Dunn et al., 2008; Hausdorf et al., 2010) and even a group comprising Polyplacophora, Cephalopoda and Phoronida (Bourlat et al., 2008). In contrast to their placement within the lophotrochozoan phylogeny, the monophyly and inner systematics of annelids are well supported by morphological data and, since the inclusion of rather unusual groups like Echiura, Sipuncula, Pogonophora or Myzostomida, also based on molecular data (e.g. Purschke, 2002; Bleidorn et al., 2003; Bleidorn et al., 2007; Struck et al., 2007; Pleijel et al., 2009; Dordel et al., 2010; Struck et al., 2011; Weigert et al., 2014; Andrade et al., 2015; Weigert & Bleidorn, 2016; Bleidorn, 2019; Struck, 2019).

1.5 Annelid systematics and examined groups

The relevance of chaetae as a diagnostic character in the history of annelid research is reflected in their traditional systematics based on morphological characters, which differentiates between Polychaeta and Clitellata as two sister groups (Rouse & Fauchald, 1997). The nomenclature

of Polychaeta (“many chaetae”) and Oligochaeta (“few chaetae”) that comprise the majority of Clitellata is based on the number and diversity of chaetae found in representatives of both groups. With the Canalipalpata and the Aciculata, the two largest and most diverse groups of the Polychaeta were differentiated by the presence of aciculae and, thus, again by chaetal characters (Rouse & Fauchald, 1997). More recent transcriptomic approaches, however, yielded a new stable and widely accepted annelid phylogenetic tree, differing significantly from the former state of knowledge (Weigert et al., 2014; Andrade et al., 2015; Weigert & Bleidorn, 2016; Struck, 2019; Fig. 1.5.1).

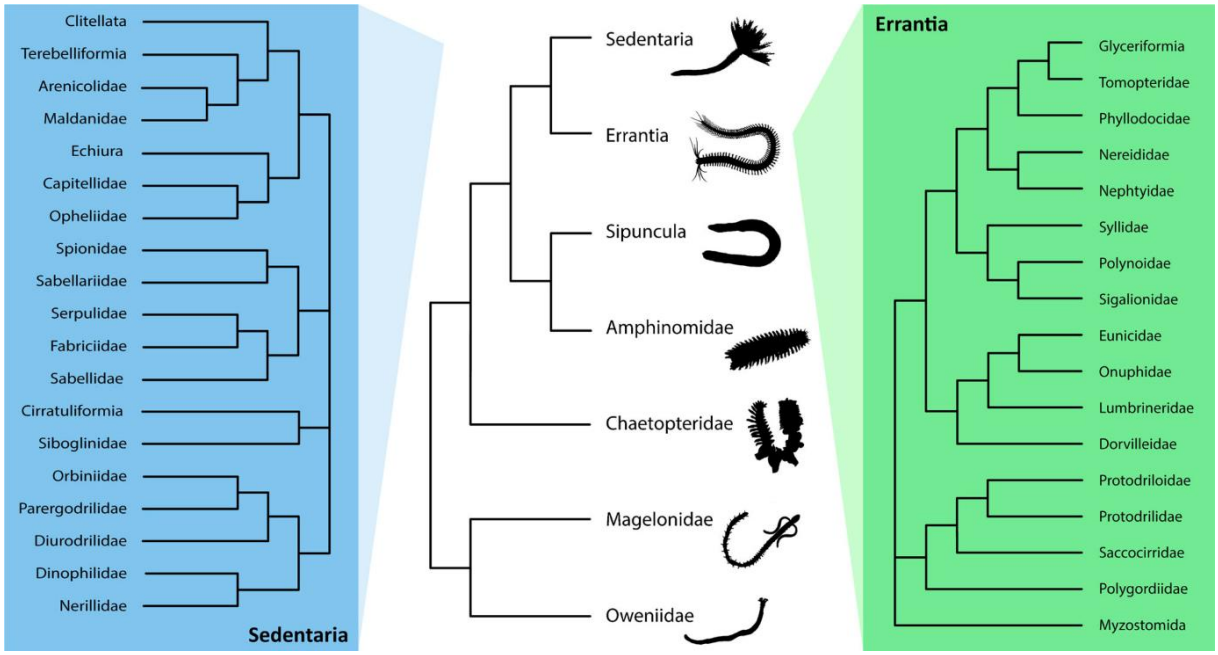

Fig. 1.5.1 The phylogenetic tree of Annelida according to the current state of knowledge based on phylogenomic analyses. From Weigert & Bleidorn (2016).

In this updated annelid systematics, Oweniidae and Magelonidae, summarized as Paleoannelida, represent the sister group to all remaining annelids. Sipuncula, formerly excluded from Annelida because of their lack of any segmentation and chaetae, turned out to be the sister group of the Amphinomida, which were primarily placed within the Aciculata (Rouse & Fauchald, 1997; Rouse & Pleijel, 2001). Errantia comprise – for the most part - the remaining aciculate groups, forming one of the two largest and most diverse groups in the new phylogeny. The second dominating group is their sister group, Sedentaria, including Clitellata

besides numerous further taxa. Those annelid groups that were examined in more detail in the course of this thesis will be presented shortly in the following.

Magelonidae

With 72 recognized species, Magelonidae constitute a rather small annelid group of burrowing suspension feeders, which are well-studied in terms of systematics, behaviour and anatomy (Jones, 1968; Fiege et al., 2000; Filippova et al., 2005; Mills & Mortimer, 2019; Mortimer et al., 2021; Parapar et al., 2021). Anatomically, they are characterized by a tagmatization into a thorax, that comprises the prostomium, peristomium, one segment without chaetae and the following 8-9 chaetigers, and an abdomen with all subsequent segments (Jones, 1968; Parapar et al., 2021). Their appearance is defined by the shovel-shaped prostomium bearing two long, papillated palps (Mortimer et al., 2020). Except for the highly variable ninth chaetiger, magelonids possess a uniform morphology, which complicates the identification of species (Jones, 1968). Therefore, parapodial details and their chaetae have been subject of detailed analyses in numerous species descriptions (Mortimer & Mackie, 2003, 2009; Clarke et al., 2010; Mortimer et al., 2012; Shakouri et al., 2017; Mills & Mortimer, 2018; Mortimer et al., 2020). Despite this focus on chaetal characteristics in magelonid literature, the arrangement and positions of formative sites are still poorly studied. Additionally, some magelonid species bear internal support chaetae in abdominal segments (Brasil, 2003). Reports on these chaetae are scarce and studies on their exact shape or ultrastructure are missing completely (Mortimer et al., 2021).

Oweniidae

Oweniidae represent an unusual annelid taxon that is characterized by several unique attributes like the lack of an elaborate cuticle, ontogenesis via a mitraria larva and an intraepidermal nervous system (Rieger & Rieger, 1976; Gardiner, 1978; Gardiner & Rieger, 1980; Smith et al., 1987; Westheide, 1997; Smart & Von Dassow, 2009). With Magelonidae they share some common features like the lack of nuchal organs or the presence of a monociliated epidermis, which support their sister group relationship (Capa et al., 2012; Parapar et al., 2021). Further similarities to magelonids, which evolved most probably convergently, are a specialized head consisting of the fused prostomium and peristomium and the subdivision into a thorax and abdomen (Nilsen & Holthe, 1985; Smart & Von Dassow, 2009). Oweniids are likewise burrowing suspension feeders, but, as opposed to magelonids, they build peculiar tubes

consisting of sand grains and shell fragments (Dales, 1957). In most oweniids, the thorax consists of three fused segments with reduced neuropodia, while numerous long, internally separated segments form the abdomen (Capa et al., 2019). While the abdominal notopodia bear bundles of long capillary chaetae, their neuropodia are equipped with huge patches of up numerous uncini, arranged in several rows (Meyer & Bartolomaeus, 1996; Capa et al., 2019). Besides the well-studied chaetogenesis of these uncini, it has been shown that they are formed at the dorsal end of the patches and degenerated at the ventral end (Meyer & Bartolomaeus, 1996). This makes them one of the very few cases of documented chaetal degeneration (Kolbasova et al., 2014). Respective data on the notochaetae of Oweniidae are still missing and would be especially interesting to improve our understanding of the formation of chaetal bundles.

Euphrosinidae

Amphinomidae and Euphrosinidae represent sister groups, together forming the clade Amphinomida (Wiklund et al., 2008). This relationship is well supported by molecular as well as morphological data (Gustafson, 1930; Borda et al., 2012; Borda et al., 2015). Amphinomida are predatory, benthic annelids with a uniform segmentation and a dorsal side covered by gills and chaetae (Hutchings, 2000a, 2000b). One of their most distinctive morphological characters is the presence of aciculae in all parapodia, which led to their former placement within Errantia, Eunicida or as an individual clade within Aciculata (Rouse & Fauchald, 1997; Rouse & Pleijel, 2001). Amphinomidae are far more diverse, species rich and, therefore, better studied than Euphrosinidae (Wiklund et al., 2008; Borda et al., 2012; Tilic et al., 2017). Amphinomidae, like the fireworm *Eurythoe complanata* (PALLAS, 1766), are notorious for carrying calcified stinging chaetae, causing skin inflammations after contact (Eckert, 1985; Schulze et al., 2017; Tilic et al., 2017). They have been proofed to be able to produce venomous substances, which, in combination with the hollow nature of their chaetae, gave rise to the hypothesis that their capillary chaetae act as venom-injecting, needle-like structures (Nakamura et al., 2008; Verdes et al., 2018; Righi et al., 2021; Simonini et al., 2021). Investigations on the chaetogenesis and ultrastructure of the chaetae, however, pointed out the artificial character of the chaetal cavities and, thus, falsified this idea (Eckert, 1985; Tilic et al., 2017; Tilic & Bartolomaeus, 2021). Due to this popularity of fire worms, substantial information on the chaetal arrangement, ultrastructure and composition of Amphinomidae are available. Equivalent investigations on Euphrosinidae could shed light on the ancestral condition of amphinomidan chaetae.

Sternaspidae

The sedentary, sediment-feeding Sternaspidae are characterized by a peculiar appearance, which differs from other annelids by derived anatomical aspects like a subdivision of the body in three distinct parts and the lack of internal segmentation (Sendall & Salazar-Vallejo, 2013). The ventral side of the posterior part of the body is covered by a cuticular shield, which contains ferric phosphate (Lowenstam, 1972). The animal's chaetae seem to contain iron components as well (Bartolomaeus, 1992). Only certain body parts bear chaetae and their identification as noto- respectively neurochaetae and especially the position of their formative sites remains unresolved to date (Sendall & Salazar-Vallejo, 2013). At the anterior body part, the retractable introvert, three segments bear two transverse rows of massive, spine-like chaetae each (Petersen, 2000). The shield is surrounded by numerous fascicles of thin capillary chaetae and two stout peg chaetae, which have been shown to actually consist of plentiful extraordinarily thin and short chaetae (Zhadan et al., 2017). The exact formation and composition of these peg chaetae is still unknown.

Nephtyidae & Glyceridae

Nephtyidae as well as Glyceridae, both belonging to the Phyllodocida, are free-living burrowers and active predators equipped with eversible pharynges (Fauchald & Jumars, 1979; Rouse & Fauchald, 1997). In glycerids, this pharynx is armed with four distinct jaws, which inject venom into their prey (Reumont et al., 2014). As members of the Phyllodocida, which are part of Aciculata, both nephtyids and glycerids possess aciculae (Rouse & Fauchald, 1997). Besides that, they bear capillary chaetae and, in the case of glycerids, compound chaetae as well (Rouse & Fauchald, 1997). Even though the chaetal type diversity is well studied for Phyllodocida, information on the chaetal arrangement or number and positions of formative sites are scarce.

1.6 Aims of the study

The newly established annelid phylogeny demands a re-evaluation of morphological characters in order to comprehend their evolution, determine potential convergences and evaluate their phylogenetic relevance (Tilic, Lehrke, & Bartolomaeus, 2015; Tilic et al., 2016; Helm et al., 2018; Beckers, Helm, & Bartolomaeus, 2019; Beckers, Helm, Purschke, et al., 2019). In the course of six chapters including three studies published in or submitted to scientific journals, chaetal characters of representatives of the annelid taxa presented above were investigated in

order to draw the before-mentioned conclusions. Altogether, the here presented results allow a broader comparison of repeatedly examined chaetal properties like formation process and ultrastructure. One of the main aspects is the analysis of different arrangement patterns including number and position of formative sites in order to enhance the understanding of their formation and to determine the ancestral state of chaetal arrangement in annelids. Furthermore, internal supportive chaetae, which are found in most of the investigated groups, will be compared regarding structure, shape, function and formation to discuss potential homologies.

Due to their newly confirmed sister group relationship to all other annelids, magelonids and oweniids have attracted increased attention in the past couple of years, resulting in numerous studies on the evolution of phylogenetically relevant morphological characters in both groups (Helm et al., 2016; Beckers, Helm, & Bartolomaeus, 2019; Beckers, Helm, Purschke, et al., 2019; Rimskaya-Korsakova et al., 2020; Carrillo-Baltodano et al., 2021; Parapar et al., 2021). The first study aims to contribute to this topic by investigating the arrangement of chaetae in *Magelona mirabilis* (JOHNSTON, 1865) and provides first ultrastructural details of the abdominal internal support chaetae of Magelonidae, which were only mentioned superficially in literature so far. The second study focusses on the poorly studied notochaetae of *Owenia fusiformis* DELLE CHIAJE, 1844 in terms of arrangement and chaetogenesis. In the course of the third study, the chaetal properties of *Euphrosine foliosa* AUDOUIN & MILNE EDWARDS 1833 and *Euphrosine* sp. were investigated with regard to their arrangement, composition and chaetogenesis and compared to equivalent data of Amphinomidae in order to shed light on the primary state of amphinomidan chaetae. Additional unpublished results concerning chaetal properties of sedentary and errant representatives are presented to cover further parts of the annelid tree. Unpublished results and supportive data include investigations on *Sternaspis scutata* (RANZANI, 1817), *Glycera fallax* QUATREFAGES, 1850, *Nephtys hombergii* SAVIGNY IN LAMARCK, 1818, *Chloeia euglochis* EHLERS, 1887, *Hermodice carunculata* PALLAS, 1766, *Archinome levinae* BORDA ET AL., 2013 and *Archinome jasoni* BORDA ET AL., 2013.

Materials & Methods 2

2.1 Specimens

Specimens of *Magelona mirabilis* have been collected during low tide in Wimereux (Hauts-de-France, France, 2012), Pouldohan (Brittany, France, 2015) and Morgat (Brittany, France, 2021). All specimens from *Owenia fusiformis* were collected in Pouldohan during low tide and have been kept in the aquarium of the Institute for Evolutionary Biology and Ecology at the University of Bonn. One specimen of *Euphrosine* sp. has been collected in the lagoon of Manatee Cay (Belize, 2006), two specimens of *Euphrosine foliosa* in Le Cabellou (Brittany, France, 2019). Specimens of *Sternaspis scutata*, provided by the Center of Marine Research, Ruđer Bošković Institute in Zagreb, were collected in Rovinj (Istria, Croatia, 2015), while one young specimen was collected in Banyuls-sur-Mer (Occitany, France, 1991). All specimens of *Nephtys hombergii* and *Glycera fallax* were collected in Concarneau (Brittany, France, 2016) during low tide. Further evaluated specimens comprise *Chloeia euglochis*, collected in the Florida Straits, south-southwest of Dry Tortugas Keys (Florida, USA, 2006); *Hermodice carunculata*, collected in Bocas del Toro (Panama, 2009); *Archinome levinae*, collected in the Guaymas Basin (Gulf of California, Mexico, 2003); and *Archinome jasoni*, collected in Kilo Moana, Lau Back-arc Basin (2005).

Prior to examination, all animals were relaxed in a 7% $MgCl_2$ solution (1:1 mixed with seawater). Additionally, the oweniid specimens were carefully removed from their sediment tubes. Fixation of specimens was obtained either with a 5% Formol solution at 4°C overnight, 4% paraformaldehyde at 4°C for 1h, Bouin's fluid (80 ml stock solution (1 g Picrid acid solved in 100 ml Ethanol) + 20 ml 35% Formol + 2 ml of Acetic acid) at room temperature overnight or 2.5% glutaraldehyde buffered in 0.05 M phosphate 0.3 M NaCl saline (PBS) at room temperature for 1h. Regardless of the respective fixation method, specimens were washed with and transferred to 70% ethanol after fixation.

2.2 Micro-computed tomography (µCT)

One whole specimen of *M. mirabilis* (from Morgat) and *E. foliosa* each was fixed with Bouin's fluid, while one specimen of *O. fusiformis* was fixed with glutaraldehyde and *S. scutata* with Formol. All animals were stained with 0.3% phosphotungstic acid (PTA) in 70% ethanol for at least one week. Using a SkyScan 1272 µCT system (Bruker) the specimens were scanned in 70% ethanol at resolutions of 3 µm (*M. mirabilis*), 8 µm (*E. foliosa*), 2.7 µm (*O. fusiformis*) and 7µm (*S. scutata*). The scan data were reconstructed with Nrecon (Bruker), the image stacks

were processed with ImageJ (Schindelin et al., 2012). Surface renderings of all specimens were generated using Drishti 2.6.5 (Limaye, 2012).

2.3 Scanning electron microscopy (SEM)

Specimens of *M. mirabilis* (from Pouldohan) were fixed with Bouin's fluid, those of *O. fusiformis*, *N. hombergii* and *G. fallax* with glutaraldehyde. In the case of *E. foliosa*, the same specimen that was used for µCT was examined. All specimens were dissected and then dehydrated in an ascending ethanol respectively acetone series. Afterwards, the samples were critically point dried with CO_2 (CPD 030, BAL-TEC) and placed on metal plates. Finally, they were coated with gold (SCD 005, BAL-TEC) and studied with a scanning electron microscope (SEM; FEI Verios 460L).

2.4 Azan-stained histology

The *M. mirabilis* specimen was fixed with Bouin's fluid and dehydrated via an ascending ethanol series, butanol-ethanol and butanol. Afterwards, the specimen was preincubated in Histoplast (Thermo Scientific) at 60°C. During the following three days, the medium was changed several times. Then, the specimen was embedded in Paraplast (McCormick Scientific) and serial transverse sections of 5 µm thickness were generated using a microtome (Autocut 2050, Reichert-Jung, Leica). After transferring the sections to albumen-glycerin-coated glass slides, they were stained with Azan.

2.5 Masson-Goldner's trichrome stained histology

The young *S. scutata* specimen from Banyuls-sur-Mer, fixed with Bouin's fluid, was dehydrated via an ethanol series and embedded in Malinol. Serial transverse sections of 10 µm thickness were produced using a microtome (Autocut 2050) and transferred to glass slides. The sections were stained with a Masson-Goldner's trichrome stain.

2.6 Semi-thin sections and transmission electron microscopy (TEM)

Specimens of *M. mirabilis* (from Pouldohan), *O. fusiformis*, *E. foliosa*, *N. hombergii* and *G. fallax* were dissected and fixed with glutaraldehyde with the addition of some ruthenium red. Then, postfixation was carried out for 30 min with 1% OsO_4 buffered in PBS at 4 °C, followed by dehydration in an ethanol series. Afterwards, the samples were embedded in araldite and serial semi-thin sections of 0.5-1.0 µm thickness were obtained using an ultramicrotome

(Ultracut S, Leica). The sections were placed on object slides and stained with toluidine blue. Ultra-thin sections of 70 nm were transferred to Formvar-covered, singer-slot copper grids and stained with 2% uranyl acetate and 2.6% lead citrate in an automated TEM stainer (QG-3100, Boeckeler Instruments). They were examined using a transmission electron microscope (TEM; EM 10CR, ZEISS) and recorded with phosphor imaging plates (Ditabis).

2.7 Confocal laser scanning microscopy (CLSM)

After fixation in paraformaldehyde, one specimen of *O. fusiformis*, *N. hombergii* and *G. fallax* each was stored in 0.1 M PBS containing 0.01% NaN_3. Single segments, separated from each other by dissection, were permeabilized in four 5-min changes of PBS with 0.1 % Triton X-100 (Fisher Scientific). The samples were stained overnight in 4 °C with TRITC phalloidin at a dilution of 1:100 and rinsed in several changes of PBS with 0.1 % Triton of up to 10 min and one 10 min rinse in pure PBS. After dehydration in an ascending series of isopropanol and clearing in three 15 min changes of Murray's Clear (BABB, benzyl alcohol, benzyl benzoate), the samples were investigated using the confocal laser scanning microscope system (CLSM; TCS SPE, Leica).

2.8 Energy Dispersive Spectrometry (EDS)

Specimens of *Euphrosine* sp., *Archinome levinae*, *Archinome jasoni*, *Chloeia euglochis* and *Hermodice carunculata* were either fixed in Formol or fixed and preserved in 95% ethanol. After transitioning bundles of chaetae or whole specimens to 100% ethanol followed by air-drying, the samples were placed on aluminium pin stubs and coated with carbon. The elemental composition was analysed using an FEI Quanta 600 SEM installed with an energy dispersive spectrometer at the University of California San Diego with a beam current of 15 kV.

2.9 Processing of data and modelling

All histological and semi-thin sections were studied and photographed using a microscope (BX-51, Olympus) equipped with a camera (CC12, Olympus) and a dot.slide 2.2 scanning system. Digitized serial histological and semi-thin sections were aligned using Imod (Kremer et al., 1996) and Imod align (https://www.q-terra.de/biowelt/3drekon/guides/imod_first_aid. pdf). Aligned image stacks were analysed and confocal Z-projections were obtained using ImageJ. Photographs have been processed with Affinity Photo 1.7 (Serif) and schematic drawings as well as figure plates have been prepared with Affinity Designer 1.7 (Serif). In order to

reconstruct the chaetal arrangement as a three-dimensional model, the aligned image stacks were analysed and certain sections marking the beginning and end of each chaeta were selected. Based on these sections, set into distances according to their respective position within the stack, cylindrical models were placed and oriented in the three-dimensional room simulating the arrangement of chaetae using 3ds-Max (Autodesk 3ds Max 2018).

2.10 Sample deposition

The samples and voucher specimens used for EDS analyses are deposited at the Scripps Institution of Oceanography Benthic Invertebrate Collection (SIO-BIC, see supplementary material Fig. A.1.2). All other specimens, samples or histological, semi-thin and ultra-thin sections are deposited at the Institute for Evolutionary Biology and Ecology of the University of Bonn. The reconstructed µCT datasets are accessible via the following links:

M. mirabilis: https://doi.org/10.5281/zenodo.5705611
O. fusiformis: https://doi.org/10.5281/zenodo.5222921
E. foliosa: https://doi.org/10.5281/zenodo.5205841
S. scutata: https://doi.org/10.5281/zenodo.6275179

Results 3

3.1 *Magelona mirabilis*

> Müller, J. & Bartolomaeus, T. (in Revision). Chaetal arrangement and type diversity in *Magelona mirabilis* (Magelonidae, Annelida) with ultrastructural details of the internal support chaetae. *Journal of Morphology*.

The appearance of Magelonidae is characterized by the shovel-shaped head with two long palps (Fig. 3.1.1A). The body is subdivided into an anterior thorax and a posterior abdomen (Fig 3.1.1A). Altogether, the thorax comprises ten segments, but the first segment after the peristomium lacks any chaetae (Fig. 3.1.1A). Therefore, chaetae-bearing thoracic segments are designated as chaetigers in the following. The first eight thoracic chaetigers are shaped uniformly with a medium length and barely visible separation (Fig. 3.1.1A). *In Magelona mirabilis*, the ninth chaetiger stands out by being distinctly shorter (Fig. 3.1.1A). The abdominal segments are approximately half as long as the first eight thoracic chaetigers (Fig. 3.1.1A). Along the trunk, segmentation is recognizable by serially arranged parapodia (Fig. 3.1.1A). All parapodia protrude slightly from the body surface and carry different types of chaetae (Fig. 3.1.1B). Noto- and neuropodia of each segment, however, show the same chaetal forms.

In the thorax, parapodia of the first eight chaetigers are oriented laterally and bear one transverse row of long, slender capillary chaetae per ramus (Fig. 3.1.1B, C). The parapodia of the ninth chaetiger are larger, with the notopodium pointing dorsally and the neuropodium ventrally (Fig. 3.1.1B). Here, far more chaetae than in the first eight chaetigers are present, forming a broader, staggered transverse row in each parapodial ramus (Fig. 3.1.1D). Chaetae in this segment are likewise long and slender, but, as opposed to the capillary chaetae of the first eight chaetigers, these mucronate chaetae terminate in a thickened, bulbous end (Fig. 3.1.1D, E). Towards the ventral end of the notopodium (and the dorsal end in the neuropodium), however, the chaetal tips are straight and slender, only characterized by some crinkled appearance (Fig. 3.1.1F). The notopodium of the ninth chaetiger examined via SEM, shows three newly formed chaetae dorsally, medially and ventrally along the posterior axis of the row (Fig. 3.1.1D). The dorsal and the medial new chaetae already show the bulb end, while the ventral one has a straight, crinkled tip equivalent to the fully-grown chaetae at this region.

In all investigated segments, noto- and neuropodium revealed corresponding results regarding chaetal type diversity as well as their number, arrangement and the position of the

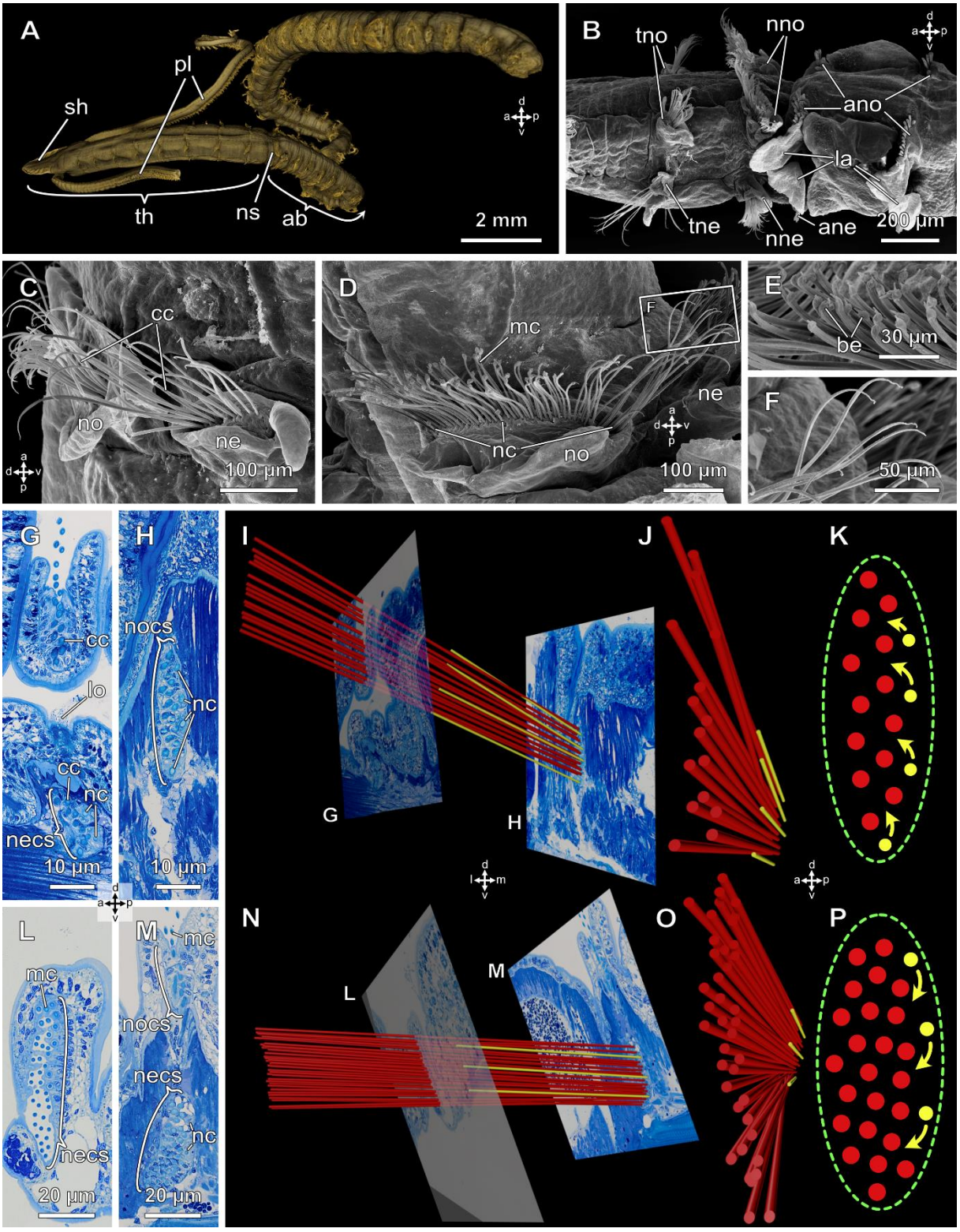

Fig. 3.1.1 Shape and arrangement of thoracic chaetae in *Magelona mirabilis*. **A** Surface rendering of a µCT-scan of a whole specimen showing the subdivision of the body into thorax and abdomen. The left palp has been dissected digitally to allow the view on all parapodia. **B** SEM showing the parapodia of the eighth and ninth thoracic chaetiger and the first two abdominal segments. **C** SEM of the thoracic noto- and neuropodium with transverse rows of capillary chaetae. **D** SEM notopodium of the ninth segment, bearing mucronate chaetae in a multi-layered row. (Continued on next page).

◄ Note the three newly formed chaetae at the posterior margin of the chaetal bundle. Rectangle marks section shown in F. (Continued on next page). **E** SEM close-up of several mucronate chaetae with specialized bulb tips. **F** SEM close-up of the tips of the ventral-most notopodial chaetae of the ninth chaetiger, lacking the specialized mucronate ending. **G & H** Transverse semi-thin sections through noto- and neuropodium of the eighth thoracic chaetiger at different levels. **I** 3D model of the arrangement of notopodial capillary chaetae. Chaetae are represented by coloured cylinders. Semi-thin sections from G and H are included for orientation. View from posterior. **J** Chaetal model from I shown from lateral. **K** Schematic drawing of the chaetal arrangement of the thoracic notopodial capillary chaetae. **L & M** Transverse semi-thin sections through noto- and neuropodium of the ninth thoracic chaetiger at different levels. **N** 3D model of the arrangement of neuropodial mucronate chaetae. Semi-thin sections from L and M are included for orientation. View from posterior. **O** Chaetal model from N shown from lateral. **P** Schematic drawing of the chaetal arrangement of the neuropodial mucronate chaetae. *ab* abdomen, *ane* abdominal neuropodium, *ano* abdominal notopodium, *be* bulbous ends, *cc* capillary chaetae, *la* lamellae, *lo* lateral organ, *mc* mucronate chaetae, *nc* newly formed chaetae, *ne* neuropodium, *necs* neuropodial chaetal sac, *nne* neuropodium of ninth chaetiger, *nno* notopodium of ninth chaetiger, *no* notopodium, *nocs* notopodial chaetal sac, *ns* ninth chaetiger, *pl* palps, *sh* shovel-shaped head, *th* thorax, *tne* thoracic neuropodium, *tno* thoracic notopodium, *a* anterior, *d* dorsal, *l* lateral, *m* medial, *p* posterior, *v* ventral, legend to schematic drawings: *green dashed line* chaetal sac, *red* fully grown chaetae, *yellow* new chaetae, *yellow arrow* movement of new chaetae during growth. Figure modified after Müller and Bartolomaeus (in revision).

formative sites. All thoracic chaetae arise from one single chaetal sac per parapodial ramus. More proximally, the chaetae of the first eight chaetigers are arranged in a doubled, staggered transverse row (Fig. 3.1.1G, H). Newly formed chaetae are located all along the ventro-posterior margin of that row in the notopodium and dorso-posteriorly in the neuropodium (Fig. 3.1.1G-J). The highest number of new chaetae found in the notopodium was four, and three in the neuropodium. Thus, several chaetae are formed simultaneously or shortly one after another as a row and move anteriorly during growth, being added to the more compact, staggered row of fully-grown chaetae (Fig. 3.1.1K). An equivalent arrangement pattern is present in the ninth chaetiger, but here the chaetal row is much broader, constituting almost a bundle of oval shape (Fig. 3.1.1L, M). The number and posterior position of newly formed chaetae and their movement during growth is comparable to the situation in the first eight chaetigers as well (Fig. 3.1.1M-P).

In contrast to the thorax, the abdominal parapodia bear transverse rows of tridentate, hooded hooks (Fig. 3.1.2A). The openings of the hoods point towards the large lamellae of the parapodia, which lie ventrally in the notopodium and dorsally in the neuropodium (Figs. 3.1.1A, 3.1.2A). The shortest hook is always closest to the lamella. The hooks are slightly curved like

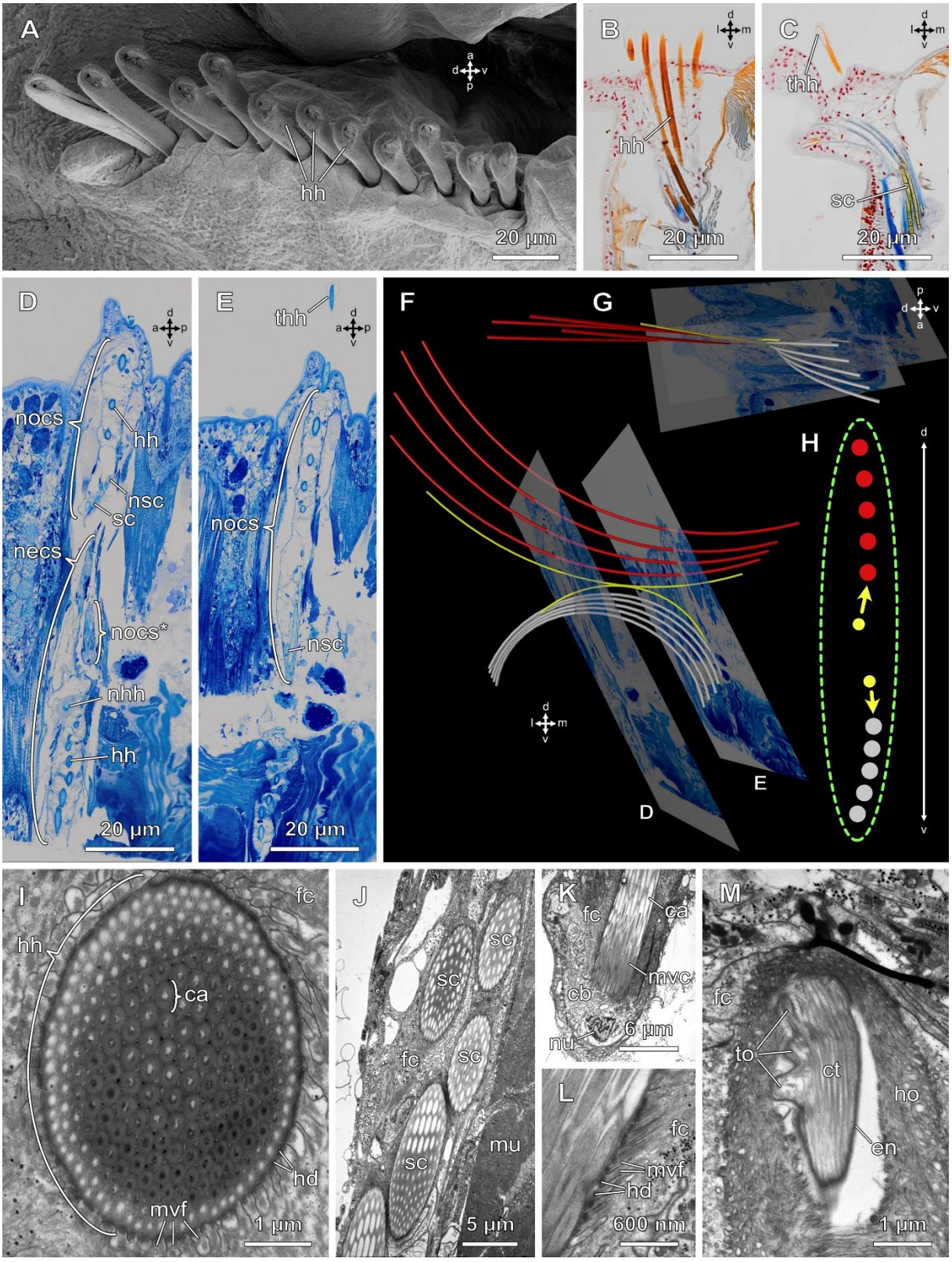

Fig. 3.1.2 Shape, arrangement and ultrastructure of abdominal chaetae in *Magelona mirabilis*. **A** SEM row of hooded hooks in an abdominal notopodium. The openings of the hoods face ventrally. **B** Azan stained histological transverse section through a notopodium of an abdominal segment showing hooded hooks and (**C**) internal support chaetae. **D & E** Transverse semi-thin sections through noto- and neuropodium of the first abdominal segment at different levels. (Continued on next page).

◄ **F** 3D model showing the arrangement of abdominal notochaetae. Chaetae are represented by coloured arcs. Semi-thin sections from D and E are included for orientation. View from posterior. **G** Chaetal model shown from lateral. **H** Schematic drawing of the chaetal arrangement of the abdominal notochaetae. **I** TEM transverse section through the basal part of a newly formed hooded hook surrounded by a follicle cell, which is closely attached to the chaeta via hemidesmosomes at the end of its microvilli. **J** Several obliquely sectioned support chaetae. **K** Basal part of the follicle of a support chaeta, showing the chaetoblast's microvilli reaching into the chaetal canals. **L** Detailed view on the border between follicle cell and support chaeta. The follicle cell's microvilli are attached to the chaeta via hemidesmosomes. **M** Apical part of a support chaeta with hood and equipped with three teeth. *ca* canal, *cb* chaetoblast, *ct* chaetal tip, *en* enamel, *fc* follicle cell, *fo* follicle, *hd* hemidesmosome, *hh* hooded hook, *ho* hood, *mu* muscle, *mvc* microvilli of chaetoblast, *mvf* microvilli of follicle cell containing intermediate filaments, *necs* neuropodial chaetal sac, *nhh* newly formed hooded hook, *nocs* notopodial chaetal sac, *nocs** second cut through the notochaetal sac due to its arcuate shape, *nsc* newly formed support chaeta, *nu* nucleus, *sc* support chaeta, *thh* tip of hook with offset hood, *to* tooth, *a* anterior, *d* dorsal, *l* lateral, *m* medial, *p* posterior, *v* ventral, legend to schematic drawings: *green dashed line* chaetal sac, *red* fully grown hooded hooks, *grey* fully grown support chaetae, *yellow* new chaetae, *yellow arrow* movement of new chaetae during growth. Figure modified after Müller and Bartolomaeus (in revision).

arcs with their bases reaching deep into the tissue (Fig. 3.1.2B). In histological sections, the hood appears as a thin, transparent structure, surrounding the narrow tip of the intensely coloured chaetal core (Fig. 3.1.2B, C). Besides the externally visible hooks, all abdominal segments contain more delicate, lighter coloured chaetae, which are embedded within the tissue and do not protrude externally (Fig. 3.1.2C). With their tips, they reach into the respective lamella of the parapodial ramus, acting as supportive structure. Because these chaetae are curved as well, but bent away from the hooks, the bases of both chaetal types are located at different positions within the tissue (Fig. 3.1.2D-F). Nonetheless, all chaetae of each parapodial ramus originate from a single chaetal sac (Fig. 3.1.2D, E). Hooks as well as support chaetae form a transverse row with corresponding numbers of 6-8 chaetae. Newly formed chaetae of both chaetal types are found most centrally in the chaetal sac and, thus, closest to the respective other type (Fig. 3.1.2D-G). Therefore, new chaetae are most probably formed simultaneously for each chaetal type. During growth, they shift dorsally in the case of notopodial hooks, while respective support chaetae move ventrally (Fig. 3.1.2H). In the neuropodium, it is the other way around.

The ultrastructure of both hooks and support chaetae is characterized by a typical honeycomb-like pattern, consisting of numerous evenly sized round canals forming a circular framework (Fig. 3.1.2I, J). Basally, these canals are filled by the chaetoblast's microvilli, which leads to their hollow nature more distally (Fig. 3.1.2K). At the proximal region, both chaetal

types lack some coating enamel layer, but are connected to microvilli of the follicle cells directly via hemidesmosomes (Fig. 3.1.2I, L). The tips of the support chaetae are characterized by three distinct teeth and here the canal framework is covered by an electron dense enamel layer (Fig. 3.1.2M). Some amorphous chitinous mass, lacking the typical hollow canals, surrounds this apical part and is connected to the follicle cells. This mass is equivalent to the hood of the externally visible hooks.

3.2 *Owenia fusiformis*

Müller, J., Bartolomaeus, T., & Tilic, E. (2022). Formation and degeneration of scaled capillary notochaetae in *Owenia fusiformis* Delle Chiaje, 1844 (Oweniidae, Annelida). *Zoomorphology*, *141*(1), 43-56. https://doi.org/10.1007/s00435-021-00547-z.

The thorax of *Owenia fusiformis* bears three pairs of laterally arranged bundles of capillary chaetae (Fig. 3.2.1A). The abdominal segments are long and uniform with only the anterior edges carrying chaetae (Fig. 3.2.1A). Here, almost the entire circumference of each segment is covered by patches of uncini so that notochaetae are only found at the very dorsal part (Fig. 3.2.1A, B). Noto- as well as neurochaetae emerge directly from the body wall without any kind of parapodial protrusion (Fig. 3.2.1A, B). The notopodia bear long and slender capillary chaetae, which are arranged in a compact, dorsally oriented and spirally twisted bundle of 40-60 chaetae each (Fig. 3.2.1B).

All chaetae in these bundles are formed within one single chaetal sac. Immunohistochemical approaches indicate ongoing formation processes of new chaetae by an increased phalloidin signal caused by the highly active f-actin in the chaetoblast's microvilli (Fig. 3.2.1C). Moreover, the bases of new chaetae are located more apically in the chaetal sac than those of fully-grown chaetae and their tips do not pierce the cuticle yet (Fig. 3.2.1C, G). All investigated notopodial chaetal sacs show newly formed chaetae of differing numbers from 0-7 in the periphery of the bundles (Fig. 3.2.1C-G). The exact positions of these new chaetae within the bundles' periphery are variable and topologically unspecific. Number and positions of new chaetae are independent from the size of the chaetal sacs and the segment's position within the animal. In contrast to formation processes, degenerating chaetae are found more centrally in the chaetal bundles (Fig. 3.2.1F, G). Even though the notopodial bundles lack a definite formative site, the relative positions of newly formed and degenerated chaetae indicate that chaetae are formed in one curled up row (Fig. 3.2.1H). New chaetae push older ones towards the centre of the bundle along this row, where they degenerate.

Regarding their shape, the notochaetae of *O. fusiformis* are subdivided into a distal part, which is densely covered by scales, and a proximal part with an almost smooth surface, only characterized by slight longitudinal grooves (Fig. 3.2.2A). Each scale emerges from the ridge between two of these grooves (Fig. 3.2.2A). The blade-shaped scales are approximately 2-3 µm long and 1 µm wide and arise spirally around the chaeta, being oriented distally (Fig. 3.2.2B). Along the scaled part, the diameter of the chaeta decreases constantly (Fig. 3.2.2A). The interior

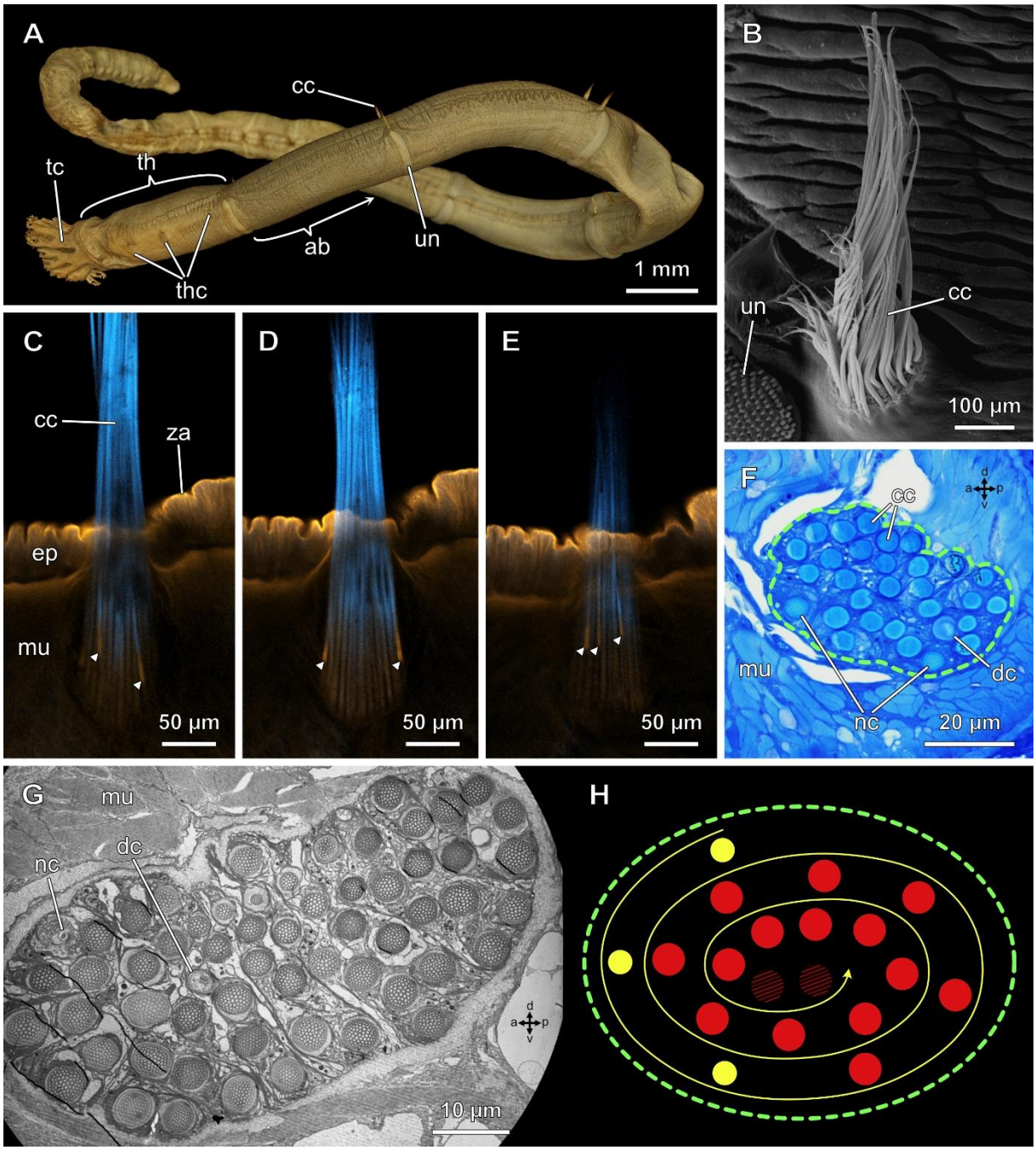

Figure 3.2.1 Arrangement of capillary chaetae in *Owenia fusiformis*. **A** µCT-based 3D rendering of *O. fusiformis*, showing the distinct body parts and indicating the positions of the respective chaetae. **B** SEM bundle of notopodial capillary chaetae with a spiral twist. **C-E** Immunohistochemistry. Longitudinal sections through a phalloidin-stained bundle of capillary chaetae, each showing newly formed chaetae. **F** Semi-thin, toluidine blue stained transverse section through a notopodial bundle with two newly formed chaetae in the periphery and one degeneration process. **G** TEM transverse section through a notopodial bundle with one young and one degenerating chaeta. **H** Schematic drawing illustrating the chaetal arrangement in the notopodium. *ab* abdomen, *cc* capillary chaeta, *dc* degenerating chaeta, *ep* epidermis, *mu* musculature, *nc* newly formed chaeta, *tc* tentacle crown, *th* thorax, *thc* thoracic chaetae, *un* uncini, *za* zonula adhaerens, *a* anterior, *d* dorsal, *p* posterior, *v* ventral, *arrowheads* chaetal formation processes, legend to schematic drawings: *green dashed line* chaetal sac, *red* capillary chaetae, (Continued on next page)

◄ *shaded red* degenerating chaetae, *yellow* new chaetae, *yellow arrow* movement of new chaetae during growth. Figure modified after Müller et al. (2022).

of the scales is dominated by a cavity without an apical pore, which proceeds proximally as part of the chaetal meshwork (Fig. 3.2.2C). The formation process, which leads to this subdivision into a scaled and smooth part, can be comprehended by analysing the chaetogenesis. Early during the chaetogenetic process, new microvilli are generated in successive order radially at the outer margin of the chaetoblast's microvilli brush border (Fig. 3.2.2D-F). That way, more and more constantly growing, hollow canals are added to the chaetal meshwork with lengths decreasing from the centre of the chaeta to its periphery. This procedure results in the cone-like tip of the chaetae (Fig. 3.2.2A).

At the distal part of a chaeta, which did not pierce the cuticle yet, flat canals are attached to the chaeta's periphery (Fig. 3.2.2G-I). A few micrometres more distally, the tips of the outermost canals lose contact to the chaeta (Fig. 3.2.2H). With their size decreasing rapidly, the canals approach the surrounding follicle cell, which eventually envelops the very end of the tips (Fig. 3.2.2I). This process continues radially with every canal. These terminal ends of chaetal canals are equivalent to one scale each, which explains their exteriorly visible spiral pattern.

At some point during chaetogenesis, the chaetoblast stops adding further peripheral microvilli, which marks the transition point from the scaled part to the smooth one. Regarding the ultrastructure, the smooth part is characterized by a circular arrangement of evenly sized, round canals with chitinous lamellae of uniform thickness (Fig. 3.2.2J). Due to the round aspect of the canals, the periphery of the chaeta is slightly undulated, which corresponds to the longitudinal grooves visible in the SEM images (Fig. 3.2.2A, J). The follicle cells surround the chaeta closely, following its shape precisely (Fig. 3.2.2J). Neither at the scaled part, nor at the smooth one, any chitinous enamel layer coats the chaetal surface (Fig. 3.2.2G-I, J).

Ultrastructural data provide insights into the degeneration process of the capillary chaetae in *O. fusiformis* (Fig. 3.2.2K). Each chaeta is degenerated from proximal to distal so that it becomes shorter and the distance of its bases to the cuticle decreases constantly. The spot of the chaeta, which is undergoing degeneration is characterized by an extraordinarily thin, hexagonal chitinous framework, which is partially dissolved, especially at the periphery (Fig. 3.2.2K). The follicular space is widened and filled with some amorphous mass. Protrusions of the subjacent cell, which contains lysosomes fill out some of the chaetal canals (Fig. 3.2.2K). This cell probably constitutes the former chaetoblast of the degenerated chaeta.

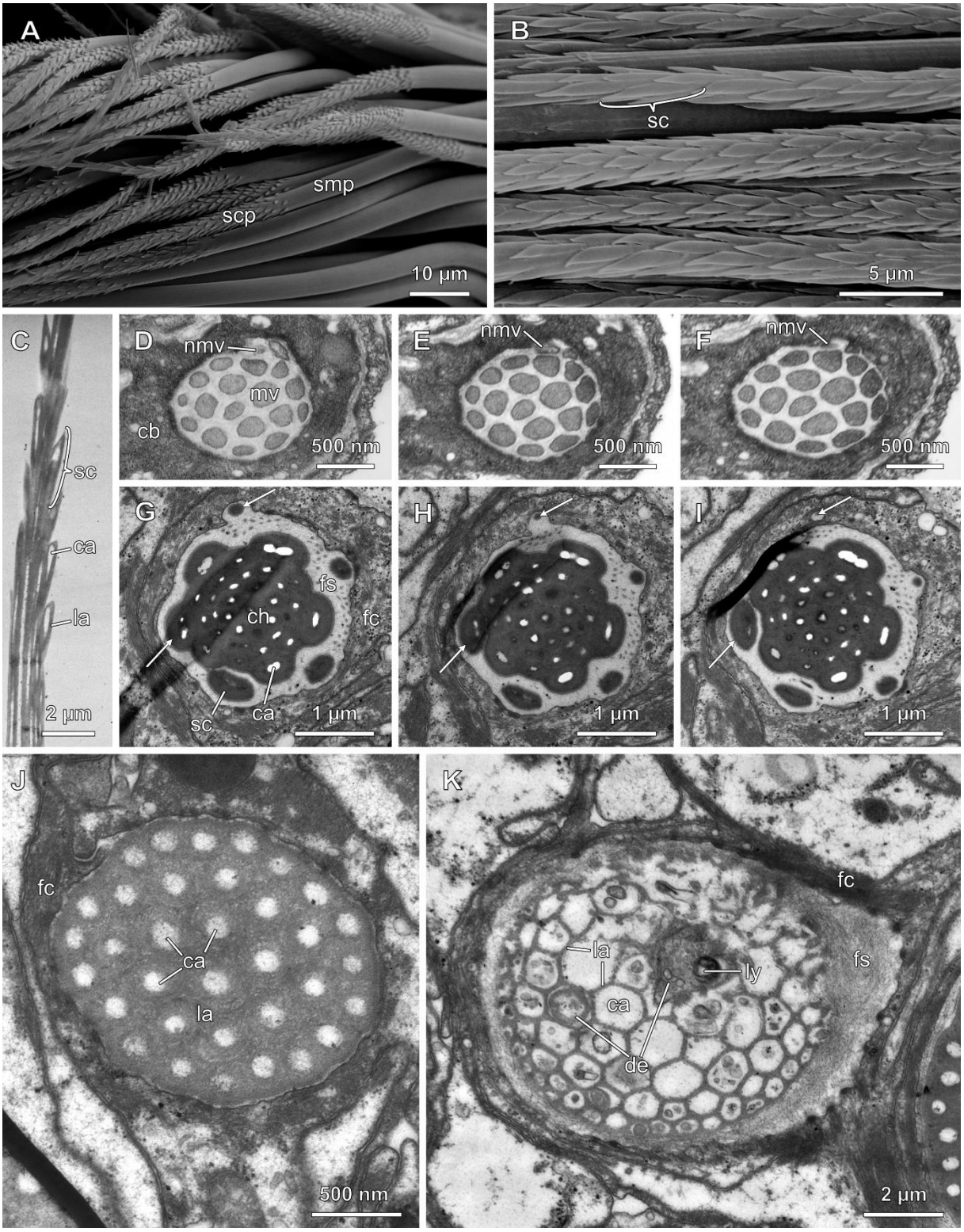

Figure 3.2.2 Shape and ultrastructure of capillary chaetae in *Owenia fusiformis*. **A** SEM notopodial chaetae with focus on the transition between smooth and scaled part, which is located at the same respective length of each chaeta. Note the slight grooves in the surface of the smooth part, with each ridge culminating in one scale. **B** Close-up of the scaled part of several chaetae, highlighting the blade-like shape of the scales. **C** TEM longitudinal section through the scaled part of a capillary chaeta, highlighting the hollow character of the scales. **D-F** TEM sections through a microvilli brush border of a growing chaetoblast at three different levels 0.5 µm apart from each other. (Continued on next page).

◄ Note the addition of a new microvillus in the periphery, which is significantly shorter than the others. **G-I** TEM Transverse sections of the scaled part of a chaeta within the follicle at three different levels 0.5 µm apart from each other. The scales are wrapped by the follicle cell at their tips. **J** TEM Transverse section through the smooth part of a capillary chaeta with thick chitinous lamellae and equally sized canals. The follicle cell closely envelops the chaeta. **K** TEM detailed view on the degeneration process of a capillary chaeta. Note the wide follicular space and the thin chitinous lamellae. The degenerating cell, which is filled with lysosomes, protrudes into the canals and breaks through the dissolving chaetal meshwork. *ca* canal, *cb* chaetoblast, *ch* chaeta, *de* degenerating cell, *fc* follicle cell, *fs* follicular space, *la* lamellae, *ly* lysosome, *mv* microvillus, *nmv* new microvillus, *sc* scale, *scp* scaled part, *smp* smooth part, *arrows* marking the same two scales in all images to comprehend the interaction between follicle cell and scales of the chaeta. Figure modified after Müller et al. (2022).

3.3 *Euphrosine foliosa* & *Euphrosine* sp.

Müller, J., Schumacher, A., Borda, E., Rouse, G. W., Bartolomaeus, T., & Tilic, E. (2021). "Brittleworms": Ultrastructure and arrangement of the calcified chaetae of *Euphrosine* (Amphinomida, Annelida). *Invertebrate Biology*, *140*(4), e12353. https://doi.org/10.1111/ivb.12353.

Euphrosine foliosa is a uniformly segmented annelid with a convex dorsal and a flat ventral side (Fig. 3.3.1A). Segments are short and each parapodial ramus bears one large bundle of long capillary chaetae (Fig. 3.3.1A, B). The parapodia do not protrude from the body surface. (Fig. 3.3.1B). Neurochaetae are oriented laterally, while notochaetae point dorsally so that almost the entire exposed surface of the animal is covered with chaetae (Fig. 3.3.1A, B). Additionally, segments bear long cirri and branched gills. Besides capillary chaetae, both parapodial rami bear several aciculae, which pierce the cuticle (Fig. 3.3.1C, D).

All chaetae of each ramus arise from a single chaetal sac, containing numerous chaetae, which are arranged in a grid-like, crescent-shaped bundle (Fig. 3.3.1C, D). These bundles consist of several transverse arc-shaped rows with their convex side oriented anteriorly (Fig. 3.3.1H). In the notopodium, the posteriormost row comprises all aciculae of the chaetal sac, while in the neuropodium they form the anterior row (Fig. 3.3.1C, D, F-H). In both cases, the bases of the aciculae are located much deeper within the tissue than those of the capillary chaetae (Fig. 3.3.1E). In return, they pierce the cuticle only with their very tip. The notopodia contain an average of 9 aciculae, while the neuropodia bear 12 of them. Regarding the capillary chaetae, the neuropodia carry notably more chaetae as well. Newly formed chaetae can be found at the dorsal end of the transverse rows in both parapodial rami (Fig. 3.3.1F, G). Each row, including that of the aciculae, is therefore simultaneously elongated by one new chaeta (Fig. 3.3.1H). Due to the crescent shape of the bundle, the new chaetae extend ventrally along the posterior side of the sac (Fig. 3.3.1D, H).

Two different types of capillary chaetae can be distinguished in *E. foliosa*. The neuropodium bears bifurcate chaetae with two straight prongs (Fig. 3.3.2A). In these chaetae, the larger prong is approximately 4 times longer than the shorter one. The aciculae of both parapodial rami terminate in an equivalent bifurcation. In addition to chaetae with this straight bifurcation, the notopodium shows specialized bifurcate chaetae with curved prongs (Fig.

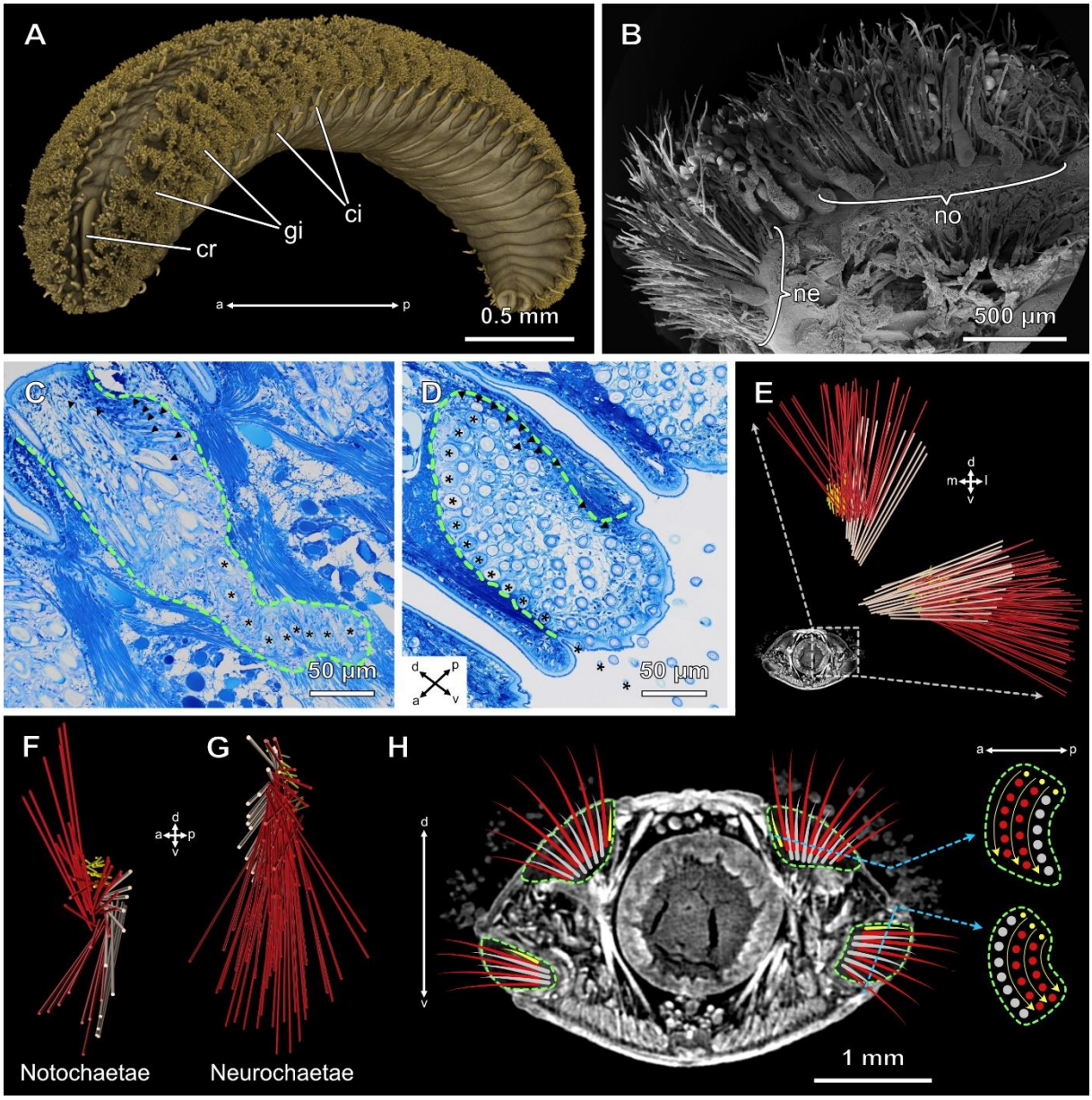

Figure 3.3.1 Chaetal arrangement in *Euphrosine foliosa*. **A** Surface rendering of a µCT scan of a whole specimen. **B** SEM cross-sectional view of the left half of a segment from posterior. **C** Sagittal semithin section of the notopodium. **D** Sagittal semithin section of the neuropodium. **E** 3D model of all chaetae of one parapodium, with a µCT cross section of the animal for orientation. Chaetae are represented by coloured cylinders. View from anterior. **F**, **G** Distal views of notopodial (F) and neuropodial 3D models (G). With shared orientation plane. **H** A µCT transverse section, with schematic drawings of the chaetae within the chaetal sacs and transverse-sectional schemes of one notopodial and one neuropodial chaetal sac. *ci* cirri, *cr* caruncle, *gi* gills, *ne* neuropodium, *no* notopodium, *a* anterior, *d* dorsal, *l* lateral, *m* medial, *p* posterior, *v* ventral, orientation plane from D valid for C, *arrowheads* newly formed chaetae, *asterisks* aciculae, legend to schematic drawings and models: *green dashed line* chaetal sac, *red* capillary chaetae, *grey* aciculae, *yellow* new chaetae, *yellow arrows* movement of new chaetae during growth, *blue dashed arrows* position of the schematic transverse sections. Figure modified after Müller et al. (2021).

3.3.2B). Here, the longer prong measures 2 times the length of the shorter one and their oppositely lying sides are characterized by numerous transverse ridges. Both chaetal types are covered by some additional brittle, mantle-like layer, which partially flakes off the chaetal core (Fig. 3.3.2A, B). Before newly formed curved bifurcate chaetae pierce the cuticle, these ridges are mirrored by the follicle cells but not yet present on the chaetae themselves (Fig. 3.3.2C).

All different types of chaetae in *E. foliosa* are characterized by a large, inner cavity, measuring approximately half of the chaeta's diameter and even extending into their prongs (Fig. 3.3.2C, D). This cavity lacks an apical as well as a basal pore (Fig. 3.3.2D). It is filled with some amorphous, coarse-grained substance and demarcated from the chaetal material by an electron-dense, thin layer (Fig. 3.3.2D, E). The ultrastructure of the chaetae is defined by the typical hollow canals, which are largest close to the cavity and decrease in size towards the chaeta's periphery (Fig. 3.3.2E). The outermost part of the chaeta consists of a dense chitinous mass, the enamel, which lacks any canals. This enamel is overlain by an additional, thin enamel layer of a differing electron density, which remains undamaged even in a disrupted follicle (Fig. 3.3.2E). This additional layer probably contains calcium, since it disappeared under acidic conditions.

The chaetoblast’s microvilli brush border constitutes a compact, circular pattern without any gaps between the evenly sized microvilli (Fig. 3.3.2F). This is represented in ultrastructural transverse sections of some chaetae, which do not show a fully pronounced cavity, but a more or less complete canal pattern in its centre (Fig. 3.3.2G). This chitinous framework, however, is characterized by a brittle and partially damaged nature, especially towards the chaeta’s centre, where the lamellae are thinnest (Fig. 3.3.2G). These chaetae’s enamel is surrounded by an additional narrow enamel layer as well, which is connected to the follicle cells via hemidesmosomes (Fig. 3.3.2.G).

An energy-dispersive X-ray spectrometry (EDS) of a chaetal shaft of *Euphrosine* sp. showed exceptionally high levels of calcium, carbon and oxygen as well as increased amounts of magnesium and phosphorus (Fig. 3.3.2H). Similar results have been obtained by analysing chaetae of other amphinomidan taxa (see supplementary material Fig. A.1.2).

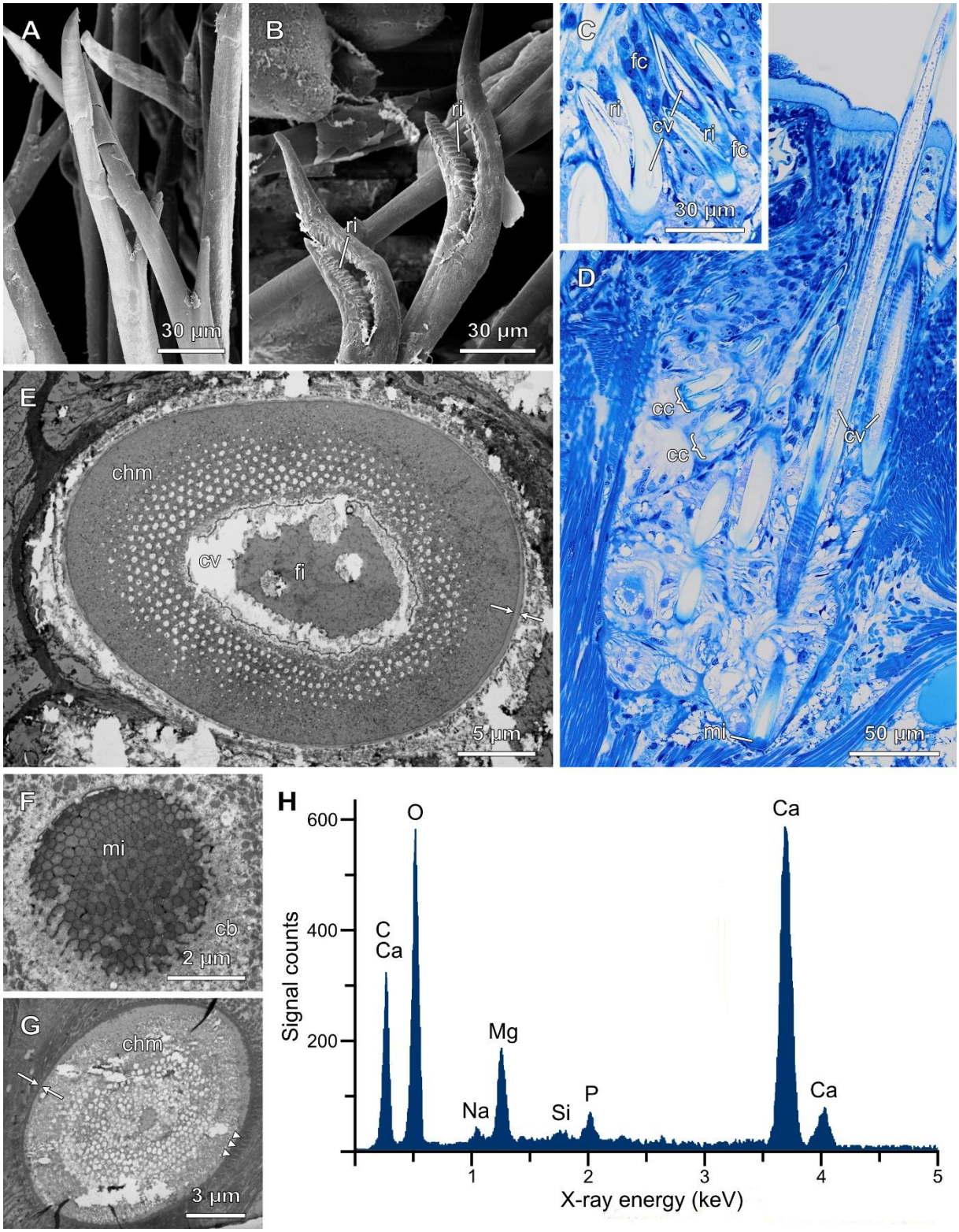

Figure 3.3.2 Details on chaetae of *Euphrosine foliosa* and an EDS-analysis of *Euphrosine* sp. **A** SEM close-up of the tips of bifurcate capillary chaetae, which are present in both parapodial rami. **B** SEM close-up of the tips of curved bifurcate chaetae, only found in the notopodium. Note the ridges on the prongs. **C** Semithin section showing curved bifurcate chaetae within the tissue, with the ridges being formed by the follicle cells. **D** Semithin section through a notopodium with longitudinally cut chaetae, with a cavity inside filled with some coarse-grained substance. (Continued on next page).

◄ Note the chaetal base at the lower edge of the section with a dense stria of microvilli reaching into the chaeta. **E** TEM cross section of a capillary chaeta with cavity, which is filled with an electron-dense substance. Arrows indicate external layer enveloping the chaetae. **F** TEM stria of microvilli of a chaetoblast. **G** TEM cross section through a chaeta showing a clear difference in the thickness of the canals in the inner and outer part, but missing any cavity. **H** EDS results of a chaetal shaft (carbon coated) of *Euphrosine* sp. The left-most peak combines signals from carbon and calcium. *cb* chaetoblast, *cc* capillary chaeta, *chm* chaetal material, *cv* cavity, *fc* follicle cell, *fi* filling, *mi* microvilli, *ml* mantle-like layer, *ri* ridges, *arrows* external layer enveloping the chaetae, *arrowheads* hemidesmosomes connecting chaeta and follicle cell. Figure modified after Müller et al. (2021).

Unpublished results 4

4.1 *Sternaspis scutata*

Sternaspis scutata has a peculiar appearance, characterized by a short and thick body subdivided into three parts and lacking any serially arranged parapodia (Fig. 4.1.1A). The anterior introvert is composed of the indistinct prostomium and peristomium as well as three segments bearing one transverse row of large, spine-like chaetae on each side (Fig. 4.1.1A, B). These chaetae decrease in size towards the ventral end of the rows (Fig. 4.1.1B). The following trunk represents the largest part of the animal, bearing one pair of genital papillae, but lacking any recognizable chaetae (Fig. 4.1.1A). The posterior region is characterized by the most prominent structure of the animals, a flat, hardened ventro-caudal shield (Fig. 4.1.1A, C). This nearly rectangular shield is framed by small fascicles of slender capillary chaetae protruding laterally and posteriorly (Fig. 4.1.1C). On each edge of the posterior margin of the shield, one horn-like peg chaeta can be found, which are shorter, but much broader than the surrounding capillary chaetae (Fig. 4.1.1C).

In the introvert, all spine-like chaetae of one row are formed in one chaetal sac with a dorsally located formative site (Fig. 4.1.1D). Thus, the smaller ventral chaetae are the oldest in each row, which means that the size of new chaetae increases during growth of the animal. Regarding the shield chaetae, all chaetae of one fascicle are formed within a single chaetal sac (Fig. 4.1.1E). They are arranged in an alternating pattern of 3-4 larger and 3-4 smaller chaetae, both of which decrease in size towards the ventral end of the sac (Fig. 4.1.1E). New chaetae of both magnitudes within these fascicles are formed simultaneously at the dorsal end of the chaetal sac (Fig. 4.1.1E). Histological sections reveal that the peg chaetae are not large, singular chaetae like the spine-like chaetae, but actually consist of numerous thin and short capillary chaetae (Fig. 4.1.1F). These chaetae do not ultimately pierce the body surface, but stay embedded in and wrapped by cuticular material as a densely packed bundle, resulting in their appearance as a singular structure. This bundle is composed of six distinct rows of 5-6 capillary chaetae, which belong to a separate chaetal sac each (Fig. 4.1.1G & H). These chaetal sacs respectively possess a dorsal formative site (Fig. 4.1.1I).

4.2 *Nephtys hombergii*

Nephtys hombergii has large parapodia with separated noto- and neuropodial protrusions, covering the whole lateral surface of the animal (Fig, 4.2.1A). The notopodium can be identified

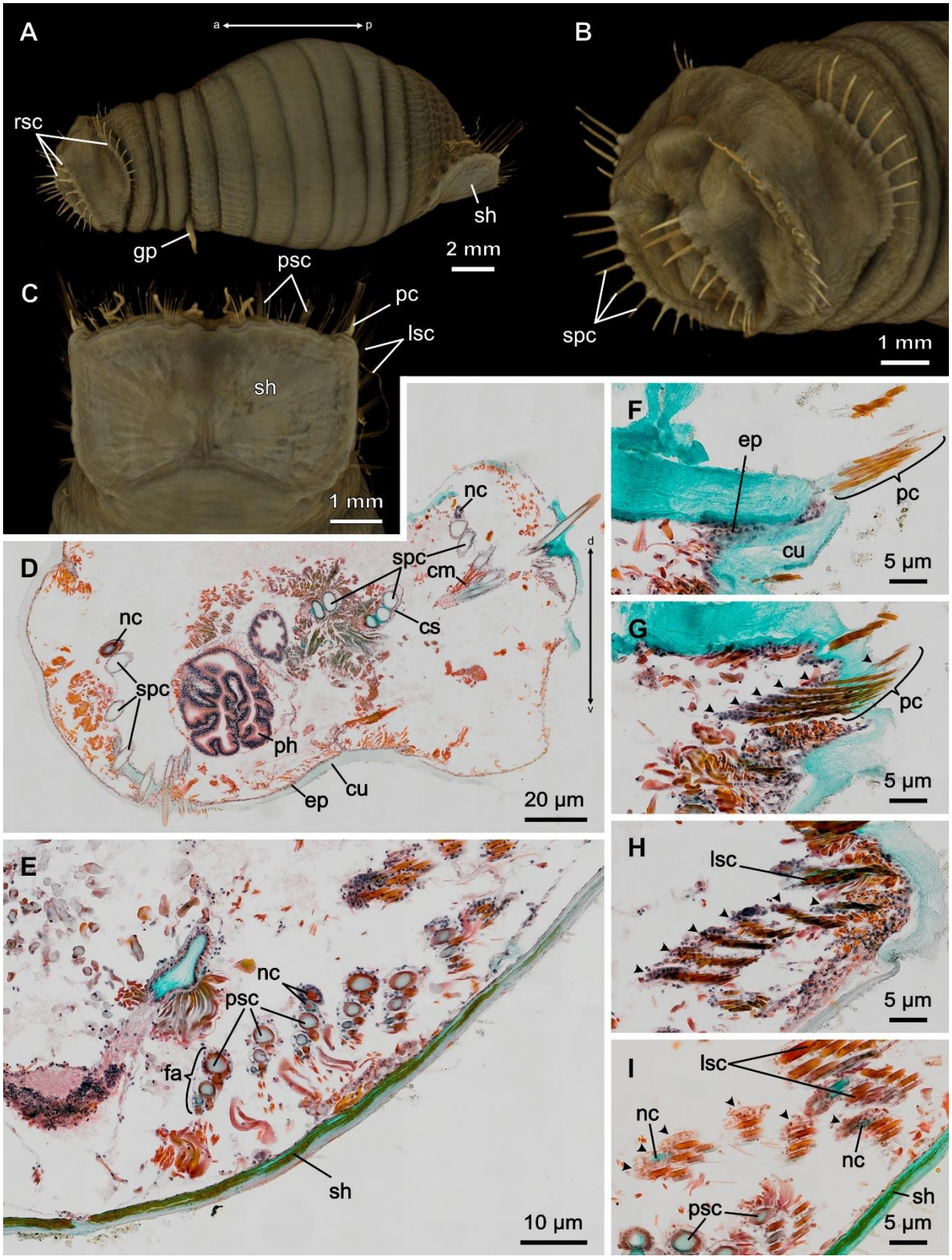

Fig. 4.1.1 Chaetal arrangement and details on peg chaetae of *Sternaspis scutata*. **A** Surface rendering of a µCT scan of the whole animal from a lateral view. **B** Detailed view of the anterior part of the animal with the three transverse rows of large spine-like chaetae. **C** Ventral view of the posterior part with the cuticular shield framed by lateral and posterior fascicles of capillary chaetae. Both posterior edges of the shield bear a single cone-shaped peg chaeta. (Continued on next page).

◄ **D** Transverse section through the anterior part, including all chaetae of one of the left rows and parts of all three right rows. Newly formed chaetae are found at the dorsal end of two rows. **E** Transverse section through the shield region with several fascicles of posterior shield chaetae with likewise dorsally located formative sites. Note the greenish shield embedded in the cuticle. **F-I** Transverse sections through a peg chaeta at different levels. **F** Peg chaeta consisting of numerous capillary chaetae being wrapped by cuticular material. **G** The capillary chaetae are arranged in six distinct rows. **H** Every row is formed within its own chaetal sac. **I** Each chaetal sac has one dorsally located formative site. *cm* chaetal musculature, *cs* chaetal sac, *cu* cuticle, *ep* epidermis, *fa* fascicle, *gp* genital papilla, *lsc* lateral shield chaetae, *nc* newly formed chaetae, *pc* peg chaetae, *ph* pharynx, *psc* posterior shield chaetae, *rsc* row of spine-like chaetae, *sh* shield, *spc* spine-like chaetae, *a* anterior, *d* dorsal, *p* posterior, *v* ventral, *arrow heads* distinct rows of capillary chaetae forming a peg chaeta, coordinate arrow of D valid for E-I.

by the presence of a cirrus, while the neuropodium carries a lamella (Fig. 4.2.1A). Notopodia as well as neuropodia bear two distinct transverse rows of capillary chaetae with the anterior row consisting of far less chaetae than the posterior one (Fig. 4.2.1A).

Both parapodial rami are equipped with one massive acicula each with a much wider diameter than the capillary chaetae and a stout ending (Fig. 4.2.1B). These aciculae are large enough to observe their composition of large canals in the centre and thicker chitinous lamellae in its periphery plus an outer enamel layer even via light microscopy (Fig. 4.2.1D). The bases of the aciculae are located much more proximally than those of the capillary chaetae and attached to a strong muscular system. Their follicles are apically open and connected to the outer medium with the tip of the notopodial acicula even piercing the cuticle (Fig. 4.2.1B).

Transverse sections through parapodia show that all chaetae of each parapodial ramus including the aciculae are formed within one chaetal sac, but two spatially separated groups of capillary chaetae can be distinguished within this sac respectively. In the neuropodium, a smaller group is located dorsally and a larger one ventrally to the acicula (Fig. 4.2.1C, D). In the notopodium, the small group lies ventrally and the large one dorsally (Fig. 4.2.1E). The small group is arranged as a simple row, while the large one constitutes a bundle formed by multiple rows (Fig. 4.2.1C-E). Due to a spiral twist of the chaetal sac, the smaller chaetal groups turn out as the anteriorly located small rows, which are exteriorly visible. Correspondingly, the large groups represent the posterior rows when piercing the cuticle. One to three newly formed chaetae are found in the distal region of each chaetal group in both parapodial rami (Fig. 4.2.1C-E). Thus, new chaetae are added simultaneously to both chaetal groups in each chaetal sac and shift closer to the acicula during growth.

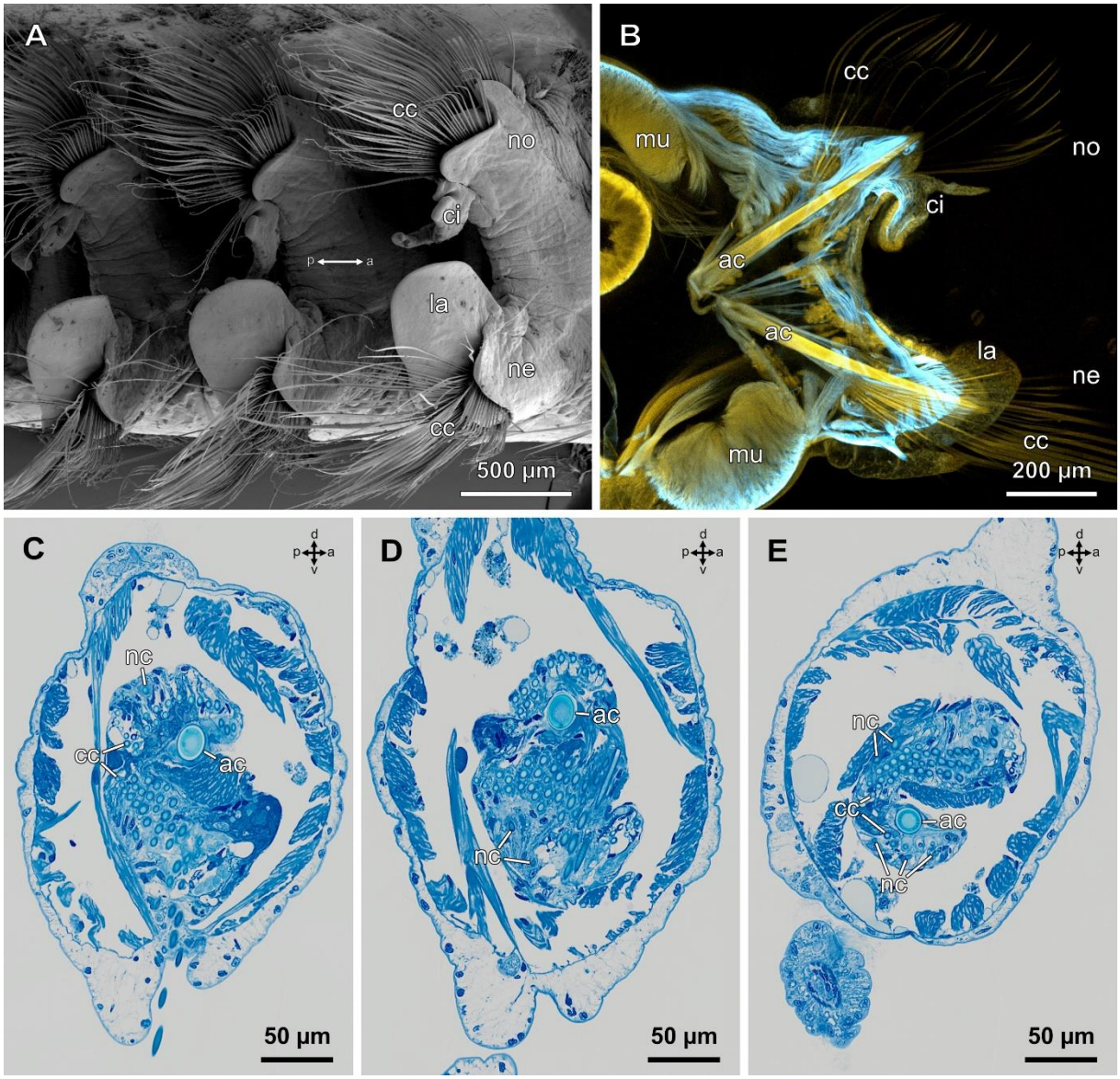

Fig. 4.2.1 *Nephtys hombergii*. **A** SEM showing three parapodia with each ramus carrying one large and one small row of long, slender capillary chaetae. **B** Confocal z-projection of a phalloidin-stained parapodium. **C-E** Semi-thin toluidine blue stained sections through a neuropodium (C-D) and a notopodium (E). *ac* acicula, *cc* capillary chaetae, *ci* cirrus, *la* lamella, *mu* musculature, *nc* newly formed chaeta, *ne* neuropodium, *no* notopodium, *a* anterior, *d* dorsal, *p* posterior, *v* ventral.

4.3 *Glycera fallax*

Parapodia of *Glycera fallax* are relatively small and indistinct. They constitute short, flat protrusions, folding around a few chaetae (Fig. 4.3.1A). Noto- and neuropodium are fused together forming one protrusion, but both are distinguishable by each carrying one large bulge. Both parapodial rami bear two spatially separated rows of chaetae (Fig. 4.3.1A). In both cases,

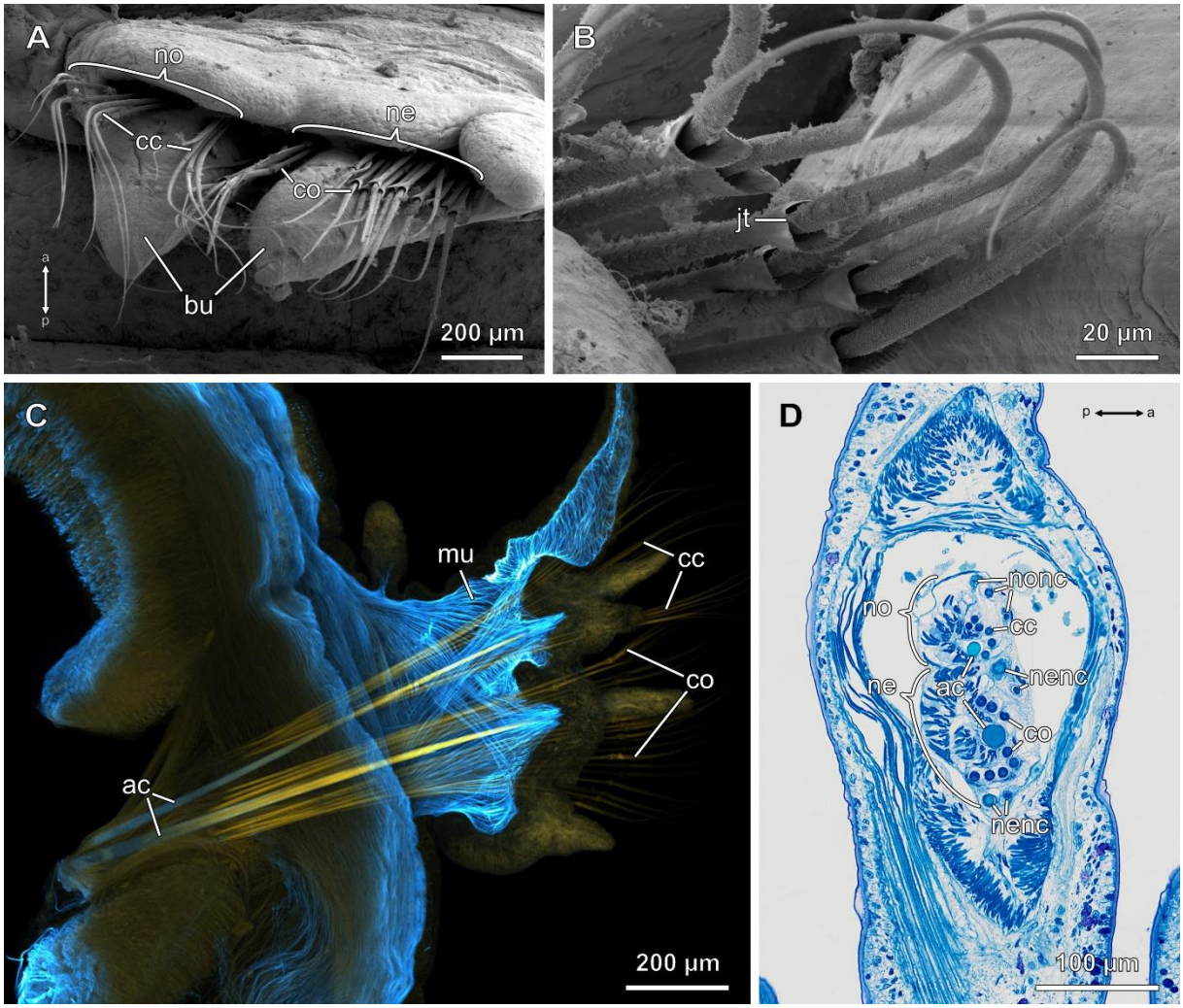

Fig. 4.3.1 *Glycera fallax*. **A** SEM of one parapodium. **B** SEM close-up of several compound chaetae with joints. **C** Confocal z-projection of a phalloidin-stained parapodium. **D** Semi-thin toluidine blue stained section through a parapodium. *ac* acicula, *bu* bulge, *cc* capillary chaetae, *co* compound chaetae, *jt* joint, *mu* musculature, *ne* neuropodium, *nenc* newly formed neurochaetae, *no* notopodium, *nonc* newly formed notochaetae, *a* anterior, *p* posterior.

the smaller row lies closest to the respective other parapodial ramus. While the notopodium bears capillary chaetae, the neuropodium carries compound chaetae (Fig. 4.3.1A). The joint of these compound chaetae is characterized by a widened, serrated margin, marking the transition point from a proximal part with a smooth surface to a distal part, which is densely covered by numerous tiny nodules, creating a rough surface (Fig. 4.3.1B).

Besides capillary or compound chaetae, each parapodial ramus is equipped with one large acicula, which lies between both chaetal rows of the respective ramus (Fig. 4.3.1C). The bases of these aciculae are located much deeper within the tissue than those of the other chaetae (Fig. 4.3.1C). Distally, the aciculae reach into the bulges, but do not pierce the cuticle. Both

aciculae represent simple chaetae with a stout end. All chaetae are embedded into a complex system of parapodial musculature (Fig. 4.3.1C, D). Transverse sections through the parapodium show that all notochaetae and all neurochaetae are formed within on chaetal sac each. The chaetae accumulate closely around the aciculae in a crescent form (Fig. 4.3.1D). More proximally, the arrangement of the capillary respectively compound chaetae into two rows becomes increasingly indistinct. Nonetheless, in the neuropodium new chaetae are formed in two clearly separated sites, one being located dorsally and the other one ventrally in the chaetal sac (Fig. 4.3.1D). Both formative sites show two newly formed chaetae of correspondingly differing lengths. In the notopodium, however, three newly formed chaetae can be found at the dorsal margin of the chaetal sac with equivalent distances to each other.

Discussion 5

Chaetae are probably the best studied and most representative morphological character of annelids (Hausen, 2005a). Their huge diversity and the possibility to study them easily via fast methods like SEM or photography established chaetae as a highly significant trait in terms of phylogenetic analyses and species descriptions (Fauchald, 1977; Fitzhugh, 1989; Fauchald & Rouse, 1997; Rouse & Fauchald, 1997; Bartolomaeus et al., 2005). In the course of this thesis, chaetal properties of different annelid taxa have been investigated. The main aspects were the arrangement with number and positions of formative sites and the ultrastructure of chaetae. Moreover, chaetal type diversity, chaetogenesis and chemical composition were examined. In the following, these results will be discussed with the aim to help comprehending the evolution of chaetal traits and to draw conclusions about their primary state found in the annelid ground pattern.

5.1 Formation, composition and degeneration of annelid chaetae

Chaetogenesis and ultrastructure

During chaetogenesis, the chaetoblast secretes polymerized β-chitin, which is complexed with proteins resulting in the peculiar hard but elastic structure of the chaetal material (George & Southward, 1973; O'Clair & Cloney, 1974). This chitinous mass accumulates between the microvilli of the chaetoblast and is pushed apically through the follicular space by constant secretion (O'Clair & Cloney, 1974). As soon as this substance reaches the terminal end of the microvilli, longitudinal, hollow canals arise at the microvilli's positions, which draw through the entire length of the chaeta. Their diameters are equivalent to those of the microvilli. That way, the typical honeycomb-like pattern is formed, which is even visible in light microscopy (Chapter 3.2, 4.2). The canal meshwork of the chaetae is highly variable and depends on the shapes and sizes of the chaetoblast's microvilli during chitin secretion (O'Clair & Cloney, 1974).

The simplest potential composition of this chaetal framework is a circular pattern of evenly sized canals with a consistent thickness of the chitinous lamellae throughout the transverse sectional level. A comparable ultrastructure has been presented in the first two studies in the hooded hooks of Magelonidae and the notochaetae of Oweniidae (Chapters 3.1 & 3.2). It is more common, however, that the canal size varies within a chaeta. In most cases, the centre of the chaeta is characterized by wide canals with thin chitinous lamellae. Towards the periphery, the size of these canals decreases, while the lamellae increase in thickness so that

the outermost region of the chaeta is basically composed of a compact and solid mass (George & Southward, 1973; Hausen, 2005a; chapter 3.3). Depending on the lamellae's thickness, this honeycomb-like pattern ensures an enormous stability and sustains flexibility at the same time (Kryvi & Sørvig, 1990; Merz & Woodin, 1991).

Another peculiar ultrastructural characteristic of the oweniid notochaetae is the lack of an enamel layer, coating the canal framework (Chapter 3.2). This leads to the grooved surface of the smooth part and is a prerequisite for the formation of the apical scales. Each scale arises from a single canal, which is set off the chaetal centre at its tip. With an outer enamel layer, the canals, and therefore the scales, would be covered by chitin. A missing enamel layer has also been reported by Kristensen and Nørrevang (1982) for psammodrilid aciculae, which they interpreted as a primitive trait. However, since all other studied annelid chaetae and even the neurochaetae in Oweniidae possess an enamel, its lack has to be considered as a derived condition (Meyer & Bartolomaeus, 1996). The enamel layer in annelid chaetae is generally considered to be contributed by the follicle cells. Actually, several studies suppose that the follicle cells secrete the largest part of chaetal chitin (O'Clair & Cloney, 1974; Zavarzin & Sergovskaya, 1979; Bartolomaeus, 1998; Hausen & Bartolomaeus, 1998; Tilic, Döhren, et al., 2015). In *Owenia fusiformis*, the complete lack of an enamel either questions this idea or at least marks oweniid notochaetae as an exception from this concept. The mentioned oweniid scales resemble fine hair-like structures or barbs found in chaetae of other annelids like *Aphrodita* or *Sthenelanella*, but these have been shown to be part of the enamel and, therefore, to be formed by the follicle cells as well (Tilic, Geratz, et al., 2021; Tilic, Neunzig, & Bartolomaeus, 2021)**.**

Adding inorganic components

In a few documented cases the organic chaetal mass consisting of chitin and proteins is modified by the inclusion of inorganic substances, added during chaetogenesis by the chaetoblast and follicle cells. Generally, mineralization of organic tissues often occurs in form of an incorporation of iron or calcium compounds, which can be for example found in the shells and radula of molluscs or the echinoderm skeleton (Towe & Lowenstam, 1967; Pearse & Pearse, 1975; Lowenstam, 1981; Weiss et al., 2002). In annelids, the most remarkable example of incorporated minerals may be the ventro-caudal shield of *Sternaspis scutata*, which contains iron in form of ferric phosphate (Lowenstam, 1972). Moreover, this species' chaetae have been shown to contain mineralized iron, probably also ferric phosphate, as well as calcium phosphate

(Lowenstam, 1972; Bartolomaeus, 1992). Calcium is often incorporated in organic tissues in association with either phosphate or carbonate (Lowenstam, 1972, 1981). Examples for other calcium incorporations among annelids are the jaws of Eunicida, the opercular plates of Serpulidae and the introvert plates in Sipuncula (Voss-Foucart et al., 1973; Bubel, 1983; Paxton, 2009). Regarding chaetae, the only record of calcification besides *S. scutata* comes from Amphinomidae. The first evidence of calcium compounds was obtained for *Chloeia* species by treating the chaetae with acetic and oxalic acid (McIntosh, 1876; Gustafson, 1930). Furthermore, it was shown that carbonate is incorporated (Horst, 1912). The more modern approach of an EDS revealed the inclusion of phosphorus in the chaetae of *Hermodice carunculata* (Righi et al., 2021). Similar examinations have not been obtained for Euphrosinidae yet, but the here presented results confirm that the chaetae of *Euphrosine foliosa* show an elemental composition similar to that of Amphinomidae (Chapter 3.3). Additional EDS analyses of four further amphinomid species, including *H. carunculata* and *Chloeia euglochis*, confirm the results of the above-mentioned studies (Chapter A1.2). The corresponding elemental composition of chaetae detected for representatives of Euphrosinidae and Amphinomidae substantiates their sister group relationship and indicates that calcification of chaetae constitutes an apomorphy of Amphinomida (Gustafson, 1930; Wiklund et al., 2008; Borda et al., 2012; Borda et al., 2015).

The high values of carbon and phosphorus in the chaetae of Amphinomida support the hypothesis that calcium is incorporated as compound of calcium carbonate ($CaCO_3$) as well as hydroxyapatite ($Ca_5(PO_4)_3(OH)$) (Righi et al., 2021). The peak of magnesium can be explained by its role in the crystallization process of calcium carbonate (Wang et al., 1997). As a result of the calcification the chaetae become rigid and brittle, which can be noticed in ultrastructural data, showing an atypical, damaged and partially broken chitinous framework (Chapter 3.3). Due to this, the chaetae break easier after contact, which possibly enhances their defensive purpose by physically hurting potential predators (Schulze et al., 2017; Tilic et al., 2017). In the centre of the chaetae, where the chitinous lamellae are thinnest, the calcification leads to a degradation of the central framework resulting in the formation of the inner cavity, typical for amphinomids. Moreover, an additional enamel layer of a lighter electron density as the chaetal lamellae surrounds the chaetae (Chapter 3.3). It can also be seen in SEM images, flaking off the chaetae and forming ornamentations such as the ridges of the curved bifurcate chaetae in *E. foliosa* and serrations or barbs in other amphinomids. These ornamentations vanish completely

after treatment with acid, which indicates that this additional enamel layer predominantly consists of calcium compounds (Gustafson, 1930; Tilic et al., 2017).

Degeneration of chaetae

While the formation process of annelid chaetae is well investigated, data on their degeneration are scarce (Kolbasova et al., 2014). Pilgrim (1977) reported that chaetae of *Clymenella torquata* (LEIDY, 1855) are degraded by coelomocytes after deposition within the coelomic cavity. Another form of degeneration has been observed in *Pseudopotamilla reniformis* (BRUGUIÈRE, 1789) and *Capitella capitata* (FABRICIUS, 1780) as well as for the neurochaetae of *O. fusiformis*. In these species, the chaeta and the follicle are directly dissolved, which is associated with numerous lysosomes in the follicle cells and the chaetoblast (Meyer & Bartolomaeus, 1996; Schweigkofler et al., 1998; Kolbasova et al., 2014). In the course of the here presented second study, the latter descriptions of chaetal degeneration could be confirmed by corresponding observations for oweniid notochaetae (Chapter 3.2). Additionally, the results support the hypothesis that the former chaetoblast participates in the disintegration process and show that this form of degeneration includes a widened follicular space filled with an amorphous electron light substance, possibly the dissolved chaetal mass.

5.2 Chaetal type diversity as a result of functional adaptation

The highly dynamic nature of the chaetoblast's microvilli pattern during the chaetogenetic process allows the precise and detailed formation of chaetae and, therefore, leads to a broad variety of numerous different shapes (Bartolomaeus, 1995b; Bartolomaeus & Meyer, 1997; Bartolomaeus, 1998; Hausam & Bartolomaeus, 2001; Merz & Woodin, 2006; Tilic, Döhren, et al., 2015). Often, several chaetal shapes can even be found in single individuals (Chapters 3.1-3.3, 4.3). Similar types of chaetae, however, are not necessarily homologous, which is well illustrated by the evolution of hooked chaetae, especially those of Magelonidae and Oweniidae. Despite being sister groups, the development of their hooks has to be considered the result of convergent evolution, which is indicated by their dispersion along the animals' bodies. In Magelonidae, hooks are found in both parapodial rami of all abdominal segments (starting with the 10th chaetiger), while in Oweniidae only the neuropodia of the abdomen (starting with the 4th chaetiger) carry hooks and the notopodia are equipped with capillary chaetae (Chapters 3.1, 3.2). Additionally, the convergence of both species' hooks is supported by their structure differing in the presence (Magelonidae) and absence (Oweniidae) of a terminal hood. Besides

Magelonidae, hooded hooks occur in several annelid taxa like Eunicida (Tilic et al., 2016), Spionidae (Hausen & Bartolomaeus, 1998) or Capitellidae (Schweigkofler et al., 1998), but based on the phylogenetic distances between these groups, it has to be assumed that hooded hooks evolved several times independently. Therefore, the evolution of hooked chaetae, to stay with this example, is strongly driven by the essential functional criterion of anchoring the worm within its tube (Merz & Woodin, 2000). The concept of a function-driven evolution of different chaetal types is applicable for annelid chaetae in general and facilitated by their dynamic morphology and the fact that they constitute external structures, which stay in direct contact with a rapidly changing environment (Merz & Woodin, 2006).

Interpreting the functional aspect of chaetae, however, remains highly speculative, especially when statistical and experimental data are scarce or missing. Besides hooks, jointed chaetae, for example, have been analysed with regard to their function. Merz and Edwards (1998) showed that such chaetae in *Oxydromus pugettensis* (JOHNSON, 1901) support the worm's locomotion in terms of undulatory walking movements as well as swimming strokes. A similar purpose can be expected for the compound chaetae of *Glycera fallax*, especially since they occur, equivalent to *O. pugettensis*, only in the neuropodia (Chapter 4.3). In contrast to this, capillary chaetae have been shown to fulfil diverse tasks in tube-building annelid taxa. These include stabilization during peristaltic movements within a tube or serving as mechanical sensor while building the tube. (Sendall et al., 1995; Woodin et al., 2003; Merz & Woodin, 2006). One of these functions would be imaginable for the capillary chaetae of the likewise tube-building *O. fusiformis*, but experimental data are necessary to test this. The oweniid capillary chaetae, however, differ significantly from other ones by the reduction of the enamel layer and the presence of scales. A potential benefit of these scales could be that they act like barbs on bird feathers, improving the connection between the chaetae and, thus, strengthening the bundle's statics (Sullivan et al., 2016).

As mentioned above, the calcification of the chaetae in *E. foliosa* makes them extraordinarily brittle so that they break easily after physical contact (Gustafson, 1930). Although Euphrosinidae are not notorious for their hurtful stinging chaetae as Amphinomidae, it is quite possible that their chaetae act as defensive structures as well (Schulze et al., 2017; Simonini et al., 2021). An exception from a defensive purpose would be the aciculae, which are deeply embedded within the tissue and serve as skeletal supporting structures and attachment point for musculature (Chapter 3.3). Chaetae of equivalent function are found in numerous annelid taxa, mostly designated as aciculae as well. Different to Amphinomida, aciculae in

Aciculata do not resemble the respective capillary chaetae of the parapodium, but are generally characterized by their large size and simple appearance with a stout end (Gustus & Cloney, 1973; Fauchald, 1974b; Hausen, 2005a; chapters 4.2, 4.3). Psammodrilid aciculae, on the other hand, constitute the only chaetae in the respective parapodium, but show a unique ultrastructure with chitinous fibres that are not connected by chaetal material (Kristensen & Nørrevang, 1982). They protrude into the thoracic cirri of the animals, similar to the magelonid abdominal support chaetae, originally also called aciculae, which reach into the parapodial lamellae (Hartmann, 1965; Jones, 1968). The magelonid support chaetae, however, represent internal hooded hooks and, therefore, the same type as the exteriorly visible abdominal chaetae (Chapter 3.1). Furthermore, the support chaetae are not present in all magelonid species so that they have to be considered as a derived characteristic, which evolved within Magelonidae, possibly even several times independently (Brasil, 2003; Mortimer et al., 2021).

These differences in morphology and formation as well as the phylogenetic positions of the respective taxa demonstrate that the term “aciculae” fulfils only a semantic purpose. Instead of indicating a homologous structure, which could potentially be present in the common ancestor of annelids, it merely describes chaetae with a specific function serving as supportive structures (Hoffmann & Hausen, 2007).

5.3 Variations of chaetal arrangement

Phylogenetic significance

The shape of chaetae always served as a reliable phylogenetic indicator and is consistently consulted as significant character in species descriptions (Jones, 1963, 1971; Koh et al., 2003; Barroso et al., 2017; Silva & Lana, 2017). However, as described above, the chaetal shape is highly dependent on functional aspects and extremely flexible due to the dynamic chaetogenetic process so that the occurrence of almost identical forms by convergent evolution can hardly be excluded hampering phylogenetic conclusions (Tilic et al., 2014; Tilic, Döhren, et al., 2015; Tilic et al., 2016). In contrast to that, the arrangement of chaetae within a chaetal sac in combination with the number and positions of formative and degenerative sites attracted increasing attention over the past two decades when it comes to phylogenetic conclusions (Hausen, 2005a; Hoffmann & Hausen, 2007; Kieselbach & Hausen, 2008; Tilic et al., 2014; Tilic, Döhren, et al., 2015; Tilic et al., 2019).

The simplest arrangement pattern is a transverse row with a single formative site. This pattern can be found in several sedentary annelid taxa, often with a ventral formative site in the

notopodium and a dorsal one in the neuropodium (Hausen & Bartolomaeus, 1998; Hausen, 2005a). The here presented results of *S. scutata* substantiate the phylogenetic relevance of the chaetal arrangement by identifying a dorsal formative site in the transverse rows of the anterior spine-like chaetae (Chapter 4.1). This is typical for the neurochaetae in Cirratuliformia, to which Sternaspidae have been associated repeatedly (Rousset et al., 2007; Struck et al., 2007; Andrade et al., 2015; Drennan et al., 2019). Correspondingly, Petersen (2000) found small, rudimentary chaetae located dorsally to the spine-like chaetae of the introvert, which classifies the latter ones as neurochaetae. The shield chaetae of *S. scutata* possess a dorsal formative site as well so that it can be assumed that these also represent neurochaetae (Chapter 4.1). It remains unclear, though, whether posterior notochaetae are either rudimentary like the anterior notochaetae and have simply not been detected yet, or if they have been lost completely within Sternaspidae.

Other possible arrangement patterns found in Sedentaria include transverse rows with an inverted position of the formative site, small chaetal fascicles or an additional longitudinal row per parapodial ramus with its own formative site (Bartolomaeus & Meyer, 1997; Hausen & Bartolomaeus, 1998; Hausen, 2001, 2005a). In contrast to that, Errantia are quite understudied regarding their chaetal arrangement. Similar to most Sedentaria, Chrysopetalidae show a single formative site in the noto- as well as neuropodium (Tilic et al., 2019). In Lumbrineridae, on the other hand, the exteriorly visible chaetae in the neuropodium are arranged in two groups, one located dorsally, the other one ventrally to the aciculae and each group contains its own formative site (Tilic et al., 2014). The notopodium, however, is often rudimentary or completely reduced in Eunicida (Paxton, 2000; Tilic et al., 2016). The lumbrinerid arrangement pattern resembles the state found in both parapodial rami in Nephtyidae and Glyceridae (Chapters 4.2, 4.3). In Lumbrineridae and Glyceridae, it can be recognized that the chaetae of both groups per chaetal sac are arranged in rows, even though they have a crescent shape in the case of Glyceridae. Nephtyid chaetae, however, form a double row in one group and larger patches in the other one. Similar arrangement patterns like this that deviate from a simple row, are common among annelids, but the formation of such patterns is more complicated to comprehend and far less studied than that of rows. A more detailed view on this subject could help answering the question whether annelid chaetae were primarily arranged in rows or bundles.

From a row to a bundle

Basically, in the context of chaetal arrangement the term “bundle” can describe a variety of differently shaped patterns. This starts with small fascicles of chaetae, which lack a distinct order of formation (Bartolomaeus & Meyer, 1997; Bartolomaeus, 2002; Hausen, 2005a). This is also true for the shield chaetae of *S. scutata*, which occur in groups of 6-8 chaetae (Bartolomaeus, 1992; Zhadan et al., 2017). As histological sections show, these are actually arranged in a double transverse row with a dorsal formative site (Chapter 4.1). The sternaspid peg chaetae, likewise associated to the caudo-ventral shield, have been shown to constitute a bundle of numerous small and thin capillary chaetae that are actually arranged in six rows and embedded in a matrix so that they appear as a solid structure (Zhadan et al., 2017). The here presented results confirm the reported number of exactly six rows forming one peg chaeta and contribute the finding that each row possesses its own dorsally located formative site and arises from its own chaetal sac (Chapter 4.1). These chaetal sacs are then summed up to one bundle resulting in the peg chaeta. The results differ regarding the total number of included chaetae, which probably means that peg chaetae grow constantly by adding new chaetae to each row simultaneously. It remains unclear, though, if any degeneration process takes place.

Several rows, which are formed simultaneously and added up to a bundle can also arise from a common chaetal sac. Such an arrangement pattern can be observed in *E. foliosa* (Chapter 3.3). Here, a single formative site regularly produces a whole new transverse row of chaetae, which then shifts anteriorly, resulting in a large bundle. A similar but less structured mechanism creates the staggered rows in the thorax of magelonids. Varying numbers of new chaetae appear at differing positions all along the posterior margin of the chaetal sac and shift anteriorly (Chapter 3.1). That way, the transverse row gets expanded successively by new chaetae, which leads to a broadened bundle-like arrangement, especially in the ninth chaetiger. This corresponds to the neuropodial patches in Apistobranchidae, which are of a more circular shape, but new chaetae are formed at the posterior margin as well (Hausen, 2001).

An especially interesting clade regarding the arrangement of chaetae are Oweniidae. While hooked chaetae are widely spread among annelids, the vast majority, such as Serpulidae, Arenicolidae, Sabellidae, Maldanidae or Terebellidae, bears distinct transverse rows of hooks (Woodin & Merz, 1987; Duchêne & Bhaud, 1988; Fitzhugh, 1991; Bartolomaeus, 1995b; Bartolomaeus & Meyer, 1997; Hausen & Bartolomaeus, 1998; Schweigkofler et al., 1998; Radashevsky & Fauchald, 2000; Bartolomaeus, 2002; Hausen, 2005a; Hausen & Bleidorn, 2006; Kieselbach & Hausen, 2008; Tilic, Döhren, et al., 2015; chapter 3.1). Oweniids, however,

possess large patches of numerous hooks (Capa et al., 2019). No distinct transverse rows are recognizable within these patches, but several formation processes can be noticed simultaneously at their dorsal ends, while degeneration takes place ventrally (Meyer & Bartolomaeus, 1996). Examining young individuals shortly after metamorphosis, though, revealed that early during ontogenesis hooks are formed in single transverse rows with a dorsal formative site (Chapter A1.1). Thus, it has to be assumed that the neurochaetal patches in Oweniidae are formed by multiplication of this single row. The oweniid notochaetae show an even more specialized and uncommon form of chaetal arrangement. The scaled capillary chaetae form a densely packed circular bundle without any notable increase of the chaetae's size or age in a certain direction (Chapter 3.2). Indeed, histological approaches demonstrate that new chaetae can be formed at any anatomical direction of the chaetal sac, but occur only in its periphery. In contrast to that, degenerating chaetae are exclusively found in the centre of the bundle. It can be concluded that notochaetae in Oweniidae are formed in a modified, curled-up row with one formative and one degenerative site, leading to a spiral arrangement of chaetae. The exteriorly visible spiral twist of the bundle may support this hypothesis. Spiral arrangements of capillary chaetae based on modified rows have already been reported from Sabellidae (Knight-Jones, 1981; Kieselbach & Hausen, 2008).

Altogether, it can be summarized that bundle-like arrangements of chaetae can often be explained as a modification of one row with a single formative site. These modifications include multiplication of formative sites, curling of rows or dense aggregation of several separate rows. Therefore, it has to be concluded that one distinct transverse row with a single, laterally located formative site per parapodial ramus represents the primary state of chaetal arrangement in annelids.

5.4 Outlook to a broader comparison with other lophotrochozoan taxa

As mentioned previously, a distinct arrangement of chaetae is considered as an apomorphy of annelids (Bartolomaeus, 1998). The focus on the arrangement as a restricting property is necessary, because extracellular, epidermal, chitinous structures comparable to chaetae are found in other lophotrochozoan taxa as well. Actually, before the advent of molecular methods and our current understanding of the annelid systematics, chaetae-like structures have been considered to be virtually widespread among lophotrochozoans. Remarkable similarities between annelid chaetae and structures found in Pogonophora, Myzostomida and Echiura concerning their development and ultrastructure led to well substantiated homology hypotheses

(Gupta & Little, 1970; George & Southward, 1973; Specht, 1988). Such hypotheses were confirmed when these groups were included into annelids (McHugh, 1997; Bleidorn et al., 2007).

Today, similar homology hypotheses regarding annelid chaetae and equivalent structures found in Barachiopoda are supported by molecular data as well as similarities in their formation, ultrastructure and composition (Zakrzewski, 2011; Schiemann et al., 2017). These brachiopod chaetae are composed of evenly sized, hollow chitinous canals arranged in a circular pattern surrounded by an enamel layer and a surface covered with barbs (Gustus & Cloney, 1972; Orrhage, 1973; Lüter & Bartolomaeus, 1997). In fact, they resemble the oweniid scaled notochaetae, but the presence of an enamel layer in brachiopod chaetae and the fact that the mentioned traits in oweniid chaetae are considered as derived within annelids contradicts a homologous evolution of these exact shapes (Gustus & Cloney, 1972; Lüter, 2001). Several molecular as well as morphological studies, however, support a sister group relationship of Brachiopoda and Phoronida (Dunn et al., 2008; Helmkampf et al., 2008b; Hausdorf et al., 2010; Kocot et al., 2017). Thus, the assumption of a common origin of brachiopod and annelid chaetae would imply that Phoronida lost their chaetae secondarily. A complete or partial secondary loss of chaetae, however, is known from several annelid groups as well (Vejdovský, 1882; Tzetlin & Purschke, 2006; Sket & Trontelj, 2008; Tilic, Lehrke, & Bartolomaeus, 2015).

Other chaetae-like structures among Lophotrochozoa are the gizzard teeth in Bryozoa and epidermal projections in juvenile octopods called Kölliker's organs (Brocco et al., 1974; Gordon, 1975). Both structures are formed by a single specialized epidermal cell that secretes chitin, which accumulates between this cell's microvilli. Therefore, they also show a framework of hollow canals typical for annelid and brachiopod chaetae, but further ultrastructural and molecular data of these structures are necessary to evaluate a potential homology.

Conclusions 6

The formation of annelid chaetae constitutes a highly dynamic process, which facilitates the development of a huge diversity of chaetal types. Since chaetae, as extracellular epidermal structures, are in direct contact with the animal's environment, their morphology is highly driven by functional aspects, which can be of mechanical, sensory or defensive nature for example. Detailed analyses of the exact formation process, ultrastructure and composition of different chaetal types allow drawing conclusions about their homologous or convergent evolution and explaining phylogenetic relationships of the respective taxa bearing these types.

The flexibility of the chaetogenetic process has been demonstrated in the second study by explaining the formation process of the notochaetae of *Owenia fusiformis* (Chapter 3.2). The lack of an enamel layer and the successive spiral addition of new microvilli during the chaetal formation process is unique among annelids and leads to the delicate scaled surface of these chaetae. The comparison with chaetae in their sister group, Magelonidae, shows that these features of oweniid notochaetae constitute a derived condition. Furthermore, the first study provides evidence that the magelonid abdominal support chaetae actually represent internal hooded hooks and, therefore, evolved secondarily within Magelonidae (Chapter 3.1). Comparisons of further supportive chaetae like those of Euphrosinidae and Errantia, highlight the semantic nature of the term "aciculae", describing chaetae fulfilling a skeletal function, which evolved independently in several annelid taxa (Chapters 3.1, 3.3, 4.2, 4.3). The data on euphrosinid chaetae presented in the third study also indicate that calcification of chaetae is present in the ground pattern of Amphinomidae and must be considered as apomorphy substantiating their monophyly (Chapter 3.3).

All results presented in the course of this thesis point out the phylogenetic significance of the arrangement of chaetae and the number and positions of formative sites within a chaetal sac. Altogether, it can be concluded that one transverse row per parapodial ramus with a single formative site located ventrally in the notopodium and dorsally in the neuropodium constitutes the ancestral state of chaetal arrangement in Annelida (Chapters 3.1, 4.1). Deviations from this pattern include the formative site to extend (Chapters 3.1, 3.3), shift (Chapter 3.1) or multiply (Chapters 3.2, 4.2, 4.3). Combined with a transformation of the shape of the chaetal sac, this eventually leads to the formation of derived patterns like staggered rows, circular bundles or large patches.

References 7

Aguinaldo, A.M. A., Turbeville, J.M., Linford, L.S., Rivera, M.C., Garey, J.R., Raff, R.A., & Lake, J.A. (1997). Evidence for a clade of nematodes, arthropods and other moulting animals. *Nature*, *387*(6632), 489–493. https://doi.org/10.1038/387489a0

Andrade, S.C., Novo, M., Kawauchi, G.Y., Worsaae, K., Pleijel, F., Giribet, G., & Rouse, G.W. (2015). Articulating "Archiannelids": Phylogenomics and annelid relationships, with emphasis on meiofaunal taxa. *Molecular Biology and Evolution*, *32*(11), 2860–2875. https://doi.org/10.1093/molbev/msv157

Balavoine, G. (2014). Segment formation in Annelids: patterns, processes and evolution. *International Journal of Developmental Biology*, *58*, 469–483.

Barnes, R.D. (1964). Tube-building and feeding in the chaetopterid polychaete, *Spiochaetopterus oculatus*. *The Biological Bulletin*, *127*(3), 397–412. https://doi.org/10.2307/1539244

Barnes, R.D. (1965). Tube-building and feeding in chaetopterid polychaetes. *The Biological Bulletin*, *129*(2), 217–233. https://doi.org/10.2307/1539840

Barroso, R., Ranauro, N., & Kudenov, J.D. (2017). A new species of *Branchamphinome* (Annelida: Amphinomidae) from the South-western Atlantic, with an emendation of the genus. *Journal of the Marine Biological Association of the United Kingdom*, *97*(5), 835–842. https://doi.org/10.1017/S0025315417000054

Bartolomaeus, T. (1992). On the ultrastructure of the cuticle, the epidermis and the gills of *Sternaspis scutata* (Annelida). *Microfauna Marina*, *7*, 237–252.

Bartolomaeus, T. (1994). On the ultrastructure of the coelomic lining in the Annelida, Sipuncula and Echiura. *Microfauna Marina*, *9*, 171–220.

Bartolomaeus, T. (1995a). Secondary monociliarity in the Annelida: Monociliated epidermal cells in larvae of *Magelona mirabills* (Magelonida). *Microfauna Marina*, *10*, 327–332.

Bartolomaeus, T. (1995b). Structure and formation of the uncini in *Pectinaria koreni*, *Pectinaria auricoma* (Terebellida) and *Spirorbis spirorbis* (Sabellida): implications for annelid phylogeny and the position of the Pogonophora. *Zoomorphology*, *115*(3), 161–177. https://doi.org/10.1007/BF00403171

Bartolomaeus, T. (1998). Chaetogenesis in polychaetous Annelida: Significance for annelid systematics and the position of the Pogonophora. *Zoology*, *100*, 348–364.

Bartolomaeus, T. (1999). Structure, function and development of segmental organs in Annelida. In A. W. C. Dorresteijn & W. Westheide (Eds.), *Reproductive Strategies and Developmental Patterns in Annelids* (pp. 21–37). Springer Netherlands. https://doi.org/10.1007/978-94-017-2887-4_2

Bartolomaeus, T. (2002). Structure and formation of thoracic and abdominal uncini in *Fabricia stellaris* (Müller, 1774) – Implication for the evolution of Sabellida (Annelida). *Zoologischer Anzeiger - a Journal of Comparative Zoology*, *241*(1), 1–17. https://doi.org/10.1078/0044-5231-00015

Bartolomaeus, T., & Meyer, K. (1997). Development and phylogenetic significance of hooked setae in Arenicolidae (Polychaeta, Annelida). *Invertebrate Biology*, *116*(3), 227–242. https://doi.org/10.2307/3226899

References

Bartolomaeus, T., Purschke, G., & Hausen, H. (2005). Polychaete phylogeny based on morphological data – a comparison of current attempts. *Hydrobiologia*, *535*(1), 341–356. https://doi.org/10.1007/s10750-004-1847-5

Beckers, P., Helm, C., & Bartolomaeus, T. (2019). The anatomy and development of the nervous system in Magelonidae (Annelida) – insights into the evolution of the annelid brain. *BMC Evolutionary Biology*, *19*(1). https://doi.org/10.1186/s12862-019-1498-9

Beckers, P., Helm, C., Purschke, G., Worsaae, K., Hutchings, P.A., & Bartolomaeus, T. (2019). The central nervous system of Oweniidae (Annelida) and its implications for the structure of the ancestral annelid brain. *Frontiers in Zoology*, *16*(1), 1–21. https://doi.org/10.1186/s12983-019-0305-1

Blake, J.A. (1969). Systematics and ecology of shell-boring polychaetes from New England. *American Zoologist*, *9*(3), 813–820. https://doi.org/10.1093/icb/9.3.813

Bleidorn, C. (2019). Recent progress in reconstructing lophotrochozoan (spiralian) phylogeny. *Organisms Diversity & Evolution*, *19*(4), 557–566. https://doi.org/10.1007/s13127-019-00412-4

Bleidorn, C., Eeckhaut, I., Podsiadlowski, L., Schult, N., McHugh, D., Halanych, K.M., Milinkovitch, M.C., & Tiedemann, R. (2007). Mitochondrial genome and nuclear sequence data support Myzostomida as part of the annelid radiation. *Molecular Biology and Evolution*, *24*(8), 1690–1701. https://doi.org/10.1093/molbev/msm086

Bleidorn, C., Vogt, L., & Bartolomaeus, T. (2003). New insights into polychaete phylogeny (Annelida) inferred from 18S rDNA sequences. *Molecular Phylogenetics and Evolution*, *29*(2), 279–288. https://doi.org/10.1016/S1055-7903(03)00107-6

Bobin, G. (1944). *Morphogénèse des soies chez les annélides polychètes* [Doctoral dissertation]. RIS.

Borda, E., Kudenov, J.D., Bienhold, C., & Rouse, G.W. (2012). Towards a revised Amphinomidae (Annelida, Amphinomida): description and affinities of a new genus and species from the Nile Deep-sea Fan, Mediterranean Sea. *Zoologica Scripta*, *41*(3), 307–325. https://doi.org/10.1111/j.1463-6409.2012.00529.x

Borda, E., Yáñez-Rivera, B., Ochoa, G.M., Kudenov, J.D., Sanchez-Ortiz, C., Schulze, A., & Rouse, G.W. (2015). Revamping Amphinomidae (Annelida: Amphinomida), with the inclusion of *Notopygos*. *Zoologica Scripta*, *44*(3), 324–333. https://doi.org/10.1111/zsc.12099

Bouligand, Y. (1967). Les soies et les cellules associées chez deux Annélides Polychètes. *Zeitschrift Für Zellforschung*, *79*(3), 332–363. https://doi.org/10.1007/BF00335480

Bourlat, S.J., Nielsen, C., Economou, A.D., & Telford, M.J. (2008). Testing the new animal phylogeny: a phylum level molecular analysis of the animal kingdom. *Molecular Phylogenetics and Evolution*, *49*(1), 23–31. https://doi.org/10.1016/j.ympev.2008.07.008

Brasil, A.C. d. S. (2003). *Filogenia de Magelonidae Cunningham & Ramage, 1888 (Annelida - Polychaeta) com base na morfologia externa* [Doctoral dissertation]. Universidade Federal do Paraná, Brazil.

Britayev, T.A., & Martin, D. (2019). 5.3 Chaetopteridae Audouin & Milne Edwards, 1833. In G. Purschke, M. Böggemann, & W. Westheide (Eds.), *Handbook of Zoology, 2193-4231: Vol. 1. Annelida* (156-175). De Gruyter.

References

Brocco, S.L., O'Clair, R.M., & Cloney, R.A. (1974). Cephalopod integument: The ultrastructure of Kölliker's organs and their relationship to setae. *Cell and Tissue Research*, *151*(3), 293–308. https://doi.org/10.1007/BF00224540

Bubel, A. (1983). A fine structural study of the calcareous opercular plate and associated cells of a polychaete annelid. *Tissue and Cell*, *15*(3), 457–476. https://doi.org/10.1016/0040-8166(83)90076-9

Capa, M., Parapar, J., & Hutchings, P.A. (2012). Phylogeny of Oweniidae (Polychaeta) based on morphological data and taxonomic revision of Australian fauna. *Zoological Journal of the Linnean Society*, *166*(2), 236–278. https://doi.org/10.1111/j.1096-3642.2012.00850.x

Capa, M., Parapar, J., & Hutchings, P.A. (2019). 4.1 Oweniidae Rioja, 1917. In G. Purschke, M. Böggemann, & W. Westheide (Eds.), *Handbook of Zoology, 2193-4231: Vol. 1. Annelida* (pp. 91–112). De Gruyter.

Carrillo-Baltodano, A.M., Seudre, O., Guynes, K., & Martín-Durán, J.M. (2021). Early embryogenesis and organogenesis in the annelid *Owenia fusiformis*. *EvoDevo*, *12*(1), 5. https://doi.org/10.1186/s13227-021-00176-z

Clarke, D.T., Paterson, G.L., Florence, W.K., & Gibbons, M.J. (2010). A new species of *Magelona* (Polychaeta: Magelonidae) from southern Namibia. *African Natural History*, *6*, 77–82. http://www.scielo.org.za/scielo.php?script=sci_arttext&pid=S2305-79632010000100002&nrm=iso

Cuvier, G. (1817). *Le régne animal distribué d'aprés son organisation, pour servir de base á l'histoire naturelle des animaux et d'introduction á l'anatomie comparée: Contenant les Reptiles, les Poissons, les Mollusques et les Annélides* (Vol. 2). Chez Déterville.

Dales, R.P. (1957). The feeding mechanism and structure of the gut of *Owenia fusiformis* delle Chiaje. *Journal of the Marine Biological Association of the United Kingdom*, *36*(1), 81–89. https://doi.org/10.1017/S0025315400017082

Díaz-Castañeda, V., & Reish, D.J. (2009). Polychaetes in Environmental Studies. In D. H. Shain (Ed.), *Annelids in Modern Biology* (pp. 205–227). John Wiley & Sons, Ltd.

Dordel, J., Fisse, F., Purschke, G., & Struck, T.H. (2010). Phylogenetic position of Sipuncula derived from multi-gene and phylogenomic data and its implication for the evolution of segmentation. *Journal of Zoological Systematics and Evolutionary Research*, *48*(3), 197–207. https://doi.org/10.1111/j.1439-0469.2010.00567.x

Drennan, R., Wiklund, H., Rouse, G.W., Georgieva, M.N., Wu, X., Kobayashi, G., Yoshino, K., & Glover, A.G. (2019). Taxonomy and phylogeny of mud owls (Annelida: Sternaspidae), including a new synonymy and new records from the Southern Ocean, North East Atlantic Ocean and Pacific Ocean: challenges in morphological delimitation. *Marine Biodiversity*, *49*(6), 2659–2697. https://doi.org/10.1007/s12526-019-00998-0

Duchêne, J.-C., & Bhaud, M.R. (1988). Uncinial patterns and age determination in terebellid polychaetes. *Marine Ecology Progress Series*, *49*(3), 267–275. http://www.jstor.org/stable/24827637

Dunn, C.W., Hejnol, A., Matus, D.Q., Pang, K., Browne, W.E., Smith, S.A., Seaver, E., Rouse, G.W., Obst, M., Edgecombe, G.D., Sørensen, M.V., Haddock, S.H. D., Schmidt-Rhaesa, A., Okusu, A., Kristensen, R.M., Wheeler, W.C., Martindale, M.Q., & Giribet, G. (2008). Broad

phylogenomic sampling improves resolution of the animal tree of life. *Nature*, *452*(7188), 745–749. https://doi.org/10.1038/nature06614

Eckert, G.J. (1985). Absence of toxin-producing parapodial glands in amphinomid polychaetes (fireworms). *Toxicon*, *23*(2), 350–353. https://doi.org/10.1016/0041-0101(85)90160-6

Eernisse, D.J., Albert, J.S., & Anderson, F.E. (1992). Annelida and Arthropoda are not sister taxa: a phylogenetic analysis of spiralian metazoan morphology. *Systematic Biology*, *41*(3), 305–330. https://doi.org/10.1093/sysbio/41.3.305

Fauchald, K. (1974a). Polychaete phylogeny: A problem in protostome evolution. *Systematic Biology*, *23*(4), 493–506. https://doi.org/10.1093/sysbio/23.4.493

Fauchald, K. (1974b). Sphaerodoridae (Polychaeta: Errantia) from world-wide areas. *Journal of Natural History*, *8*(3), 257–289. https://doi.org/10.1080/00222937400770241

Fauchald, K. (1977). *The polychaete worms. Definitions and keys to the orders, families and genera*. *Science Series: Vol. 28*. Natural History Museum of Los Angeles County.

Fauchald, K., & Jumars, P.A. (1979). The diet of worms: a study of polychaete feeding guilds. *Oceanography and Marine Biology Annual Review*, *17*, 193–284.

Fauchald, K., & Rouse, G. (1997). Polychaete systematics: Past and present. *Zoologica Scripta*, *26*(2), 71–138. https://doi.org/10.1111/j.1463-6409.1997.tb00411.x

Fiege, D., Licher, F., & Mackie, A.S. Y. (2000). A partial review of the European Magelonidae (Annelida: Polychaeta): *Magelona mirabilis* redefined and *M. johnstoni* sp. nov. distinguished. *Journal of the Marine Biological Association of the United Kingdom*, *80*(2), 215–234. https://doi.org/10.1017/S0025315499001800

Filippova, A., Purschke, G., Tzetlin, A.B., & Müller, M.C. M. (2005). Reconstruction of the musculature of *Magelona* cf. *mirabilis* (Magelonidae) and *Prionospio cirrifera* (Spionidae) (Polychaeta, Annelida) by phalloidin labeling and cLSM. *Zoomorphology*, *124*(1), 1–8. https://doi.org/10.1007/s00435-004-0106-7

Fitzhugh, K. (1989). A systematic revision of the Sabellidae-Caobangiidae-Sabellongidae complex (Annelida, Polychaeta). *Bulletin of the AMNH*, *192*, 1–104.

Fitzhugh, K. (1991). Uncini and the anchor-function hypothesis: empirical tests and causal explanations. *Bulletin of Marine Science*, *48*(2), 574–583.

Gardiner, S.L. (1978). Fine structure of the ciliated epidermis on the tentacles of *Owenia fusiformis* (Polychaeta, Oweniidae). *Zoomorphology*, *91*(1), 37–48. https://doi.org/10.1007/BF00994152

Gardiner, S.L. (1992). Chapter 2: Polychaeta: External Anatomy. In F. W. Harrison & S. L. Gardiner (Eds.), *Microscopic anatomy of invertebrates. Vol.7, Annelida* (11-17). Wiley-Liss.

Gardiner, S.L., & Rieger, R.M. (1980). Rudimentary cilia in muscle cells of annelids and echinoderms. *Cell and Tissue Research*, *213*(2), 247–252. https://doi.org/10.1007/BF00234785

George, J.D., & Southward, E.C. (1973). A comparative study of the setae of Pogonophora and polychaetous Annelida. *Journal of the Marine Biological Association of the United Kingdom*, *53*(2), 403–424. https://doi.org/10.1017/S0025315400022359

References

Giribet, G., & Ribera, C. (1998). The position of arthropods in the animal kingdom: a search for a reliable outgroup for internal arthropod phylogeny. *Molecular Phylogenetics and Evolution*, *9*(3), 481–488. https://doi.org/10.1006/mpev.1998.0494

Glasby, C.J., & Timm, T. (2008). Global diversity of polychaetes (Polychaeta; Annelida) in freshwater. In E. V. Balian, C. Lévêque, H. Segers, & K. Martens (Eds.), *Freshwater Animal Diversity Assessment* (pp. 107–115). Springer Netherlands. https://doi.org/10.1007/978-1-4020-8259-7_13

Glover, A.G., Källström, B., Smith, C.R., & Dahlgren, T.G. (2005). World-wide whale worms? A new species of *Osedax* from the shallow north Atlantic. *Proceedings of the Royal Society B: Biological Sciences*, *272*(1581), 2587–2592. https://doi.org/10.1098/rspb.2005.3275

Gordon, D.P. (1975). The resemblance of bryozoan gizzard teeth to "annelid-like" setae. *Acta Zoologica*, *56*(4), 283–289. https://doi.org/10.1111/j.1463-6395.1975.tb00105.x

Gouveneaux, A., Gielen, M.-C., & Mallefet, J. (2018). Behavioural responses of the yellow emitting annelid *Tomopteris helgolandica* to photic stimuli. *Luminescence*, *33*(3), 511–520. https://doi.org/10.1002/bio.3440

Grzimek, B. (Ed.). (1971). *Grzimeks Tierleben: Enzyklopädie des Tierreichs: Band I: Niedere Tiere* (Vol. 1). Kindler Verlag.

Gupta, B.L., & Little, C. (1970). Studies on Pogonophora. 4. Fine structure of the cuticle and epidermis. *Tissue and Cell*, *2*(4), 637–696. https://doi.org/10.1016/S0040-8166(70)80035-0

Gustafson, G. (1930). *Anatomische Studien über die Polychäten-Familien Amphinomidae und Euphrosynidae* [Doctoral dissertation]. Universität Uppsala, Uppsala.

Gustus, R.M., & Cloney, R.A. (1972). Ultrastructural similarities between setae of brachiopods and polychaetes. *Acta Zoologica*, *53*(2), 229–233. https://doi.org/10.1111/j.1463-6395.1972.tb00590.x

Gustus, R.M., & Cloney, R.A. (1973). Ultrastructure of the larval compound setae of the polychaete *Nereis vexillosa* Grube. *Journal of Morphology*, *140*(3), 355–366. https://doi.org/10.1002/jmor.1051400308

Halanych, K.M., Bacheller, J.D., Aguinaldo, A.M. A., Liva, S.M., Hillis, D.M., & Lake, J.A. (1995). Evidence from 18S ribosomal DNA that the lophophorates are protostome animals. *Science*, *267*(5204), 1641–1643. https://doi.org/10.1126/science.7886451

Hartmann, O. (1965). Deep-water benthic polychaetous annelids off New England to Bermuda and other North Atlantic areas. *Allan Hancock Found. Publ. Occas. Pap.*, *28*, 1–378.

Hausam, B., & Bartolomaeus, T. (2001). Ultrastructure and development of forked and capillary setae in the polychaetes *Orbinia bioreti* and *Orbinia latreillii* (Annelida: Orbiniidae). *Invertebrate Biology*, *120*(1), 13–28. https://doi.org/10.1111/j.1744-7410.2001.tb00022.x

Hausdorf, B., Helmkampf, M., Nesnidal, M.P., & Bruchhaus, I. (2010). Phylogenetic relationships within the lophophorate lineages (Ectoprocta, Brachiopoda and Phoronida). *Molecular Phylogenetics and Evolution*, *55*(3), 1121–1127. https://doi.org/10.1016/j.ympev.2009.12.022

Hausen, H. (2001). *Untersuchungen zur Phylogenie ''spiomorpher'' Polychaeten (Annelida)*. Logos Verlag. https://pub.uni-bielefeld.de/record/2434530

Hausen, H. (2005a). Chaetae and chaetogenesis in polychaetes (Annelida). *Morphology, Molecules, Evolution and Phylogeny in Polychaeta and Related Taxa*, *179*, 37–52. https://doi.org/10.1007/1-4020-3240-4_4

Hausen, H. (2005b). Comparative structure of the epidermis in polychaetes (Annelida). *Hydrobiologia*, *535*(1), 25–35. https://doi.org/10.1007/s10750-004-4442-x

Hausen, H., & Bartolomaeus, T. (1998). Setal structure and chaetogenesis in *Scolelepis squamata* and *Malacoceros fuliginosus* (Spionidae, Annelida). *Acta Zoologica*, *79*(3), 149–161. https://doi.org/10.1111/j.1463-6395.1998.tb01154.x

Hausen, H., & Bleidorn, C. (2006). Significance of chaetal arrangement for maldanid systematics (Annelida, Maldanidae). *Scientia Marina*, *70*(S3), 75–79. https://doi.org/10.3989/scimar.2006.70s375

Helm, C., Beckers, P., Bartolomaeus, T., Drukewitz, S.H., Kourtesis, I., Weigert, A., Purschke, G., Worsaae, K., Struck, T.H., & Bleidorn, C. (2018). Convergent evolution of the ladder-like ventral nerve cord in Annelida. *Frontiers in Zoology*, *15*(1), 36. https://doi.org/10.1186/s12983-018-0280-y

Helm, C., Vöcking, O., Kourtesis, I., & Hausen, H. (2016). *Owenia fusiformis* – a basally branching annelid suitable for studying ancestral features of annelid neural development. *BMC Evolutionary Biology*, *16*(1), 129. https://doi.org/10.1186/s12862-016-0690-4

Helmkampf, M., Bruchhaus, I., & Hausdorf, B. (2008a). Multigene analysis of lophophorate and chaetognath phylogenetic relationships. *Molecular Phylogenetics and Evolution*, *46*(1), 206–214. https://doi.org/10.1016/j.ympev.2007.09.004

Helmkampf, M., Bruchhaus, I., & Hausdorf, B. (2008b). Phylogenomic analyses of lophophorates (brachiopods, phoronids and bryozoans) confirm the Lophotrochozoa concept. *Proceedings of the Royal Society B: Biological Sciences*, *275*(1645), 1927–1933. https://doi.org/10.1098/rspb.2008.0372

Hoffmann, S., & Hausen, H. (2007). Chaetal arrangement in Orbiniidae (Annelida, Polychaeta) and its significance for systematics. *Zoomorphology*, *126*(4), 215–227. https://doi.org/10.1007/s00435-007-0042-4

Horst, R.R. (1912). Polychaeta Errantia of the Siboga Expedition. Part I. Amphinomidae. *Siboga Expeditie*, *24*, 1–43. https://www.biodiversitylibrary.org/part/92902

Hutchings, P.A. (1998). Biodiversity and functioning of polychaetes in benthic sediments. *Biodiversity & Conservation*, *7*(9), 1133–1145. https://doi.org/10.1023/A:1008871430178

Hutchings, P.A. (2000a). Family Amphinomidae. In P. L. Beesley, G. Ross, & C. J. Glasby (Eds.), *Fauna of Australia: 4A. Polychaeta, Myzostomida, Pogonophora, Echiura, Sipuncula. Polychaetes & Allies: The Southern Synthesis* (4A. Polychaeta, Myzostomida, Pogonophora, Echiura, Sipuncula, pp. 144–148). CSIRO Publishing.

Hutchings, P.A. (2000b). Family Euphrosinidae. In P. L. Beesley, G. Ross, & C. J. Glasby (Eds.), *Fauna of Australia: 4A. Polychaeta, Myzostomida, Pogonophora, Echiura, Sipuncula. Polychaetes & Allies: The Southern Synthesis* (4A. Polychaeta, Myzostomida, Pogonophora, Echiura, Sipuncula, pp. 148–151). CSIRO Publishing.

References

Irvine, S.Q., & Martindale, M.Q. (2000). Expression patterns of anterior Hox genes in the polychaete *Chaetopterus*: Correlation with morphological boundaries. *Developmental Biology*, *217*(2), 333–351. https://doi.org/10.1006/dbio.1999.9541

Jennings, J.B., & Gelder, S.R. (1976). Observations on the feeding mechanism, diet and digestive physiology of *Histriobdella homari* van Beneden 1858: an aberrant polychaete symbiotic with North American and European lobsters. *The Biological Bulletin*, *151*(3), 489–517. https://doi.org/10.2307/1540502

Jones, M.L. (1963). Four new species of *Magelona* (Annelida, Polychaeta) and a redescription of *Magelona longicornis* Johnson. *American Museum Novitates*, *2164*, 1–31. http://hdl.handle.net/2246/3338

Jones, M.L. (1968). On the morphology, feeding, and behavior of *Magelona sp*. *The Biological Bulletin*, *134*(2), 272–297. https://doi.org/10.2307/1539604

Jones, M.L. (1971). *Magelona berkeleyi* n.sp. from Puget Sound (Annelida: Polychaeta), with a further redescription of *Magelona longicornis* Johnson and a consideration of recently described species of *Magelona*. *Journal of the Fisheries Research Board of Canada*, *28*(10), 1445–1454. https://doi.org/10.1139/f71-223

Kieselbach, D., & Hausen, H. (2008). Chaetal arrangement provides no support for a close relationship of Sabellidae and Sabellariidae (Annelida). *Journal of Morphology*, *269*(1), 104–117. https://doi.org/10.1002/jmor.10537

Knight-Jones, P. (1981). Behaviour, setal inversion and phylogeny of Sabellida (Polychaeta). *Zoologica Scripta*, *10*(3), 183–202. https://doi.org/10.1111/j.1463-6409.1981.tb00495.x

Kocot, K.M., Struck, T.H., Merkel, J., Waits, D.S., Todt, C., Brannock, P.M., Weese, D.A., Cannon, J.T., Moroz, L.L., Lieb, B., & Halanych, K.M. (2017). Phylogenomics of Lophotrochozoa with consideration of systematic error. *Systematic Biology*, *66*(2), 256–282. https://doi.org/10.1093/sysbio/syw079

Koh, B.-S., Bhaud, M.R., & Jirkov, I.A. (2003). Two new species of *Owenia* (Annelida: Polychaeta) in the northern part of the North Atlantic Ocean and remarks on previously erected species from the same area. *Sarsia*, *88*(3), 175–188. https://doi.org/10.1080/00364820310001318

Kolbasova, G.D., Tzetlin, A.B., & Kupriyanova, E.K. (2014). Chaetal loss and replacement in *Pseudopotamilla reniformis* (Sabellida, Annelida). *Invertebrate Biology*, *133*(3), 261–273. https://doi.org/10.1111/ivb.12061

Krantzberg, G. (1985). The influence of bioturbation on physical, chemical and biological parameters in aquatic environments: A review. *Environmental Pollution Series A, Ecological and Biological*, *39*(2), 99–122. https://doi.org/10.1016/0143-1471(85)90009-1

Kremer, J.R., Mastronarde, D.N., & McIntosh, J. (1996). Computer visualization of three-dimensional image data using IMOD. *Journal of Structural Biology*, *116*(1), 71–76. https://doi.org/10.1006/jsbi.1996.0013

Kristensen, R.M., & Nørrevang, A. (1982). Description of *Psammodrilus aedificator* sp.n. (Polychaeta), with notes on the arctic interstitial fauna of Disko Island, W. Greenland. *Zoologica Scripta*, *11*(4), 265–279. https://doi.org/10.1111/j.1463-6409.1982.tb00538.x

Kryvi, H., & Sørvig, T. (1990). Internal organization of limbate polychaete setae (*Sabella penicillus*), with notes on bending stiffness. *Acta Zoologica*, *71*(1), 25–31. https://doi.org/10.1111/j.1463-6395.1990.tb01177.x

Labrune, C., Grémare, A., Amouroux, J.-M., Sardá, R., Gil, J., & Taboada, S. (2007). Assessment of soft-bottom polychaete assemblages in the Gulf of Lions (NW Mediterranean) based on a mesoscale survey. *Estuarine, Coastal and Shelf Science*, *71*(1), 133–147. https://doi.org/10.1016/j.ecss.2006.07.007

Levin, L.A., Rathburn, A.E., Gutiérrez, D., Muñoz, P., & Shankle, A. (2003). Bioturbation by symbiont-bearing annelids in near-anoxic sediments: Implications for biofacies models and paleo-oxygen assessments. *Palaeogeography, Palaeoclimatology, Palaeoecology*, *199*(1), 129–140. https://doi.org/10.1016/S0031-0182(03)00500-5

Levin, L.A., Ziebis, W., Mendoza, G.F., Growney-Cannon, V., & Walther, S. (2006). Recruitment response of methane-seep macrofauna to sulfide-rich sediments: An in situ experiment. *Journal of Experimental Marine Biology and Ecology*, *330*(1), 132–150. https://doi.org/10.1016/j.jembe.2005.12.022

Lewis, D.B. (1968). Feeding and tube-building in the Fabriciinae (Annelida, Polychaeta). *Proceedings Linnean Society London*, *179*(1), 37–49. https://doi.org/10.1111/j.1095-8312.1968.tb01099.x

Limaye, A. (2012). Drishti: a volume exploration and presentation tool. *Developments in X-Ray Tomography VIII*, *8506*. https://doi.org/10.1117/12.935640

Lippert, W., & Gentil, K. (1963). Über den Feinbau der Schillerhaare des Polychaeten *Aphrodite aculeata* L. *Zeitschrift Für Morphologie Und Ökologie Der Tiere*, *53*(1), 22–28.

Lotmar, W., & Picken, L.E. R. (1950). A new crystallographic modification of chitin and its distribution. *Experientia*, *6*(2), 58–59. https://doi.org/10.1007/BF02174818

Lowenstam, H.A. (1972). Phosphatic hard tissues of marine invertebrates: Their nature and mechanical function, and some fossil implications. *Chemical Geology*, *9*(1), 153–166. https://doi.org/10.1016/0009-2541(72)90053-8

Lowenstam, H.A. (1981). Minerals formed by organisms. *Science*, *211*(4487), 1126. https://doi.org/10.1126/science.7008198

Lüter, C. (2001). Brachiopod larval setae - a key to the phylum's ancestral life cycle? In Brunton, C. Howard C., Cocks L. Robin M., Long, Sarah L. (Ed.), *The Systematic Association Special: Vol. 63. Brachiopods Past and Present* (Vol. 63, pp. 46–55). Taylor & Francis.

Lüter, C., & Bartolomaeus, T. (1997). The phylogenetic position of Brachiopoda - a comparison of morphological and molecular data. *Zoologica Scripta*, *26*(3), 245–253. https://doi.org/10.1111/j.1463-6409.1997.tb00414.x

Martinez-Acosta, V.G., & Zoran, M.J. (2015). *Evolutionary aspects of annelid regeneration*. *Major Reference Works*. https://doi.org/10.1002/9780470015902.a0022103.pub2

McHugh, D. (1997). Molecular evidence that echiurans and pogonophorans are derived annelids. *Proceedings of the National Academy of Sciences*, *94*(15), 8006. https://doi.org/10.1073/pnas.94.15.8006

McHugh, D. (2000). Molecular phylogeny of the Annelida. *Canadian Journal of Zoology*, *78*(11), 1873–1884. https://doi.org/10.1139/z00-141

References

McIntosh, W.C. (1876). VIII. On the Annelida of the 'Porcupine Expeditions of 1869 and 1870. *The Transactions of the Zoological Society of London*, *9*(7), 395–416. https://doi.org/10.1111/j.1096-3642.1976.tb00244.x

Merz, R.A., & Edwards, D.R. (1998). Jointed setae – their role in locomotion and gait transitions in polychaete worms. *Journal of Experimental Marine Biology and Ecology*, *228*(2), 273–290. https://doi.org/10.1016/S0022-0981(98)00034-3

Merz, R.A., & Woodin, S.A. (1991). The stiffness of capillary setae: a comparison among sedentariate polychaetes. *Ophelia*(Suppl. 5), 615.

Merz, R.A., & Woodin, S.A. (2000). Hooked setae: tests of the anchor hypothesis. *Invertebrate Biology*, *119*(1), 67–82. https://doi.org/10.1111/j.1744-7410.2000.tb00175.x

Merz, R.A., & Woodin, S.A. (2006). Polychaete chaetae: Function, fossils, and phylogeny. *Integrative and Comparative Biology*, *46*(4), 481–496. https://doi.org/10.1093/icb/icj057

Meyer, K., & Bartolomaeus, T. (1996). Ultrastructure and formation of the hooked setae in *Owenia fusiformis* delle Chiaje, 1842: implications for annelid phylogeny. *Canadian Journal of Zoology*, *74*(12), 2143–2153. https://doi.org/10.1139/z96-243

Mills, K., & Mortimer, K. (2018). Redescription of *Magelona minuta* Eliason, 1962 (Annelida), with discussions on the validity of *Magelona filiformis minuta*. *Zootaxa*, *4527*(4), 541. https://doi.org/10.11646/zootaxa.4527.4.5

Mills, K., & Mortimer, K. (2019). Observations on the tubicolous annelid *Magelona alleni* (Magelonidae), with discussions on the relationship between morphology and behaviour of European magelonids. *Journal of the Marine Biological Association of the United Kingdom*, *99*(4), 715–727. https://doi.org/10.1017/S0025315418000784

Mortimer, K., Cassà, S., Martin, D., & Gil, J. (2012). New records and new species of Magelonidae (Polychaeta) from the Arabian Peninsula, with a re–description of *Magelona pacifica* and a discussion on the magelonid buccal region. *Zootaxa*, *3331*(1), 1. https://doi.org/10.11646/ZOOTAXA.3331.1.1

Mortimer, K., Fitzhugh, K., Brasil, A.C. d. S., & Lana, P.C. (2021). Who's who in Magelona: phylogenetic hypotheses under Magelonidae Cunningham & Ramage, 1888 (Annelida: Polychaeta). *PeerJ*, *9*, e11993. https://doi.org/10.7717/peerj.11993

Mortimer, K., & Mackie, A.S. Y. (2003). The Magelonidae (Annelida: Polychaeta) from the Seychelles, with the description of three new species. In E. Sigvaldadóttir, A. S. Y. Mackie, G. V. Helgason, D. J. Reish, J. Svavarsson, S. A. Steingrímsson, & G. Guðmundsson (Eds.), *Advances in polychaete research* (pp. 163–173). Springer Netherlands.

Mortimer, K., & Mackie, A.S. Y. (2009). Magelonidae (Polychaeta) from Hong Kong, China, with discussions on related species and redescriptions of three species. *Zoosymposia*, *2*(1), 179–199. https://doi.org/10.11646/ZOOSYMPOSIA.2.1.15

Mortimer, K., Mills, K., Jordana, E., Pinedo, S., & Gil, J. (2020). A further review of European Magelonidae (Annelida), including descriptions of *Magelona equilamellae* and *Magelona filiformis*. *Zootaxa*, *4767*(1), zootaxa.4767.1.4. https://doi.org/10.11646/zootaxa.4767.1.4

Müller, J., & Bartolomaeus, T. (in revision). Chaetal arrangement and type diversity in *Magelona mirabilis* (Magelonidae, Annelida) with ultrastructural details of the internal support chaetae. *Journal of Morphology*.

Müller, J., Bartolomaeus, T., & Tilic, E. (2022). Formation and degeneration of scaled capillary notochaetae in *Owenia fusiformis* Delle Chiaje, 1844 (Oweniidae, Annelida). *Zoomorphology*, *141*(1), 43–56. https://doi.org/10.1007/s00435-021-00547-z

Müller, J., Schumacher, A., Borda, E., Rouse, G.W., Bartolomaeus, T., & Tilic, E. (2021). "Brittleworms": Ultrastructure and arrangement of the calcified chaetae of *Euphrosine* (Amphinomida, Annelida). *Invertebrate Biology*, *140*(4), e12353. https://doi.org/10.1111/ivb.12353

Nakamura, K., Tachikawa, Y., Kitamura, M., Ohno, O., Suganuma, M., & Uemura, D. (2008). Complanine, an inflammation-inducing substance isolated from the marine fireworm *Eurythoe complanata*. *Organic & Biomolecular Chemistry*, *6*(12), 2058–2060. https://doi.org/10.1039/B803107J

Nilsen, R., & Holthe, T. (1985). Arctic and Scandinavian Oweniidae (Polychaeta) with a description of *Myriochele fragilis* sp.n., and comments on the phylogeny of the family. *Sarsia*, *70*(1), 17–32. https://doi.org/10.1080/00364827.1985.10420615

Noffke, A., Hertweck, G., Kröncke, I., & Wehrmann, A. (2009). Particle size selection and tube structure of the polychaete *Owenia fusiformis*. *Estuarine, Coastal and Shelf Science*, *81*(2), 160–168. https://doi.org/10.1016/j.ecss.2008.10.010

O'Clair, R.M., & Cloney, R.A. (1974). Patterns of morphogenesis mediated by dynamic microvilli: Chaetogenesis in *Nereis vexillosa*. *Cell and Tissue Research*, *151*(2), 141–157. https://doi.org/10.1007/BF00222219

Øresland, V., & Pleijel, F. (1991). An ectoparasitic typhloscolecid polychaete on the chaetognath *Eukrohnia hamata* from the Antarctic Peninsula. *Marine Biology*, *108*(3), 429–432. https://doi.org/10.1007/BF01313652

Orrhage, L. (1973). Light and electron microscope studies of some brachiopod and pogonophoran setae. *Zoomorphology*, *74*(4), 253–270. https://doi.org/10.1007/BF00636879

Paps, J., Baguñà, J., & Riutort, M. (2009). Lophotrochozoa internal phylogeny: new insights from an up-to-date analysis of nuclear ribosomal genes. *Proceedings of the Royal Society B: Biological Sciences*, *276*(1660), 1245–1254. https://doi.org/10.1098/rspb.2008.1574

Parapar, J., Mortimer, K., Capa, M., & Moreira, J. (2021). On the systematics and biodiversity of the Palaeoannelida. *Diversity*, *13*(2). https://doi.org/10.3390/d13020041

Paxton, H. (2000). "Eunicidans". In P. L. Beesley, G. Ross, & C. J. Glasby (Eds.), *Fauna of Australia: 4A. Polychaeta, Myzostomida, Pogonophora, Echiura, Sipuncula. Polychaetes & Allies: The Southern Synthesis* (4A. Polychaeta, Myzostomida, Pogonophora, Echiura, Sipuncula, pp. 121–140). CSIRO Publishing.

Paxton, H. (2009). Phylogeny of Eunicida (Annelida) based on morphology of jaws. *Zoosymposia*, *2*(1), 241–264. https://doi.org/10.11646/zoosymposia.2.1.18

Pearse, J.S., & Pearse, V.B. (1975). Growth zones in the echinoid skeleton. *American Zoologist*, *15*(3), 731–751. https://doi.org/10.1093/icb/15.3.731

References

Petersen, M.E. (2000). Family Sternaspidae Carus, 1863, including a review of described species and comments on some points of confusion. In J. A. Blake, B. Hilbig, & P. H. Scott (Eds.), *Taxonomic atlas of the benthic fauna of the Santa Maria Basin and Western Santa Barbara Channel* (Vol. 7, pp. 311–336). Santa Barbara Museum of Natural History.

Pilgrim, M. (1977). The functional morphology and possible taxonomic significance of the parapodia of the maldanid polychaetes *Clymenella torquata* and *Euclymene oerstedi*. *Journal of Morphology*, *152*(3), 281–302. https://doi.org/10.1002/jmor.1051520302

Pleijel, F., Dahlgren, T.G., & Rouse, G.W. (2009). Progress in systematics: from Siboglinidae to Pogonophora and Vestimentifera and back to Siboglinidae. *Comptes Rendus Biologies*, *332*(2), 140–148. https://doi.org/10.1016/j.crvi.2008.10.007

Purschke, G. (2002). On the ground pattern of Annelida. *Organisms Diversity & Evolution*, *2*(3), 181–196. https://doi.org/10.1078/1439-6092-00042

Radashevsky, V.I., & Fauchald, K. (2000). Chaetal arrangement and homology in spionids (Polychaeta: Spionidae). *Bulletin of Marine Science*, *67*(1), 13–23.

Read, G.B. (2019). A History of Annelida Research. In G. Purschke, M. Böggemann, & W. Westheide (Eds.), *Handbook of Zoology, 2193-4231: Vol. 1. Annelida* (pp. 3–36). De Gruyter.

Read, G.B., & Fauchald, K. (2022). *World Polychaeta Database*. https://www.marinespecies.org/polychaeta

Reumont, B.M. von, Campbell, L.I., Richter, S., Hering, L., Sykes, D., Hetmank, J., Jenner, R.A., & Bleidorn, C. (2014). A polychaete's powerful punch: venom gland transcriptomics of *Glycera* reveals a complex cocktail of toxin homologs. *Genome Biology and Evolution*, *6*(9), 2406–2423. https://doi.org/10.1093/gbe/evu190

Rieger, R.M., & Purschke, G. (2005). The coelom and the origin of the annelid body plan. In T. Bartolomaeus & G. Purschke (Eds.), *Morphology, molecules, evolution and phylogeny in Polychaeta and related taxa* (pp. 127–137). Springer Netherlands. https://doi.org/10.1007/1-4020-3240-4_8

Rieger, R.M., & Rieger, G.E. (1976). Fine structure of the archiannelid cuticle and remarks on the evolution of the cuticle within the Spiralia. *Acta Zoologica*, *57*(1), 53–68. https://doi.org/10.1111/j.1463-6395.1976.tb00211.x

Righi, S., Savioli, M., Prevedelli, D., Simonini, R., & Malferrari, D. (2021). Unravelling the ultrastructure and mineralogical composition of fireworm stinging bristles. *Zoology*, *144*, 125851. https://doi.org/10.1016/j.zool.2020.125851

Rimskaya-Korsakova, N., Dyachuk, V., & Temereva, E. (2020). Parapodial glandular organs in *Owenia borealis* (Annelida: Oweniidae) and their possible relationship with nephridia. *Journal of Experimental Zoology Part B: Molecular and Developmental Evolution*, *334*(2), 88–99. https://doi.org/10.1002/jez.b.22928

Robbins, D.E. (1965). The biology and morphology of the pelagic annelid *Poeobius meseres* Heath. *Proceedings of the Zoological Society of London*, *146*(2), 197–212. https://doi.org/10.1111/j.1469-7998.1965.tb05209.x

Rouse, G.W., & Fauchald, K. (1997). Cladistics and polychaetes. *Zoologica Scripta*, *26*(2), 139–204. https://doi.org/10.1111/j.1463-6409.1997.tb00412.x

Rouse, G.W., & Pleijel, F. (2001). *Polychaetes*. Oxford university press.

Rousset, V., Plaisance, L., Erséus, C., Siddall, M.E., & Rouse, G.W. (2008). Evolution of habitat preference in Clitellata (Annelida). *Biological Journal of the Linnean Society*, *95*(3), 447–464. https://doi.org/10.1111/j.1095-8312.2008.01072.x

Rousset, V., Pleijel, F., Rouse, G.W., Erséus, C., & Siddall, M.E. (2007). A molecular phylogeny of annelids. *Cladistics*, *23*(1), 41–63. https://doi.org/10.1111/j.1096-0031.2006.00128.x

Schepotieff, A. (1903). Untersuchungen über den feineren Bau der Borsten einiger Chätopoden und Brachiopoden. *Z. Wiss. Zool.*, *74*, 656–698.

Schepotieff, A. (1904). Untersuchungen über die Borstentaschen einiger Polychäten. *Z. Wiss. Zool.*, *77*, 586–605.

Schiemann, S.M., Martín-Durán, J.M., Børve, A., Vellutini, B.C., Passamaneck, Y.J., & Hejnol, A. (2017). Clustered brachiopod Hox genes are not expressed collinearly and are associated with lophotrochozoan novelties. *Proceedings of the National Academy of Sciences*, *114*(10), E1913. https://doi.org/10.1073/pnas.1614501114

Schindelin, J., Arganda-Carreras, I., Frise, E., Kaynig, V., Longair, M., Pietzsch, T., Preibisch, S., Rueden, C., Saalfeld, S., Schmid, B., Tinevez, J.-Y., White, D.J., Hartenstein, V., Eliceiri, K., Tomancak, P., & Cardona, A. (2012). Fiji: an open-source platform for biological-image analysis. *Nature Methods*, *9*(7), 676–682. https://doi.org/10.1038/nmeth.2019

Schulze, A., Grimes, C.J., & Rudek, T.E. (2017). Tough, armed and omnivorous: *Hermodice carunculata* (Annelida: Amphinomidae) is prepared for ecological challenges. *Journal of the Marine Biological Association of the United Kingdom*, *97*(5), 1075–1080. https://doi.org/10.1017/S0025315417000091

Schweigkofler, M., Bartolomaeus, T., & Salvini-Plawen, L. von (1998). Ultrastructure and formation of hooded hooks in *Capitella capitata* (Annelida, Capitellida). *Zoomorphology*, *118*(2), 117–128.

Sendall, K.A., Fontaine, A.R., & O'Foighil, D. (1995). Tube morphology and activity patterns related to feeding and tube building in the polychaete *Mesochaetopterus taylori* Potts. *Canadian Journal of Zoology*, *73*(3), 509–517. https://doi.org/10.1139/z95-058

Sendall, K.A., & Salazar-Vallejo, S.I. (2013). Revision of *Sternaspis* Otto, 1821 (Polychaeta, Sternaspidae). *ZooKeys*, *286*, 1–74. https://doi.org/10.3897/zookeys.286.4438

Shakouri, A., Mortimer, K., & Dehani, E. (2017). A new species and new records of *Magelona* (Annelida: Magelonidae) from Chabahar Bay, Gulf of Oman, South-eastern Iran. *Journal of the Marine Biological Association of the United Kingdom*, *97*(7), 1537–1552. https://doi.org/10.1017/S002531541600076X

Shank, T.M., Fornari, D.J., Damm, K.L. von, Lilley, M.D., Haymon, R.M., & Lutz, R.A. (1998). Temporal and spatial patterns of biological community development at nascent deep-sea hydrothermal vents (9°50′N, East Pacific Rise). *Deep Sea Research Part II: Topical Studies in Oceanography*, *45*(1), 465–515. https://doi.org/10.1016/S0967-0645(97)00089-1

Shelley, R., Widdicombe, S., Woodward, M., Stevens, T., McNeill, C.L., & Kendall, M.A. (2008). An investigation of the impacts on biodiversity and ecosystem functioning of soft sediments by the non-native polychaete *Sternaspis scutata* (Polychaeta: Sternaspidae). *Journal of Experimental Marine Biology and Ecology*, *366*(1), 146–150. https://doi.org/10.1016/j.jembe.2008.07.018

References

Silva, L., & Lana, P. (2017). *Owenia caissara* sp. n. (Annelida, Oweniidae) from Southern Brazil: addressing an identity crisis. *Zoologia*, *34*, 1–7. https://doi.org/10.3897/zoologia.34.e12623

Simonini, R., Maggioni, F., Zanetti, F., Fai, S., Forti, L., Prevedelli, D., & Righi, S. (2021). Synergy between mechanical injury and toxins triggers the urticating system of marine fireworms. *Journal of Experimental Marine Biology and Ecology*, *534*, 151487. https://doi.org/10.1016/j.jembe.2020.151487

Sket, B., & Trontelj, P. (2008). Global diversity of leeches (Hirudinea) in freshwater. In E. V. Balian, C. Lévêque, H. Segers, & K. Martens (Eds.), *Freshwater Animal Diversity Assessment* (pp. 129–137). Springer Netherlands. https://doi.org/10.1007/978-1-4020-8259-7_15

Smart, T.I., & Von Dassow, G. (2009). Unusual development of the mitraria larva in the polychaete *Owenia collaris*. *The Biological Bulletin*, *217*(3), 253–268. https://doi.org/10.1086/BBLv217n3p253

Smith, P.R., Ruppert, E.E., & Gardiner, S.L. (1987). A deuterostome-like nephridium in the mitraria larva of *Owenia fusiformis* (Polychaeta, Annelida). *The Biological Bulletin*, *172*(3), 315–323. https://doi.org/10.2307/1541711

Specht, A. (1988). III. Chaetae. In C. O. Hermans & W. Westheide (Eds.), *Microfauna Marina: Vol. 4. The Ultrastructure of Polychaeta* (pp. 45–59). Gustav Fischer.

Stewart, R.J., Weaver, J.C., Morse, D.E., & Waite, J.H. (2004). The tube cement of *Phragmatopoma californica*: a solid foam. *Journal of Experimental Biology*, *207*(26), 4727–4734. https://doi.org/10.1242/jeb.01330

Struck, T.H. (2011). Direction of evolution within Annelida and the definition of Pleistoannelida. *Journal of Zoological Systematics and Evolutionary Research*, *49*(4), 340–345. https://doi.org/10.1111/j.1439-0469.2011.00640.x

Struck, T.H. (2019). Phylogeny. In G. Purschke, M. Böggemann, & W. Westheide (Eds.), *Handbook of Zoology, 2193-4231: Vol. 1. Annelida* (pp. 37–68). De Gruyter.

Struck, T.H., Paul, C., Hill, N., Hartmann, S., Hösel, C., Kube, M., Lieb, B., Meyer, A., Tiedemann, R., Purschke, G., & Bleidorn, C. (2011). Phylogenomic analyses unravel annelid evolution. *Nature*, *471*(7336), 95–98. https://doi.org/10.1038/nature09864

Struck, T.H., Schult, N., Kusen, T., Hickman, E., Bleidorn, C., McHugh, D., & Halanych, K.M. (2007). Annelid phylogeny and the status of Sipuncula and Echiura. *BMC Evolutionary Biology*, *7*(1), 57.

Sullivan, T.N., Pissarenko, A., Herrera, S.A., Kisailus, D., Lubarda, V.A., & Meyers, M.A. (2016). A lightweight, biological structure with tailored stiffness: The feather vane. *Acta Biomaterialia*, *41*, 27–39. https://doi.org/10.1016/j.actbio.2016.05.022

Tilic, E., & Bartolomaeus, T. (2021). Commentary on: "Unravelling the ultrastructure and mineralogical composition of fireworm stinging bristles" by Righi et al. 2020. *Zoology*, *144*, 125890. https://doi.org/10.1016/j.zool.2020.125890

Tilic, E., Bartolomaeus, T., & Rouse, G.W. (2016). Chaetal type diversity increases during evolution of Eunicida (Annelida). *Organisms Diversity & Evolution*, *16*(1), 105–119. https://doi.org/10.1007/s13127-015-0257-z

Tilic, E., Döhren, J. von, Quast, B., Beckers, P., & Bartolomaeus, T. (2015). Phylogenetic significance of chaetal arrangement and chaetogenesis in Maldanidae (Annelida). *Zoomorphology*, *134*(3), 383–401. https://doi.org/10.1007/s00435-015-0272-9

Tilic, E., Geratz, A., Rouse, G.W., & Bartolomaeus, T. (2021). Notopodial "spinning glands" of *Sthenelanella* (Annelida: Sigalionidae) are modified chaetal sacs. *Invertebrate Biology*, *140*(3), e12334. https://doi.org/10.1111/ivb.12334

Tilic, E., Hausen, H., & Bartolomaeus, T. (2014). Chaetal arrangement and chaetogenesis of hooded hooks in *Lumbrineris* (*Scoletoma*) *fragilis* and *Lumbrineris tetraura* (Eunicida, Annelida). *Invertebrate Biology*, *133*(4), 354–370. https://doi.org/10.1111/ivb.12066

Tilic, E., Lehrke, J., & Bartolomaeus, T. (2015). Homology and evolution of the chaetae in Echiura (Annelida). *PLOS ONE*, *10*(3), e0120002. https://doi.org/10.1371/journal.pone.0120002

Tilic, E., Neunzig, N., & Bartolomaeus, T. (2021). Hairy and iridescent chaetae of the sea mouse *Aphrodita* (Annelida, Errantia). *Acta Zoologica.* Advance online publication. https://doi.org/10.1111/azo.12395

Tilic, E., Pauli, B., & Bartolomaeus, T. (2017). Getting to the root of fireworms' stinging chaetae - chaetal arrangement and ultrastructure of *Eurythoe complanata* (Pallas, 1766) (Amphinomida). *Journal of Morphology*, *278*(6), 865–876. https://doi.org/10.1002/jmor.20680

Tilic, E., Sermelwall, S., & Bartolomaeus, T. (2019). Formation and structure of paleae and chaetal arrangement in Chrysopetalidae (Annelida). *Zoomorphology*, *138*(2), 209–220. https://doi.org/10.1007/s00435-019-00435-7

Towe, K.M., & Lowenstam, H.A. (1967). Ultrastructure and development of iron mineralization in the radular teeth of *Cryptochiton stelleri* (Mollusca). *Journal of Ultrastructure Research*, *17*(1), 1–13. https://doi.org/10.1016/S0022-5320(67)80015-7

Tzetlin, A.B., & Filippova, A.V. (2005). Muscular system in polychaetes (Annelida). *Hydrobiologia*, *535*(1), 113–126. https://doi.org/10.1007/s10750-004-1409-x

Tzetlin, A.B., & Purschke, G. (2006). Fine structure of the pharyngeal apparatus of the pelagosphera larva in *Phascolosoma agassizii* (Sipuncula) and its phylogenetic significance. *Zoomorphology*, *125*(3), 109–117. https://doi.org/10.1007/s00435-006-0025-x

Vejdovský, F. (1882). Untersuchungen über die Anatomie, Physiologie und Entwicklung von *Sternaspis*. *Mathematisch-Naturwissenschaftliche Classe*, *43*, 33–90.

Verdes, A., Simpson, D., & Holford, M. (2018). Are fireworms venomous? Evidence for the convergent evolution of toxin homologs in three species of fireworms (Annelida, Amphinomidae). *Genome Biology and Evolution*, *10*(1), 249–268. https://doi.org/10.1093/gbe/evx279

Volkenborn, N., Hedtkamp, S.I. C., van Beusekom, J.E., & Reise, K. (2007). Effects of bioturbation and bioirrigation by lugworms (*Arenicola marina*) on physical and chemical sediment properties and implications for intertidal habitat succession. *Estuarine, Coastal and Shelf Science*, *74*(1), 331–343. https://doi.org/10.1016/j.ecss.2007.05.001

Voss-Foucart, M.-F., Fonze-Vignaux, M.-T., & Jeuniaux, C. (1973). Systematic characters of some polychaetes (Annelida) at the level of the chemical composition of the jaws. *Biochemical Systematics and Ecology*, *1*(2), 119–122. https://doi.org/10.1016/0305-1978(73)90025-2

References

Wang, R.Z., Addadi, L., & Weiner, S. (1997). Design strategies of sea urchin teeth: structure, composition and micromechanical relations to function. *Philosophical Transactions of the Royal Society of London. Series B: Biological Sciences*, *352*(1352), 469–480. https://doi.org/10.1098/rstb.1997.0034

Weigert, A., & Bleidorn, C. (2016). Current status of annelid phylogeny. *Organisms Diversity & Evolution*, *16*(2), 345–362. https://doi.org/10.1007/s13127-016-0265-7

Weigert, A., Helm, C., Meyer, M., Nickel, B., Arendt, D., Hausdorf, B., Santos, S.R., Halanych, K.M., Purschke, G., Bleidorn, C., & Struck, T.H. (2014). Illuminating the base of the annelid tree using transcriptomics. *Molecular Biology and Evolution*, *31*(6), 1391–1401. https://doi.org/10.1093/molbev/msu080

Weiss, I.M., Tuross, N., Addadi, L., & Weiner, S. (2002). Mollusc larval shell formation: amorphous calcium carbonate is a precursor phase for aragonite. *Journal of Experimental Zoology*, *293*(5), 478–491. https://doi.org/10.1002/jez.90004

Welsch, U., Storch, V., & Richards, K.S. (1984). Annelida. In J. Bereiter-Hahn, A. G. Matoltsy, & K. S. Richards (Eds.), *Biology of the Integument: Invertebrates* (pp. 269–364). Springer Berlin Heidelberg.

Westheide, W. (1997). The direction of evolution within the Polychaeta. *Journal of Natural History*, *31*(1), 1–15. https://doi.org/10.1080/00222939700770011

Westheide, W., McHugh, D., Purschke, G., & Rouse, G. (1999). Systematization of the Annelida: different approaches. In A. W. C. Dorresteijn & W. Westheide (Eds.), *Reproductive Strategies and Developmental Patterns in Annelids* (pp. 291–307). Springer Netherlands. https://doi.org/10.1007/978-94-017-2887-4_18

Wiklund, H., Nygren, A., Pleijel, F., & Sundberg, P. (2008). The phylogenetic relationships between Amphinomidae, Archinomidae and Euphrosinidae (Amphinomida: Aciculata: Polychaeta), inferred from molecular data. *Journal of the Marine Biological Association of the United Kingdom*, *88*(3), 509–513. https://doi.org/10.1017/S0025315408000982

Woodin, S.A., & Merz, R.A. (1987). Holding on by their hook: anchors for worms. *Evolution*, *41*(2), 427–432. https://doi.org/10.1111/j.1558-5646.1987.tb05808.x

Woodin, S.A., Merz, R.A., Thomas, F.M., Edwards, D.R., & Garcia, I.L. (2003). Chaetae and mechanical function: tools no Metazoan class should be without. In E. Sigvaldadóttir, A. S. Y. Mackie, G. V. Helgason, D. J. Reish, J. Svavarsson, S. A. Steingrímsson, & G. Guðmundsson (Eds.), *Advances in polychaete research* (pp. 253–258). Springer Netherlands.

Zakrzewski, A.-C. (2011). *Molecular characterization of chaetae formation in Annelida and other Lophotrochozoa.* Freie Universität Berlin, Berlin.

Zanol, J., Carrera-Parra, L.F., Steiner, T.M., Amaral, A.C. Z., Wiklund, H., Ravara, A., & Budaeva, N. (2021). *The current state of Eunicida (Annelida) systematics and biodiversity*. *Diversity: Vol. 13.* https://doi.org/10.3390/d13020074

Zavarzin, A., & Sergovskaya, T.V. (1979). The application of radioautography to analyzing the mechanisms of setal growth in polychaetes. *Tsitologiya*, *21*(4), 419–423.

Zhadan, A.E., Tzetlin, A.B., & Salazar-Vallejo, S.I. (2017). Sternaspidae (Annelida, Sedentaria) from Vietnam with description of three new species and clarification of some morphological features. *Zootaxa*, *4226*(1). https://doi.org/10.11646/zootaxa.4226.1.3

Zimmermann, M.R., Luth, K.E., & Esch, G.W. (2011). Complex interactions among a nematode parasite (*Daubaylia potomaca*), a commensalistic annelid (*Chaetogaster limnaei limnaei*), and trematode parasites in a snail host (*Helisoma anceps*). *Journal of Parasitology*, *97*(5), 788–791. https://doi.org/10.1645/GE-2733.1

Appendix

A.1 Supplementary material

A.1.1 Early arrangement of hooks in a juvenile specimen of Owenia fusiformis

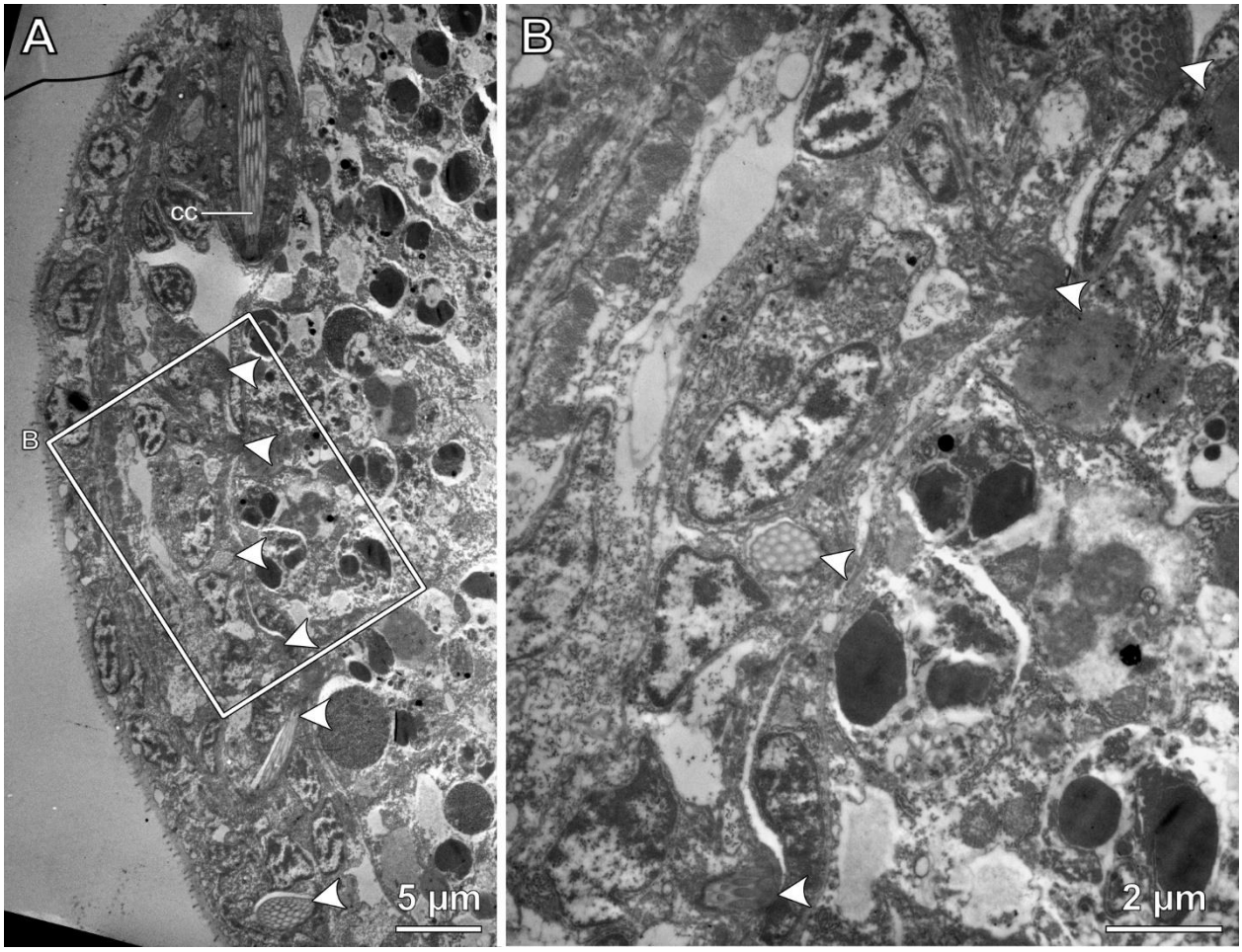

Fig. A.1.1 TEM data of a juvenile specimen of *Owenia fusiformis*. **A** Transverse section, showing six hooked chaetae during chaetogenesis, forming a row with a dorsal formative site. **B** Close-up of the framed region in A. *cc* capillary chaeta, *arrowheads* hooked chaetae

A.1.2 EDS-analyses of chaetae of various amphinomidan representatives

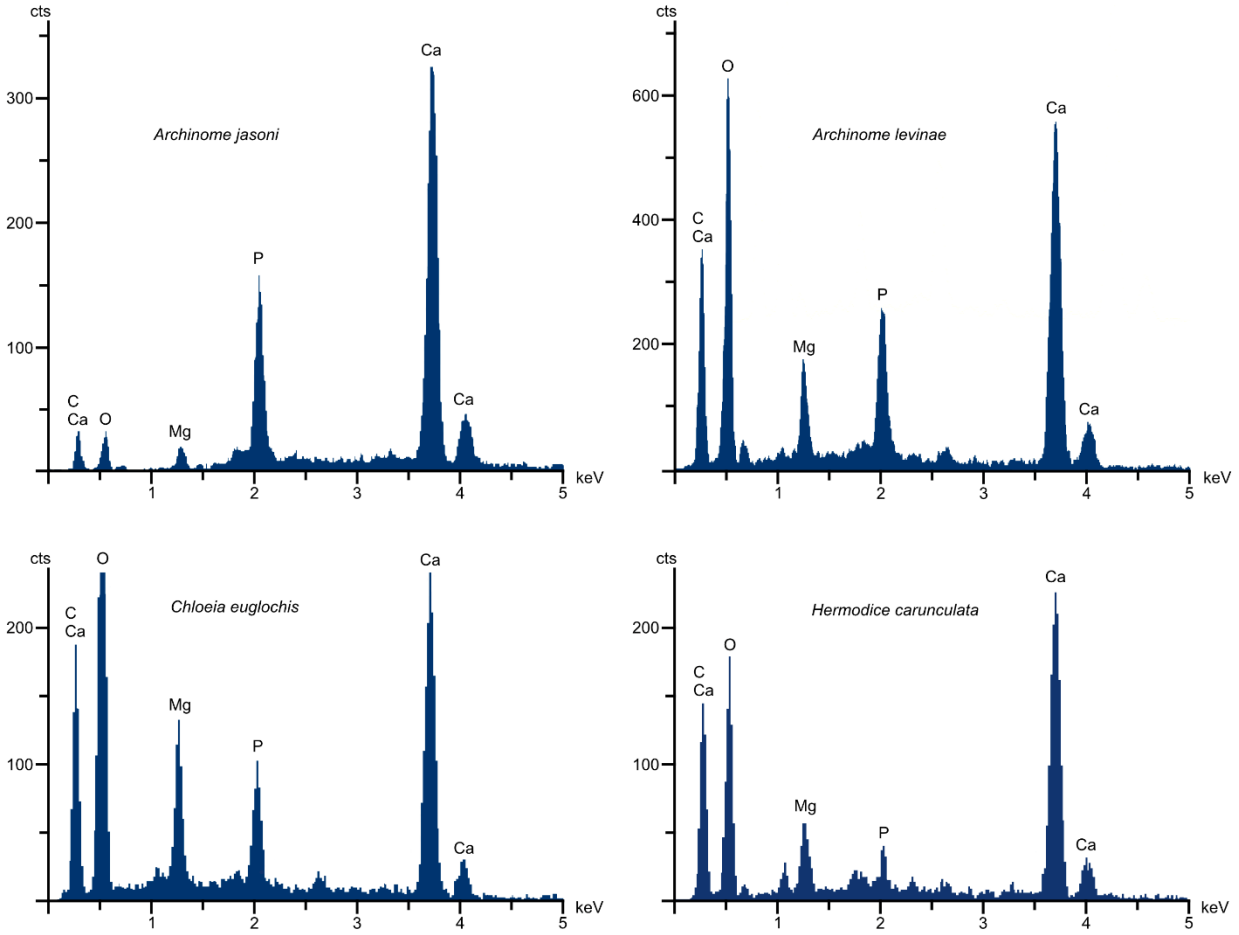

Fig. A.1.2 EDS results of chaetae (carbon coated) of *Archinome jasoni* (SIO-BIC A2368), *Archinome levinae* (SIO-BIC A2312), *Chloeia euglochis* (SIO-BIC A2760), *Hermodice carunculata* (SIO-BIC A8558).